Multifunctional Zwitterionic Surface Chemistry

for Applications in Complex Media

Norman D. Brault

A dissertation
submitted in partial fulfillment of the
requirements for the degree of

Doctor of Philosophy

University of Washington

2014

Reading Committee:

Shaoyi Jiang, Ph.D., Chairman

Daniel M. Ratner, Ph.D.

Cole A. DeForest, Ph.D.

Nathan Sniadecki, Ph.D., GSR

Program Authorized to Offer Degree:
Chemical Engineering

University of Washington

Abstract

Multifunctional Zwitterionic Surface Chemistry for Applications in Complex Media

Norman D. Brault

Chair of the Supervisory Committee:
Professor Shaoyi Jiang, Ph.D.
Chemical Engineering

The realization of personalized medicine relies on the discovery of clinically relevant biomarkers as well as on the development of corresponding assays. Due to the complexity of human blood plasma and serum, the most common sources for biomarker analysis, current attempts to integrate existing biosensing assays with analyte detection has resulted in two major shortcomings: high rates of false-positives, from non-specific binding, and a lack of assay sensitivity, due to low ligand loading. Taken together, these two factors indicate that a high signal-to-noise ratio (S/N) is vital for achieving sensitive biomarker-based diagnostics. Furthermore, a single material that can (1) exhibit non-fouling properties from undiluted human blood, (2) present abundant and easily functionalizable chemical groups for ligand attachment, and (3) possesses high immobilization capacities, would offer the most promising approach to achieving this goal. Such idealities were addressed using zwitterionic poly(carboxybetaine) (pCB) surface chemistry.

First, an important parameter was realized for identifying surface coatings suitable for real-world applications involving undiluted complex media. It was found that ultra low fouling properties using a thin film is possible if it is densely packed. While such prevention of non-specific adsorption is important, the detection of biomarkers also hinges on the ability to immobilize biologically active ligands all while maintaining the original ultra low fouling background noise of the surface coating. Hence, the dual-functionality of pCB, which provides both protein resistance and ligand functionalization, was then applied to protein arrays. Here, uniform spot morphology as well as excellent non-fouling properties

following antibody immobilization was achieved. This enabled improvements in the sensitivity for multiplexed detection of target analytes directly from undiluted human plasma.

As even the best non-fouling background combined with the highest affinity ligand would still have a limited S/N ratio due to the 2-dimensional (2-D) structure of polymer films, two efforts to improve the "signal" component were also investigated. The first method led to the development of a hierarchical architecture consisting of a thin and highly dense first layer and a loose but controlled second layer, for low fouling and high ligand loading, respectively. The second approach for improving biomarker assay performance involved taking advantage of new biosensor devices. Such novel sensor designs exhibit decreasing surface dimensions with unique geometries and enhanced theoretical sensitivities. Due to these distinct characteristics, the development of a dual-functional "graft-to" surface coating was necessary. Here, the conjugation of the adhesive molecule DOPA with pCB enabled the successful attachment to a biosensor surface while also demonstrating ultra low fouling and functionalization properties. This "graft-to" technology can be readily extended to other device platforms.

Finally, while normal immobilization conditions for pCB allow for the attachment of acidic and neutrally charged ligands, two strategies for expanding the range of ligands, to include basic proteins (i.e. with high isoelectric points), which can be coupled to an ultra low fouling zwitterionic background were also investigated. It was found that the use of reversible citraconic anhydride protection enabled the coupling of the highly basic protein lysozyme to the pCB surface. The second strategy, involving a novel zwitterionic ultra low fouling material, led to an initial characterization which indicated promising results. In summary, this work represents a multifunctional zwitterionic surface chemistry readily suitable for applications in undiluted complex media.

Table of Contents

List of Tables

List of Equations

List of Figures

Dedication

this is dedicated to my loving parents who have always kept pushing me to succeed

Chapter 1

Introduction

Personalized medicine has the potential to significantly improve the health of society. The idea behind this approach to treatment is that there exists significant heterogeneity within a given disease, at both the population level as well as within individuals themselves.[1] In the current paradigm, all patients which seemingly exhibit the same general symptoms are grouped together and subsequently administered the same therapeutic. Without accounting for the specific and unique differences between individuals, a range of desirable and undesirable responses is observed. Hence, the goal of personalized medicine is to better stratify patients into more specific and individually tailored treatments to significantly improve the number of positive outcomes.[1-3]

The realization of personalized medicine relies on the discovery and validation of clinically relevant biomarkers as well as on the development of biosensors that can be used for their detection.[4] A biomarker is defined as a biological characteristic that can be objectively evaluated as an indicator of a biological or pathological state.[5] Examples include nucleic acids (DNA and RNA), proteins, and metabolites, among others. Due to the ease of accessibility as well as the ability to represent dynamic physiological and abnormal processes, human plasma and serum are the most common sources for biomarker analysis. However, the comprehensive proteome of human blood consists of thousands of core proteins that span more than 10 orders of magnitude in concentration in which biomarkers are typically found in low abundance (at or below nanogram/milliliter quantities).[6] Attempts to integrate existing biosensing platforms or detection assays with the analysis of biomarkers from human blood has resulted in two major shortcomings: lack of sensitivity and high rates of false-positives.[7,8]

The lack of sensitivity arises from the limited immobilization capacity of molecular recognition elements which can bind to targets (biomarkers) of interest and emit a detectable signal. The use of crude samples (e.g. undiluted human blood), which allows one to achieve the best limit of detection while also minimizing assay variability,[9] has further led to a high prevalence of false-positive measurements. This is

the result of background noise caused by non-specific binding from the undiluted complex media and leads to an incorrect diagnosis.[10] Taken together, these two shortcomings indicate that a high signal-to-noise ratio (S/N) is vital for achieving the correct patient stratification using biomarker-based detection.

Traditionally, efforts to improve the S/N ratio have almost exclusively focused on increasing the signal component, primarily via significant amplification of the binding event using sandwich-based assays.[11] This method is expensive due to the requirement of developing two compatible and high affinity recognition elements (e.g. antibody ligands) per target analyte: one that can first capture the molecule and the second which is used to amplify the signal.[2] Thus, the feasibility of this approach is limited, especially in the context of the ever increasing number of biomarkers being tested and developed. While the "signal" component in the S/N ratio is the primary focus, common means to reduce background noise associated with protein fouling employ the use of blocking agents such as BSA protein or milk powder, all of which offer only minor improvements in assay performance while also exhibiting reproducibility issues.[12-15] Ideally, a single material that can achieve excellent non-fouling properties from undiluted human blood, present abundant and easily functionalizable chemical groups for ligand attachment, and possess high immobilization capacities for increasing the detectable signal, would maximize the S/N ratio and offer significant advancements to biomarker detection and personalized medicine.

The ability to significantly reduce or eliminate non-specific adsorption (i.e. background noise) from undiluted human blood plasma has almost solely been achieved using ethylene glycol-based (EG) or zwitterionic poly(carboxybetaine) (pCB) surface chemistries.[16,17] While EG-based films achieve protein resistance via a hydrogen bonding-induced hydration layer,[17] the lack of easily functionalizable groups has made it difficult to immobilize molecular recognition elements while maintaining low fouling properties.[18] In contrast, zwitterionic pCB can bind water molecules even more strongly via electrostatically-induced hydration. This has enabled surface-initiated zwitterionic pCB films to achieve ultra low fouling properties (< 5 ng/cm^2 of protein fouling) from undiluted human plasma and serum, even better than poly(ethylene glycol) films.[17,19] Furthermore, CB is a dual-functional material; the presence of a carboxylate group on each CB monomer in a polymer film enables convenient

immobilization via commonly used amino coupling chemistries. Importantly, following deactivation, pCB returns to its original zwitterionic non-fouling state.[20] Hence, the dual-functionality of pCB allows for the ability to covalently attach ligand molecules all while maintaining ultra low fouling properties to undiluted complex media on the post-functionalized polymer films, making this material an excellent choice for biomarker diagnostics.

The objective of this dissertation is to overcome the two major shortcomings associated with biomarker detection using zwitterionic pCB surface chemistry for the advancement of personalized medicine. First, in addressing the "noise" component for achieving high S/N ratios, the establishment of the physical requirements of polymer films for exhibiting ultra low fouling properties is introduced. Using pCB, a new parameter capable of characterizing and predicting protein resistance to crude complex matrices while also establishing a minimum value, is also discussed (Chapter 2). While such prevention of non-specific adsorption is important, the discovery, validation, and detection of biomarkers also hinges on the ability to immobilize biologically active ligands all while maintaining the original ultra low fouling properties of the surface coating. Furthermore, the large heterogeneity within diseases has created the need to develop biomarker panels for the detection of multiple analytes simultaneously from a single sample for improved diagnostic accuracy.[1,14] While protein arrays play a vital role in meeting this need, a single array platform capable of excellent spot morphology for multiplexed detection from crude samples is still highly desirable, thus PCB was investigated for this purpose (Chapter 3).[8,18]

As even the best non-fouling background combined with the highest affinity ligand would still have a limited maximum S/N ratio due to the 2-dimensional (2-D) structure of polymer films, two efforts to improve the "signal" component were introduced. The first includes overcoming the relatively low ligand immobilization levels of 2-D films by implementing a 3-dimensional (3-D) component. Specifically, the use of a thin and highly dense first layer, to provide ultra low fouling properties, with a loose and controlled second layer to enable high levels of ligand immobilization and improved antigen detection, is demonstrated (Chapter 4). The second approach for improving biomarker assay performance involves taking advantage of new biosensor devices. Such sensors utilize decreasing surface dimensions

and unique geometries to offer significant improvements in sensitivity.[21-23] However, their small size and design has hindered their implementation. To fully take advantage of their potential, the creation of a dual-functional “graft-to” surface coating is necessary. While simple in theory, the development of a “graft-to” coating which can be ubiquitously applied to numerous sensor platforms has proven challenging.[24] PCB conjugates exhibiting an adhesive molecule are investigated as a simple means to enable improved detection limits from complex media on such devices (Chapter 5).

Finally, as pCB is ideally suited to perform diagnostics in crude samples, it is important to enable the full range of potential ligands which are amenable to immobilization on the ultra low fouling background. Normal coupling conditions allow for the attachment of acidic and neutrally charged proteins but not basic molecules (e.g. high isoelectric point proteins). Thus, two methods to expand the range of ligands that can be covalently grafted to the surface, all while maintaining bioactivity, are explored. The first approach relies on a reversible protein modification strategy using citraconic anhydride (CA) to covalently modify basic biomolecules prior to immobilization, making them negatively charged (Chapter 6). Protein conjugation methods with CA as well as the study of the reversible nature of the modification are studied. Immobilization conditions and bioactivity of the modified ligand coupled onto the positively charged and activated pCB film was also tested. The second approach involves the use of a novel zwitterionic material (Chapter 7). This compound contains a tertiary amine and a carboxylic acid separated by a single carbon spacer and also exhibits ultra low fouling protein resistance under neutral pH conditions.[25] A key property of this material which makes it amenable to the immobilization of basic ligands involves the tertiary amine component, whose pKa decreases upon the esterification of the carboxylic acid. It is hypothesized that if a negatively charged and amine-reactive agent is used to form the ester, there will exist an immobilization pH window in which a basic ligand will be attracted to and efficiently coupled to the negatively charged surface. Here, this hypothesis is investigated.

Chapter 2

Dry Film Refractive Index as an Important Parameter for Ultra Low Fouling Surface Coatings

Here we demonstrate that the film refractive index (RI) can be an even more important parameter than film thickness for identifying nonfouling polymer films to undiluted human blood plasma and serum. The film thickness and RI are two parameters obtained from ellipsometry. Previously, film thickness has been correlated to ultra low fouling properties. Practically, the film RI can be used to characterize polymer density but is often overlooked. By varying the water content in the surface-initiated atom transfer radical polymerization of zwitterionic carboxybetaine, a minimum of ~1.5 RI units was necessary to achieve < 5 ng/cm^2 of adsorption from undiluted human serum. A model of the film structure versus water content was also developed. These results point to an important parameter and simple approach for identifying surface coatings suitable for real-world applications involving complex media. Thus, ultra low fouling using a thin film is possible if it is densely packed.

2.1 Introduction

A major challenge in the biomedical community involves the prevention of nonspecific biomolecular attachment onto surfaces. For example, nonspecific protein adsorption onto diagnostic devices has severely limited their full exploitation for sensitive detection from complex media.[26] A small amount of protein adsorption onto medical implants can propagate into a total foreign body response thereby affecting device biocompatibility.[27] The use of stealth materials in drug delivery is vital for improving drug circulation half-life and bioavailability.[28] These applications highlight the importance of achieving ultra low fouling properties (< 5 ng/cm^2 of protein fouling).

The surface-initiated atom transfer radical polymerization (SI-ATRP) of zwitterionic carboxybetaine has previously achieved ultra low fouling properties to undiluted human serum and

plasma.[29] In this study, it was determined that the level of protein resistance was related to film thickness; a value too small or too large resulted in increased protein adsorption thus requiring some optimal value. Hucknall et al. observed a minimum film thickness for the SI-ATRP of oligo(ethylene glycol) methacrylate which was necessary to achieve undetectable adsorption from protein solutions.[16] Theoretically, a brush can be characterized via its chain lengths and chain-to-chain distances.[30] Practically, however, AFM or ellipsometry provides only an effective film thickness, thus correlating this property to nonfouling is ambiguous. Dilute but long polymers (such as those grown with a low surface coverage of initiator) can have the same thickness as short but highly dense brushes. Furthermore, the polymer density, in addition to the film thickness, simultaneously changes during film growth.[30,31]

The swelling behavior of a film, determined as the ratio of wet and dry thicknesses, is one approach to study polymer density. Tightly packed polymer brushes in a good solvent will swell less than lower density brushes.[30,31] These tightly packed films have high extension in the dry state and significant further extension is limited upon swelling.[32] Ellipsometry also calculates an additional parameter, the film refractive index (RI). The film RI can be used to characterize the polymer density, but is often overlooked in practice. Since the RI measurements of films account for two factors, the medium (e.g. air, RI of ~1.0) as well as the material itself (e.g. proteins, RI of ~1.53)[33], the RI of a polymer film will increase with density.[34,35] Importantly, the RI can be measured in the dry state, thus offering a convenient and simple approach for film characterization.

In this work, SI-ATRP was used to investigate a new parameter capable of characterizing and predicting ultra low fouling properties of poly(carboxybetaine acrylamide) (pCBAA) films. SI-ATRP is a controlled radical polymerization that enables the formation of polymer brushes with low polydispersity, high density, and a desired thickness. It is based on the equilibrium reaction between activated propagating chains and those that have been capped by a deactivating complex.[36] The highly localized and low concentration of immobilized initiators in SI-ATRP (relative to solution ATRP) is a major challenge for achieving control due to the low concentration of persistent deactivator which can trap the propagating radical. The rate of polymerization is highly dependent upon the ratio of activator to

deactivator; reduction in the latter leads to fast and uncontrolled growth. This increases the film polydispersity as well as the probability of irreversible chain-chain termination events (i.e. recombination) thereby affecting the polymer density.[30,36] For aqueous ATRP, the water content has been shown to sharply affect the rate of reaction due to a significant loss of deactivator, among other side reactions.[37] This has previously enabled the use of SI-ATRP with 2-hydroxyethylmethacrylate (HEMA) to obtain a peak film thickness at some medium water concentration.[38] Since the polydispersity of a film is related to its polymer density,[32] varying the content of water during SI-ATRP enables a convenient approach for studying the effect of film thickness and polymer density on the nonfouling properties of pCBAA brushes.

Herein, the ability to obtain ultra low fouling properties of pCBAA films formed via SI-ATRP was investigated using surface plasmon resonance (SPR) biosensors. Protein resistance to undiluted human serum was studied as a function of the polymer thickness and dry refractive index, the latter representing the polymer density. The results indicated that the nonfouling properties of pCBAA films were not affected much by the polymer thickness, but were more strongly dependent on the RI. The data also enabled a model of polymer structure as a function of water content in the SI-ATRP reaction to be developed. This work points to an important parameter which may be necessary to achieve, and used to predict, ultra low fouling properties of surface polymerized films.

2.2 Experimental Section

2.2.1 Materials

All chemicals were purchased from Sigma-Aldrich (St. Louis, MO) and Decon Laboratories (King of Prussia, PA). Pooled human serum was purchased from Biochemed Services (Winchester, VA). Mercaptoundecyl bromoisobutyrate and CBAA monomer were synthesized as described previously.[39,40]

2.2.2 Preparation of pCBAA Films

UV cleaned SPR sensor chips coated with ATRP initiator self-assembled monolayers were prepared by soaking in 0.1 mM mercaptoundecyl bromoisobutyrate in pure ethanol for 24 hours. The chips were then removed, rinsed with ethanol, THF, and ethanol, and the blown dry using filtered air and placed into a custom glass tube reactor. In a separate glass tube, 8.86 mg CuBr, 57.87 mg 2,2'-bipyridine, and 600 mg of CBAA were added. Both tubes were then placed under nitrogen protection. Appropriate volumes of nitrogen purged methanol and water were then added (total volume was 4 mL) to the solids according to the necessary solvent ratio. For example, an ATRP water content of 10% was obtained by adding 3.6 mL of methanol and 0.4 mL of water. The water content was varied from 0 – 90% (v/v). After dissolving the solids (~ 15 min), the mixture was then transferred to the reactor tube under nitrogen protection and allowed to react for 3 hours at 25°C in a shaker set to 120 rpm. Following the reaction the chips were rinsed with water and then submerged overnight in PBS.

2.2.3 SPR Sensor, Chips, and Calibration of the Surface Sensitivity

A laboratory SPR sensor developed at the Institute of Photonics and Electronics, Prague, Czech Republic was used as described previously.[26] This custom built SPR is based on the Kretschmann geometry of the attenuated total reflection method with wavelength modulation. It is equipped with a four-channel flow-cell, temperature control, and uses a peristaltic pump for delivering samples. SPR sensor chips were made of a glass slide coated with an adhesion-promoting titanium film (~2 nm) followed by a gold film (~48 nm) using an electron beam evaporator. Since SPR sensitivity depends on the distance of the binding event from the SPR active surface, the sensor response due to the polymer films was calibrated using previously described methods.[26,41]

2.2.4 Determination of Polymer Film Thickness, Refractive Index, and Density

Dry and wet film thickness and refractive index measurements were determined using a multi-wavelength ellipsometer (J. A. Woollam Co., Inc., Model alpha-SE). A liquid cell with a volume of 0.5 mL was used for obtaining the wet measurements. The data was analyzed via fitting a Cauchy model for a bare SPR substrate which enabled the film thickness and refractive index to be simultaneously determined without using predetermined or assumed Cauchy coefficients. The wet and dry refractive index measurements were then used with an effective medium approximation for calculating the wet polymer density (see **Equation 2.1**).

2.2.5 Measurements of Nonspecific Protein Adsorption by SPR

Nonspecific protein adsorption of the pCBAA polymer films was determined with a SPR biosensor using a flow rate of 50 μL/min at 25°C. After first establishing a baseline using PBS, undiluted human serum was flowed for 10 minutes, followed by buffer. Protein adsorption was quantified as the difference between buffer baselines and converted to a surface coverage using the appropriate sensitivity factor.

2.3 Results and Discussion

The pCBAA films were achieved by varying the SI-ATRP water content from 0 – 90% (v/v) using a fixed reaction time. The corresponding dry film thicknesses (8 – 40 nm), dry RI values (1.48 – 1.56 RI units (RIU)), and protein adsorption to undiluted human serum are shown in **Figure 2.1**. The data indicates a maximum value for both the thickness and RI as the polymerization rate was varied. Interestingly, all films except for those made using 90% water (v/v) enabled ultra low fouling properties (**Figure 2.1c**). Thus it appears that thickness (**Figure 2.1a**) may not play a significant role in protein

resistance. Since the dry film RI is proportional to the polymer density, the relatively high fouling for the films made from 90% water is likely due to its lower polymer density (**Figure 2.1b**) with a correspondingly reduced hydration, the primary mechanism of protein resistance.[42] The SPR sensorgrams for films made using 50% and 90% water (v/v) are shown in **Figures 2.2 and 2.3**, representing ultra low fouling and high protein binding, respectively). It should be noted that in the initial stages of polymerization for a given reaction, the thickness as well as the polymer density are simultaneously changing.[30] Thus, the thickness can still serve as an indirect measure for achieving nonfouling surfaces, as observed previously.[16] However, the results here illustrate that the polymer density may be the direct and more important parameter for reflecting protein resistance. This enables one to achieve ultra low fouling with a densely packed thin film.

A comparison of **Figures 2.1b and 2.1c** indicate the existence of a minimum RI value (~1.5), representing a minimum polymer density for achieving ultra low fouling properties with pCBAA films. This requirement was further tested with two control experiments. The first was a pCBAA film made from pure methanol but for a shorter reaction time (30 min). The second was using a SPR initiator chip made from a 9:1 mol% undecanethiol:ATRP initiator ethanolic solution to reduce the surface density of initiator for growing long but loose polymer chains. This chip then underwent SI-ATRP using a water concentration of 10% (v/v) in methanol for 3 hrs to enable both reasonable control and polymer solubility. The resulting refractive indices for the first and second control experiments were 1.481 ± 0.007 RIU and 1.469 ± 0.005 RIU with corresponding protein adsorption to undiluted human serum as 12.6 ± 0.7 ng/cm^2 and 29.0 ± 0.7 ng/cm^2, respectively. These data confirm the hypothesis that a minimum dry film RI (or polymer density) is necessary for achieving ultra low fouling properties, as illustrated in **Figure 2.1d**.

As shown in **Figure 2.1a**, the pCBAA film had a peak thickness at ~ 40 nm using 20% water (v/v). Polymer films grown using 0% water enable a relatively slow reaction with low polydispersity. Under this condition, the final thickness is limited by the lower solubility of the brush in methanol which leads to confinement of the growing chain end, limiting the access of free monomer as well as the catalyst complex.[43] Increasing the amount of water will increase the accessibility of the chain end due to the

super-hydrophilicity of zwitterionic carboxybetaine materials and an increase in the polymerization rate, resulting in larger film thicknesses but with more polydispersity due to radical recombination. If such events occur too often as in the case of very high water concentrations, the film thickness can decrease, as observed in **Figure 2.1a**.[36,38]

The RI measurements shown in **Figure 2.1b** had a similar trend to the film thicknesses. Since the dry film RI is proportional to polymer density, these results indicate that the density initially increases and then rapidly decreases with the rate of the ATRP reaction. Interestingly, the films made from 0% and 90% water had the lowest densities in air, despite the former being made under the most controlled conditions (i.e. water-free) which would be expected to yield a very high density polymer brush. The films made using 10% - 60% water had the highest polymer densities. These are attributed to increased polydispersity and longer chain lengths allowing for ion-pair interactions of the loose chains, which collapse onto the surface in the presence of air, similar to a multilayer polyelectrolyte film.[44] This may also explain why the same solvent composition did not simultaneously give both the maximum RI and thickness, which were observed with a 50% and 20% water content, respectively. The long chains obtained for the latter were more uniform and hence formed fewer multilayers. This indicates that a combination of both long and polydisperse chains are responsible for increasing the dry film RI. The low value achieved for the film made from 0% water is thus due to a monodisperse brush containing few collapsed chains. The result for the film made with 90% water (v/v) was likely caused by excessive radical termination reactions which occur under this condition, thus creating little pockets for air thereby reducing the density. This is supported by the rapid decrease in thickness for films made from high water concentrations.

The wet polymer density in PBS, synonymous with the polymer volume fraction (PVF), of several films was also studied (**Figure 2.4**). A low wet density will have a large amount of solvent relative to polymer material thus enabling a large degree of swelling, corresponding to a “loose” polymer structure. The films made using 0%, 10%, 50%, and 90% water had wet densities of 62%, 48%, 35%, and 73%, respectively. The initial decrease follows the expected increase in polydispersity for the faster polymerizations,[30] such as with high water concentrations. However, the high value for 90% water was

unexpected. The expected result would have been a very “loose” structure with a low wet density due to rapid propagation. Such a high value has not been previously observed in the literature for fast polymerizations and may simply be due to the extreme scenario in which control of the reaction was absent; a combined result of both rapidly propagating acrylamide-based monomers and a high water content.[37] Therefore, since the films made using 90% water elicit widespread termination events, as indicated by the rapid decrease in thickness (**Figure 2.1a**), it is believed that such significant chain-end recombination restricted the polymer from swelling yielding a high wet density.

A summary of the results enables a model of the polymer structure as a function of water content (polymerization rate) and protein resistance to be developed (**Figure 2.5**). The water free scenario results in thin but uniform and dense polymer brushes with low polydispersity and ultra low fouling properties. As the water concentration increases, the polydispersity increases but the amount of termination is not excessive enough to significantly suppress film growth. The continued propagation enabled by the lack of recombination provides for a similarly dense base-layer to form (dashed box) and thus ultra low fouling properties can be achieved. The scenario for high water content occurs with very fast and uncontrolled reactions in which radical recombination frequently occurs. This restricts polymer growth and reduces the polymer density thereby affecting the film hydration and subsequent protein resistance.

2.4 Conclusions

In this work, protein resistance of pCBAA films made via SI-ATRP was studied as a function of film thickness and RI by varying the water content in the reaction. The results indicated that the film RI, which is proportional to the polymer density, is potentially the more important parameter for ultra low fouling properties than the film thickness, which was previously correlated to protein resistance. This finding enables one to achieve excellent nonfouling using a thin film if it is densely packed. Noteworthy, in the initial stages of polymerization for a given reaction, both the thickness and density are simultaneously changing. Thus, it is still possible to use film thickness for indirectly accessing protein

resistance. The data revealed a RI range of 1.50 – 1.56 RIU with wet polymer densities from 62 – 35% PVF that allowed zwitterionic pCBAA films to achieve < 5 ng/cm^2 of nonspecific protein adsorption from undiluted human serum. A model of the polymer structure as a function of the SI-ATRP water content was also developed. Increasing the water concentration initially leads to thicker but more polydisperse films, the latter a result of radical termination events, until excessive recombination occurs after which the thickness decreases. While the exact RI values may vary for different polymer film systems (i.e. other than pCBAA), this work points to an important parameter and a simple approach which can be used for assessing the protein resistance of surface coatings for real-world applications involving complex media.

2.5 Figures

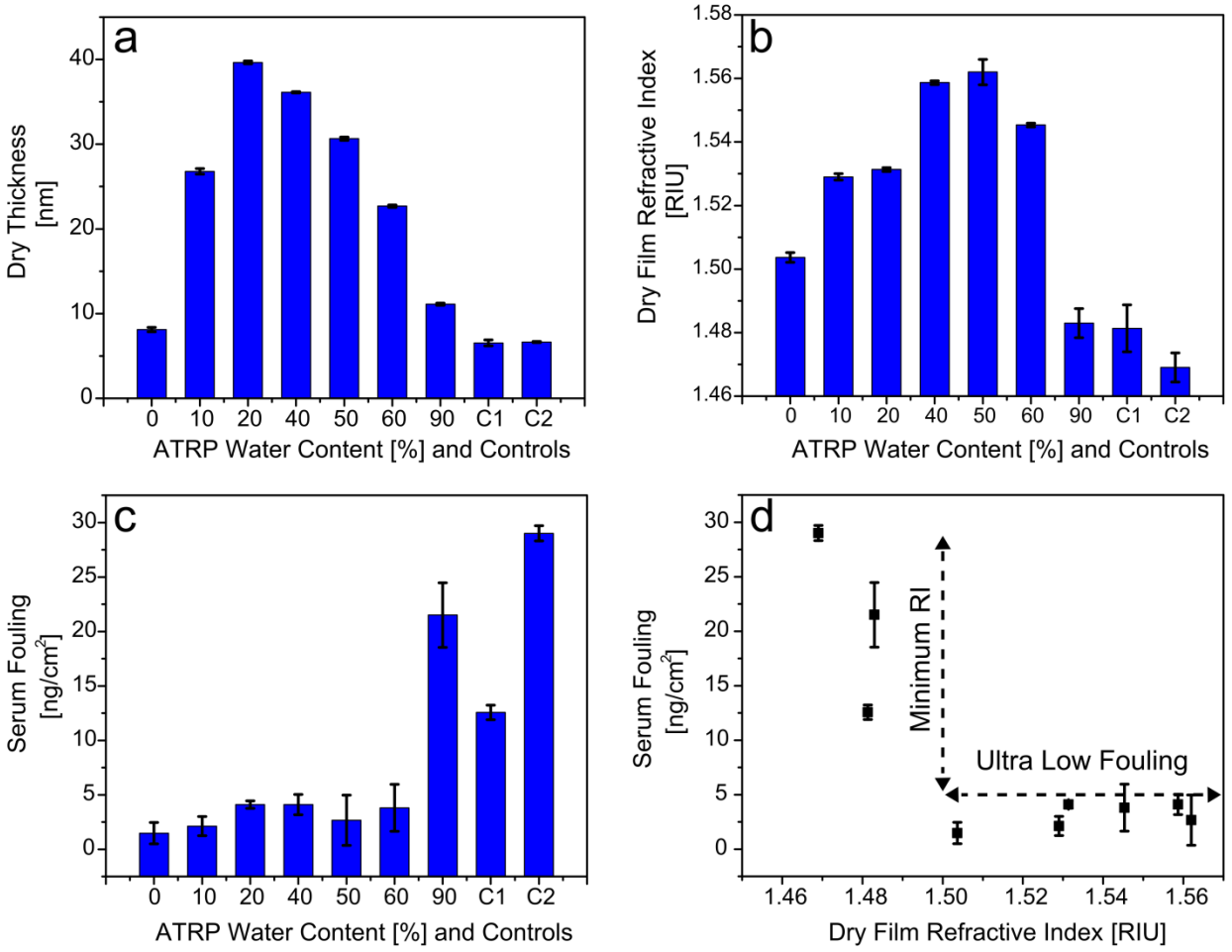

Figure 2.1. Film thickness (a), RI (b), and protein adsorption of pCBAA films to undiluted human serum (c) as a function of water content for zwitterionic pCBAA grown via SI-ATRP using a 3 hr reaction time. Two additional control experiments were also run. Control 1 (C1) represents a pCBAA film prepared from pure methanol, but with a 30 min reaction time. Control 2 (C2) represents a film prepared using a 9:1 mol% undecanethiol:ATRP initiator covered surface and 10% water (v/v) in methanol for 3 hr. (d) Serum fouling as a function of the average dry film RI for all samples tested.

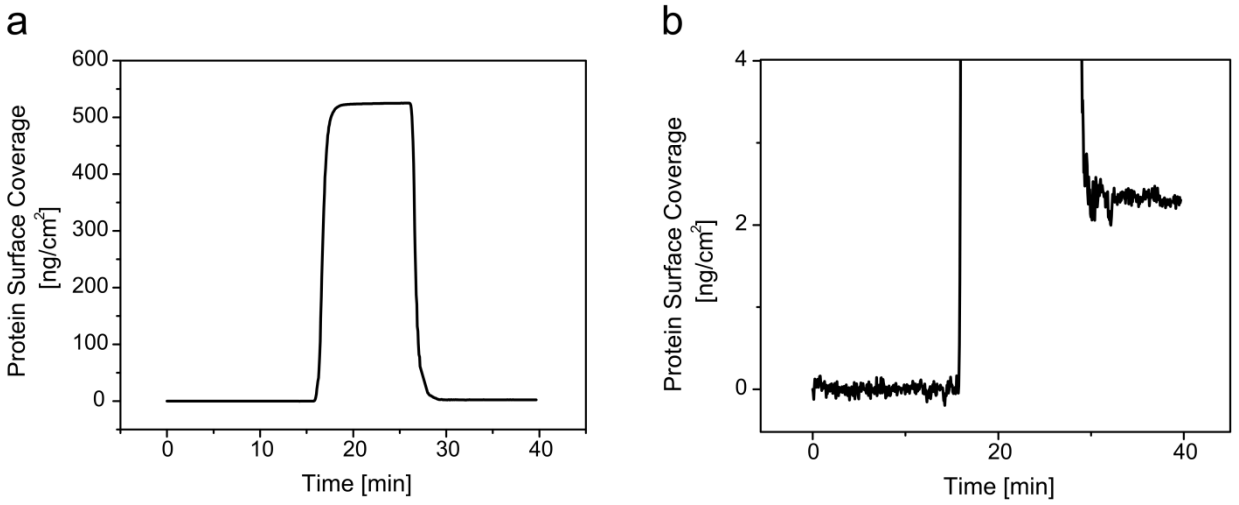

Figure 2.2. (a) The SPR sensor-gram for pCBAA films made via surface initiated atom transfer radical polymerization (SI-ATRP) with a water concentration of 50% (v/v) in methanol. (b) This result demonstrates ultra low fouling behavior (< 5 ng/cm^2 of non-specific protein adsorption) to undiluted human serum.

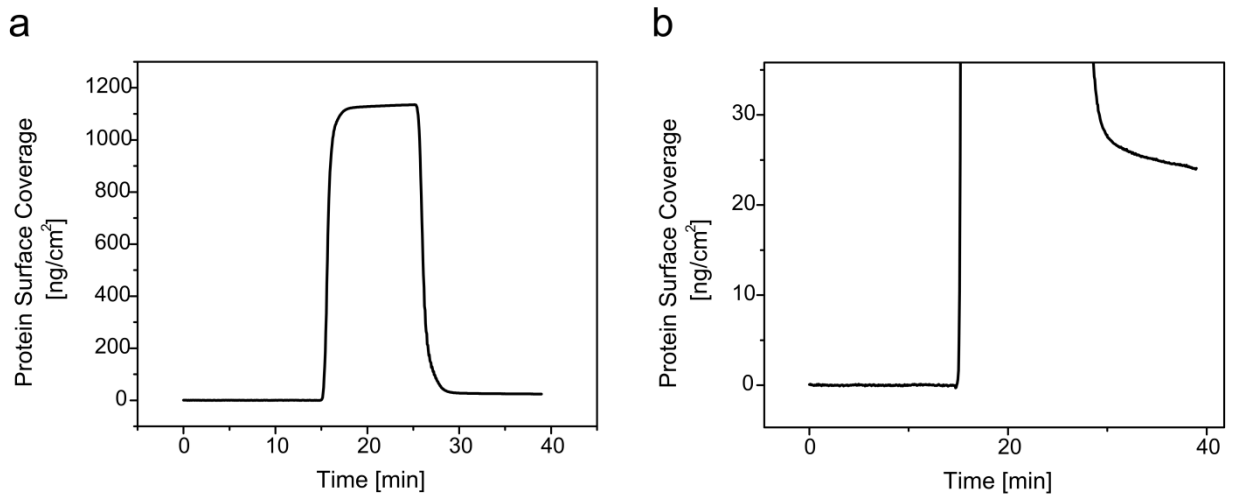

Figure 2.3. (a) The SPR sensor-gram for pCBAA films made via SI-ATRP with a water concentration of 90% (v/v) in methanol. (b) This result demonstrates high protein binding when challenged to undiluted human serum.

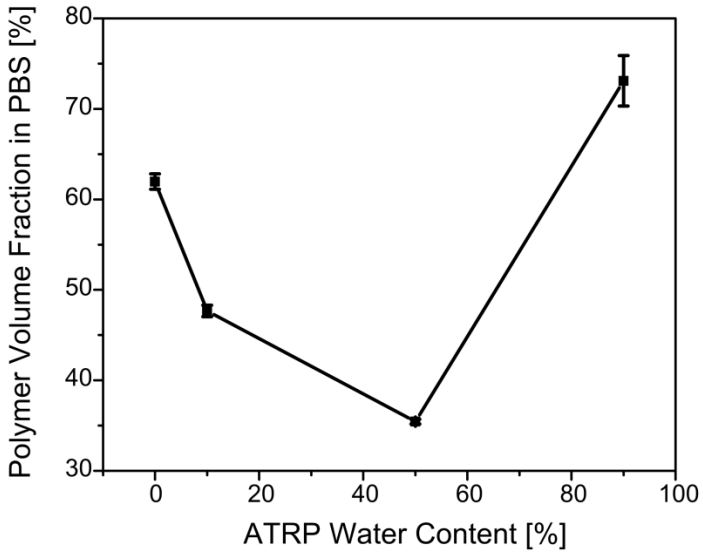

Figure 2.4. The polymer volume fraction (PVF) of pCBAA films in PBS (i.e. the wet polymer film density) as a function of SI-ATRP water content. The corresponding swell ratios for films made using 0%, 10%, 50% and 90% water content were 1.7, 1.9, 2.4, and 1.6 respectively.

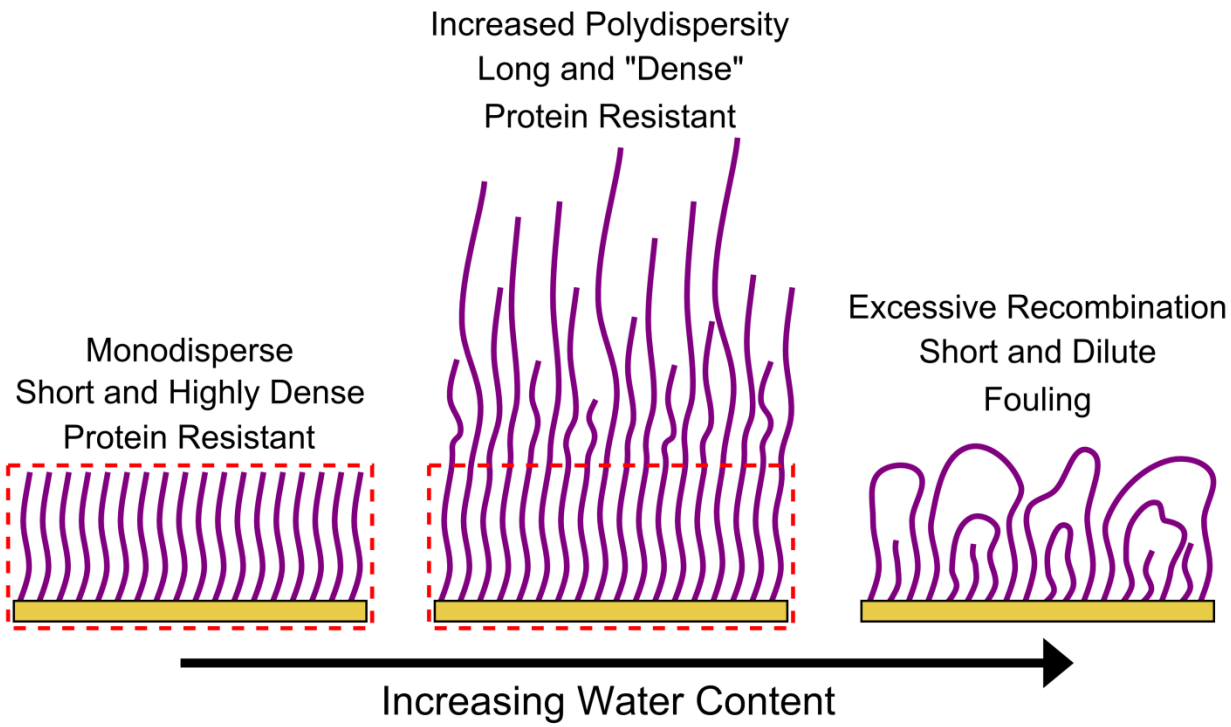

Figure 2.5. Model of polymer growth as a function of SI-ATRP water content in a good solvent. The water free scenario results in thin but uniform and dense brushes with low polydispersity. As the water content increases, the polydispersity increases but the density of all of these films is sufficient to achieve ultra low fouling properties due to a similar base layer (dashed box). Very high water contents permit fast and uncontrolled reactions in which radical recombination reduces the polymer density thereby decreasing the film hydration and the subsequent protein resistance.

2.6 Equations

Equation 2.1. Polymer Volume Fraction Calculation

The wet and dry refractive index (RI) measurements were used with an effective medium approximation[45] (Eq. 1) for calculating the wet polymer density in PBS, synonymous with the polymer volume fraction (PVF), of pCBAA films made via SI-ATRP using 0%, 10%, 50% and 90% water (v/v).

$$PVF = \frac{\left(n_p^2 - n_b^2\right)\left(n_{p-dry}^2 + 2n_b^2\right)}{\left(n_p^2 + 2n_b^2\right)\left(n_{p-dry}^2 - n_b^2\right)}$$

n_p $= RI\ of\ polymer\ brush\ in\ PBS$

n_{p-dry} $= RI\ of\ polymer\ brush\ in\ air$

n_b $= RI\ of\ PBS$, 1.333

Chapter 3

Directly Functionalizable Surface Platform for Protein Arrays in Undiluted Human Blood Plasma

Protein arrays are a high-throughput approach for proteomic profiling vital for achieving a greater understanding of biological systems in addition to disease diagnostics and monitoring therapeutic treatments. In this work, zwitterionic carboxybetaine polymer (pCB) coated substrates were investigated as an array surface platform to enable convenient amino-coupling chemistry on a single directly functionalizable and unblocked film for the sensitive detection of target analytes from undiluted human blood plasma. Using a surface plasmon resonance (SPR) imaging sensor, the antibody immobilization conditions which provided excellent spot morphology and the largest antigen response were determined. It was found that pCB functionalization and the corresponding antigen detection both increased with pH and antibody concentration. Additionally, immobilization only required an aqueous buffer without the need for additives to improve spot quality. The non-specific protein adsorption to undiluted human plasma on both the antibody immobilized pCB spots as well as the background were found to be about 9 ng/cm^2 and 6 ng/cm^2, respectively. A subsequent array consisting of three antibodies spotted onto pCB revealed little cross-reactivity for antigens spiked into the undiluted plasma. The low post-functionalized non-fouling properties combined with antibody amplification showed similar sensitivities achievable with conventional spectroscopic SPR sensors and the same pCB films, but now with high throughput capabilities. This represents the first demonstration of low fouling properties following antibody functionalization on protein arrays from undiluted human plasma and indicates the great potential of the pCB array platform for high-throughput protein analysis.

3.1 Introduction

Protein arrays play a vital role in high-throughput proteomics, personalized medicine, biomarker discovery and validation, drug discovery, and *in vitro* diagnostics among many other applications which require the simultaneous detection of multiple analytes from a single sample.[14,46-50] However, the field currently suffers from lack of standardized procedures, numerous platforms tailored to individual purposes and difficulty in achieving uniform and consistent immobilized antibody spot morphology with a high signal to noise ratio (S/N).[14] While the use of additives is typically necessary to improve spot quality, a key characteristic for the successful implementation of protein arrays in the clinic, the limit-of-detection (LOD), has been severely hindered by the inability to analyze undiluted complex media due to the large background noise associated with non-specific adsorption which also blocks analyte binding sites thereby severely decreasing the S/N which is necessary for highly sensitive detection.[18] For example, the comprehensive proteome of human blood consists of thousands of core proteins that span more than 10 orders of magnitude in concentration in which cancer biomarkers typically fall in the minority (at or below nanogram/milliliter quantities).[6] Hence, in addition to high quality binding reagents, a single array platform which provides simple and convenient surface chemistry for ligand immobilization with excellent morphology all while minimizing fouling from undiluted complex media without the use of blocking agents is highly desirable and offers the best means for achieving sensitive detection of multiple analytes.[8,18]

In order to reduce the background noise associated with protein fouling, most platforms require the use of blocking agents such as BSA protein or milk powder as well as the dilution of the sample (e.g., whole blood, plasma or serum) by at least 9:1 thereby worsening the LOD.[12-14] This has lead to the use of low fouling materials, commonly based on ethylene glycol (EG) and its derivatives, which can more effectively resist non-specific adsorption via the formation of hydrogen bond-induced hydration layer.[17] Recently, antibody arrays made from ~100 nm films of poly(oligo(ethylene glycol) methacrylate) (pOEMGA) were used to detect multiple analytes from undiluted fetal bovine serum and rabbit blood.[18]

For these films, the antibody was non-covalently adsorbed onto pOEGMA under vacuum desiccation. This process results in the removal of water from the system which can subsequently reduce the ability to prevent non-specific protein adsorption and maintain the bioactivity of the trapped antibodies.[18,42] While the fouling properties for the non-functionalized pOEGMA films (i.e., without antibody) were previously verified via SPR,[16] sandwich-based ELISA was used for the detection of multiple analytes with the pOEGMA array. This commonly used technique only accounts for the desired specific antigen-antibody interaction and hence the non-specific adsorption onto the functionalized pOEGMA antibody spots was not determined. This is especially important as fouling on EG based films typically increases following ligand immobilization.[16]

Surface grafted polymer films composed of zwitterionic carboxybetaine (CB) have also been shown to be highly attractive materials for protein resistant applications due to their ability to prevent fouling via an electrostatically induced hydration layer.[17] These films exhibit ultra low fouling properties to undiluted human serum and plasma (i.e., < 5 ng/cm^2 of non-specific protein adsorption) and possess abundant functionalizable groups to enable antibody immobilization via amino-coupling chemistry.[29] Importantly, following deactivation, pCB returns to its original zwitterionic non-fouling state, thus allowing for the sensitive detection of target analytes from undiluted complex media due to the ability to significantly reduce background noise on the functionalized film without the use of blocking agents.[20] Such surface chemistry has been previously demonstrated via the *in situ* functionalization of pCB substrates using a spectroscopic surface plasmon resonance (SPR) biosensor.

In this work, antibody arrays based on zwitterionic pCB substrates were investigated using standard pin-spotting techniques integrated with an SPR imaging sensor for the direct interrogation of both specific and non-specific protein adsorption. Using conventional amino-coupling chemistry, the necessary printing conditions for achieving uniform spot morphology and biologically active antibodies were determined. The non-fouling properties as well as the ability to detect three target analytes directly from undiluted human plasma were then studied. The antibody arrays on pCB enabled low fouling properties on both the functionalized and non-functionalized surfaces as well as improved detection limits

from the undiluted plasma. This represents the first demonstration of low fouling properties following antibody functionalization on a protein array and indicates the great potential of pCB for high throughput detection.

3.2 Experimental Section

3.2.1 Materials

Copper(I) bromide (99.999%), 2,2'-bipyridine (bpy, 99%), tetrahydrofuran (THF), methanol, phosphate buffered saline (PBS, 0.01 M phosphate, 0.138 M sodium chloride, 0.0027 M potassium chloride, pH 7.4), anhydrous acetone, and triethylamine were purchased from Sigma-Aldrich (St. Louis, MO). Ethanol (200 Proof) was purchased from Decon Laboratories (King of Prussia, PA). Sodium carbonate anhydrous were purchased from EMD Chemicals (Darmstadt, Germany). Sodium chloride (NaCl) and ether were purchased from J.T. Baker (Phillipsburg, NJ). Sodium acetate anhydrous was purchased from Fluka (subsidiary of Sigma Aldrich, St. Louis, MO). 1-Ethyl-3-(3-dimethylaminopropyl) carbodiimide hydrochloride (EDC) and N-hydroxysuccinimide (NHS) were purchased from Acros Organics (Geel, Belgium). β-propiolactone was purchased from Alfa Aesar (Ward Hill, MA). N-[3-(Dimethylamino)propyl] acrylamide (DMAPA, 98%) was purchased from TCI America (Portland, OR). Pooled human plasma was purchased from Biochemed Services (Winchester, VA). Human monoclonal antibody against the activated leukocyte cell adhesion molecule (anti-ALCAM), human polyclonal anti-ALCAM, and human recombinant ALCAM/Fc chimera (105 kDa) were purchased from R&D Systems (Minneapolis, MN). Antibody to thyroid stimulating hormone (anti-TSH) and TSH antigen (29 kDa) were purchased from ThermoFisher Scientific (Waltham, MA). Antibody to β-human chorionic gonadotropin (anti-hCG) and hCG antigen (37 kDa) were purchased from Scripps Labs (San Diego, CA). Water was purified using a Millipore water purification system with a minimum resistivity of 18.2 MΩ cm. Mercaptoundecyl bromoisobutyrate (SI-ATRP initiator) was synthesized as described previously.[51]

3.2.2 Synthesis of Carboxybetaine Acrylamide Monomer

The synthesis of (3-Acryloylamino-propyl)-(2-carboxy-ethyl)-dimethyl-ammonium (CB) is shown in **Figure 3.1**. It was synthesized by reacting 48 mL of DMAPA with 25 g of β-propiolactone in 400 mL of anhydrous acetone at 0°C under nitrogen. After removing the ice bath at 20 min, the solution was allowed to warm up to room temperature. After 6 h, the product was filtered, washed with ether, and dried under vacuum. The rough product, was re-dissolved in a 30% (v/v) triethylamine in methanol solution and stirred overnight. After concentrating the solution, the CB was precipitated with acetone and filtered. The white solids were suspended in acetone and ether, for 1 h each, filtered, dried under vacuum, and stored at 4°C. Yield: 61%. H'NMR (Bruker 500MHz, DMSO-d6): 8.61 (t, 1H,N-H), 6.28 (t, 1H, CHH=C*H*), 6.13 (t, 1H, CH*H*=CH), 5.61 (t, 1H, C*H*H=CH), 3.44 (t, 2H, N-CH_2-CH_2-COO), 3.21 (m, 4H, NH-CH_2-CH_2-CH_2), 2.97 (s, 6H, N-(CH_3)2), 2.25 (t, 2H, CH_2-COO), 1.87 (t, 2H,NH-CH_2-CH_2- CH_2).

3.2.3 Preparation of pCB Films

The preparation of pCB films is shown in **Figure 3.2**. Initiator self-assembled monolayers on SPR chips were prepared by soaking the UV-cleaned gold-coated substrate in 0.1 mM mercaptoundecyl bromoisobutyrate in pure ethanol overnight. The chips were then removed, rinsed with ethanol, THF, and ethanol, and blown dry using filtered compressed air and placed into a custom glass tube reactor. In a separate glass tube, 8.86 mg CuBr, 57.87 mg bpy, and 600 mg of CB were added. Both tubes were then placed under nitrogen protection. Nitrogen purged methanol (3.6 mL) and water (0.4 mL) were then added to the solids. Once everything completely dissolved (~ 15 min), the mixture was then transferred to the reactor and allowed to react for 3 h at 25°C in a shaker. The chips were then removed and rinsed with water and submerged overnight in PBS. The pCB film thickness was about 15 – 20 nm measured via ellipsometry as reported previously.[52]

3.2.4 SPR Imaging Sensor and Substrates

SPR imaging sensor chips were made of a glass slide coated with titanium film (~2 nm) followed by a gold film (~48 nm) using an electron beam evaporator. The SPR imaging sensor used was based on the Kretschmann geometry of the attenuated total reflection method and prism coupling with intensity self-referencing and polarization contrast developed at the Institute of Photonics and Electronics (Prague, Czech Republic) as described previously.[53] The sensor consists of a monochromatic LED light source (centered at 750 nm) made incident onto the attached chip in which the reflected light is imaged on a two-dimensional CCD detector. The intensity of the reflected light is dependent upon the strength of coupling and can be correlated to the distribution of local refractive index along the gold film. As each pixel in the CCD image represents an individual measurement of intensity, the SPR imaging sensor allows for spatially resolved label-free measurements in real-time. It is equipped with a two-channel flow-cell, temperature control for sample delivery, an LED temperature and intensity stabilizer, and uses a peristaltic pump for delivering liquid samples.

3.2.5 Micro-contact printer

The micro-contact printer used in this work was a Spotbot 2 personal arrayer purchased from TeleChem International (Sunnyvale, CA, U.S.A). The arrayer was equipped a sampling station (382-well microplate), a wash station with pump, a dry station with air compressor, a robot for positioning contact printing pins, and a humidity controller. The system was equipped with a Stealth Microspotting Pin (SMP8) capable of producing ~265 μm size spots. Programming of the robot for printing had a 1 micron resolution.

3.2.6 Protein Arrays on pCB coated substrates

The pCB chips were removed from the PBS storage solution, rinsed with water, and then dried using filtered air. The carboxylic acid groups were then activated by submerging the chip in an aqueous solution of 0.05 M NHS and 0.2 M EDC for 7 min. The substrate was removed, rinsed with water, dried and placed into the micro-contact printer. Antibody solutions were then added to the arrayer 382-well sampling station at the desired protein concentration, buffer, buffer concentration, and pH. For pH and concentration studies, anti-hCG with a pI ~6.8 was used.[54] Following printing, the spotted proteins were allowed to react for 1 hour at 70% humidity and room temperature. The chip was then deactivated in a solution of 10 mM sodium carbonate and 300 mM NaCl at pH 10 (SCNa) for 10 min to hydrolyze unreacted NHS esters and remove non-covalently bound protein. Following washing with water and drying, the substrate was loaded onto the SPR imaging sensor.

In order to quantitatively characterize and provide a statistical analysis of the uniformity/morphology of the printed antibody spots on pCB films, a new variable termed “spot variation” was introduced. The “spot variation” was defined as the standard deviation in intensity of a spot divided by the mean of the spot. A larger value corresponds to poor spot morphology (e.g., the presence of holes, bright spots, etc. within the spot) and vice versa. This statistical analysis was enabled by using the software program, ImageJ.

3.2.7 Measurements of Specific and Non-specific Protein Adsorption and Antibody Cross-Reactivity

Following the attachment of the pCB antibody array onto the SPR imaging sensor, the areas corresponding to each protein spot as well as the non-functionalized background spots were identified using PBS running buffer. Each identified spot then underwent a three point refractive index (RI) calibration consisting of PBS, PBS plus 0.4% (w/w) NaCl, and PBS plus 0.8% (w/w) NaCl exhibiting

solution refractive indices of 1.3500, 1.35050, and 1.35120 RI units (RIU), respectively. After reestablishing the buffer baseline, antigen spiked PBS, antigen spiked undiluted human plasma, or undiluted plasma was injected for 10 min followed by PBS. The non-specific or specific protein adsorption was then calculated as the difference between buffer baselines and converted to mRIU (10^{-3} RIU) which enabled comparison between different experiments as well as individual protein spots. Due to ALCAM being naturally present in human blood,[55] the cross-reactivity experiments were analyzed as the difference in response between spiked (1 µg/mL) and non-spiked plasma injections.

ALCAM was used as a model system for demonstrating the LOD achievable with the pCB array platform in both *direct* and sandwich assay formats. Here, ALCAM was injected into undiluted human plasma at 0, 1, and 10 ng/mL (1000 ng/mL was also used for the *direct* assay) and flowed over a pCB substrate spotted only with anti-ALCAM. After washing with buffer, polyclonal anti-ALCAM (5 µg/ml in PBS) was then injected for 10 min followed by rinsing with buffer. The direct detection of ALCAM was calculated as the difference between the initial PBS baseline and the buffer wash before amplification and converted to mRIU. The amplified signal was calculated as the difference in PBS baselines before and after the injection of polyclonal anti-ALCAM and converted to mRIU. The LOD was determined as the lowest spiked response greater than one standard deviation from a blank plasma control. All error bars correspond to a single standard deviation.

3.3 Results and Discussion

The strategy for demonstrating the array capabilities of pCB coated substrates is shown in **Figure 3.3**. There were several key features in this process. First, the formation of NHS-esters upon the activation of pCB transforms the film from superhydrophylic to slightly hydrophobic. This was important for achieving uniform antibody spot morphology without having the protein solution wet out on the chip, as would occur for the un-activated and superhydrophylic zwitterionic film.[56] Furthermore, activation also produces a slight positive charge on the surface. Thus, spotting the antibodies at a pH greater than the

isoelectric point of the protein offers the most efficient approach for immobilization as it takes advantage of favorable electrostatic interactions. Subsequent deactivation using a basic buffer removes un-reacted NHS-esters on the non-spotted pCB background and non-covalently attached antibody.[20,57]

3.3.1 Antibody Printing Conditions

Standard pin-spotting arrays are well known to be influenced by a number of variables including buffer type and concentration, protein concentration, humidity, temperature, and the addition of additives among others.[58] Hence, the appropriate conditions for establishing uniform and biologically active antibody spots on pCB substrates was first determined. Shown in **Figure 3.4a**, as the antibody solution pH increased, the amount and uniformity of the antibody spot also increased (seen as brighter and a more uniform redness, respectively). This result was further confirmed via quantitative analysis with the "spot variation" variable (**Figure 3.5**) as the lowest spot variations (i.e., the best morphology) was achieved at the highest solution pH. This was expected due to the slight positive charge on the pCB surface following activation.[20,57] For these experiments, anti-hCG (pI ~6.8)[54] was used. Thus, the higher the antibody solution pH (from 8 – 12), the more negatively charged the protein, thus providing more favorable electrostatic interactions and higher and more uniform immobilization levels. In order to verify the biological activity for each condition, antigen spiked into PBS (1 µg/mL) was then injected into the sensor. The increasing response to antigen with pH confirmed the observed trends with the immobilization levels and also indicated stable and functional antibodies. **Figure 3.4a** also exhibited the "coffee ring" morphology for the lower pH conditions. This well-known and frequently observed effect with arrays is attributed to micro advection as each tiny droplet dries. This results in small concentration gradients and the enrichment of molecules near the outer edge of each spot as the liquid evaporates which can greatly affect the subsequent bioactivity (molar ratio of antigen binding to antibody immobilized) of the attached antibody and may have reduced the antigen response for the lower pH conditions.[59]

The effect of antibody concentration was also investigated as shown in **Figure 3.4b**. As one would suspect, the larger protein content enabled higher immobilization levels and improved morphology, which subsequently gave larger antigen responses. This was also confirmed via the "spot variation" variable (**Figure 3.6**). A comparison of **Figure 3.4a**, made using 100 mM sodium carbonate (SC) with an antibody concentration of 1 mg/mL, with that of **Figure 3.4b**, made using 100 mM boric acid (BA) at a pH of 10, also shows the effect of the different buffers on the pCB array platform. The pH 10 SC antibody spot resulted in more uniform and complete morphology compared to the pH 10 BA spot. Based on the "coffee-ring" effect described above, this may be attributed to differences in viscosity of the two buffers which affected the rate of evaporation of the water. Regardless, due to the ability of 100 mM sodium carbonate pH 11 and 12 to enable excellent spot morphology, high immobilization levels, and the highest biological activity of the attached antibody, without the use of additives (e.g., glycerol), both conditions were used for the remainder of this work. A typical SPR image is shown in **Figure 3.7** which consists of 144 antibody spots (~265 μm) on a pCB sensor chip. Complete removal of non-covalently bound antibody during the immobilization procedure with SCNa was confirmed via achieving a stable PBS baseline prior to running any detection assays.

The ability to achieve excellent spot morphology on pCB is crucial for its application to high – throughput protein analysis from undiluted complex media. The statistical analysis of antibody spotting for the three antibodies on pCB films is shown in **Figure 3.8** using the "spot variation" variable. This data shows the median spot variation with error bars representing the 95% confidence interval, each maximum and minimum with representative antibody images. As presented, the median variation for all three antibodies fell near the lower confidence interval indicating that most antibody spots have consistently good morphology, but also with outliers of poor morphology due in part to image artifacts (see image insets at top of bars in **Figure 3.8**). Achieving similar median variations amongst all three antibodies further implies small differences between the individual proteins thus demonstrating consistent spotting between different ligands. Taken together, these results indicate the ability of pCB films to achieve the desired spot morphology which is necessary for highly sensitive analyte detection.

3.3.2 pCB Protein Array Non-fouling Properties and Antibody Cross-Reactivity

Arrays consisting of three antibodies, each printed in a row of six spots per channel as shown in **Figure 3.7**, were then used to evaluate the non-specific protein adsorption. Six non-functionalized background spots were also used. The post-functionalized antibody spots and the non-functionalized pCB background had fouling levels of 0.092 ± 0.048 mRIU and 0.056 ± 0.004 mRIU, respectively. These correspond to protein surface coverage values of ~9 ng/cm^2 for each antibody spot and ~6 ng/cm^2 for the background, indicating very low non-fouling properties of the functionalized film.[13] The raw data presented in protein surface coverage units is shown in **Figure 3.9**. As a comparison, *in situ* antibody functionalized OEG-OH/COOH self assembled monolayers showed ~100 ng/cm^2 of fouling to undiluted human plasma thus indicating the ability of pCB films to create an array platform with low background noise.[20]

Arrays consisting of three antibodies on the pCB coated substrates were then subjected to individual solutions of each single antigen spiked into undiluted human plasma (1 µg/mL) to evaluate the cross-reactivity of the corresponding antibodies. Due to the natural presence of ALCAM in human plasma (~ 84 ng/mL),[55] these results were compared to un-spiked plasma and the results are shown in **Figure 3.10**. Both hCG and TSH are also naturally present in blood but with negligible concentrations.[60,61] The plots indicate little cross-reactivity between individual antigens and the three corresponding immobilized antibodies, an analysis enabled by the low post-functionalized non-fouling properties of the pCB array (0.092 ± 0.048 mRIU). Noteworthy, due to the very high viscosity of human plasma (relative to typical PBS buffer solutions), a gasket configuration which gradually increased to the size of the channel from the liquid injection port in the SPR imaging sensor flow cell was required in order to achieve uniform results across all 6 spots in each row. Such design enables nearly all types of solutions or media to be used for analysis.

3.3.3 pCB Protein Array Detection from Undiluted Human Plasma

In order to take advantage of the low fouling properties on the pCB antibody arrays for enabling high throughput and sensitive detection of multiple analytes, the limit of detection was then demonstrated using the cancer biomarker ALCAM. This analyte was chosen due to the ability to compare the result to previous reports in which the protein was detected from undiluted human plasma but using *in situ* functionalized pCB substrates with spectroscopic SPR sensors.[20] Here, anti-ALCAM was spotted onto the pCB substrate and used for evaluating the sensitivity. After establishing an initial PBS baseline, ALCAM spiked undiluted human plasma was injected into the SPR imaging sensor followed by washing with buffer. The LOD for the *direct* detection of ALCAM was found to be 10 ng/mL (**Figure 3.11**) which was comparable to that achieved from buffer using the pCB protein array (LOD of 10 ng/mL) as well as with pCB films and spectroscopic SPR sensors and *in situ* antibody immobilization (LOD of 7.8 ng/mL)[20]. These results indicate that the sensitivity of the pCB array is not affected by the media used (i.e., buffer versus plasma) due to its low fouling properties, and that SPR imaging can achieve comparable sensitivity to conventional SPR sensors and with high throughput capabilities. The LOD on the pCB array platform is also a five-time improvement in sensitivity over the detection of ALCAM from diluted plasma samples with antibodies immobilized onto an oligo-ethylene glycol self assembled monolayer.[13] In order to improve the sensitivity and further verify the non-fouling background, a sandwich assay was then performed in which polyclonal anti-ALCAM in PBS (5 µg/mL) was injected to amplify the binding signal following the PBS buffer wash. The results for blank, 1 ng/mL, and 10 ng/mL of ALCAM spiked into undiluted human plasma are shown in **Figure 3.12** which indicate a LOD of 1 ng/mL. The use of antibody amplification was able to increase the sensitivity by about one order of magnitude compared to direct detection. Importantly, no detectable signal of polyclonal anti-ALCAM was observed on the background pCB spots thereby verifying the protein resistant properties. While only a model system of ALCAM/Anti-ALCAM was used for determining the limit of detection from undiluted human plasma, similar results would be expected for other antigen-antibody pairs, thereby demonstrating the significant

advantage of low fouling pCB protein array platforms for high throughput and sensitive detection of multiple analytes.

3.4 Conclusions

Using a SPR imaging biosensor, a novel protein array platform based on zwitterionic CB was shown to be a single directly functionalizable and unblocked polymer film capable of the sensitive detection of target analytes from undiluted human blood plasma. It was found that the antibody immobilization and antigen binding capacity both increased with the solution pH and the antibody concentration. The optimal conditions, 100 mM sodium carbonate at pH 11 or 12 without additives and a protein concentration of 750 µg/mL, enabled 144 antibody spots with excellent morphology which was attributed to the increase in hydrophobicity following pCB activation. Following deactivation, low post-functionalized fouling (9 ng/cm^2) was demonstrated for the first time from undiluted human plasma for a protein array. Subsequent experiments with spiked plasma revealed little cross-reactivity between three immobilized antibodies. The LOD achieved using direct detection from undiluted plasma with the pCB array (10 ng/mL) was comparable to that achieved with pCB substrates with *in situ* antibody immobilization and spectroscopic SPR sensors (7.8 ng/mL). The use of antibody amplification for the array further improved the sensitivity to 1 ng/mL. Collectively, these illustrate the unique properties of pCB surface chemistry for achieving sensitive detection directly from undiluted human plasma and its successful integration with a high throughput SPR imaging device. The 144 spots demonstrated here serve only as an example of this technology which can be readily extended to thousands or more printed proteins. Furthermore, the relatively low pCB film thickness (15 – 20 nm) makes this platform adaptable to other biosensing devices in addition to SPR. Taken together, the results indicate the great potential of pCB protein arrays as a simple and convenient platform capable of achieving a high S/N, a large analyte response with low background noise, from undiluted complex media which is necessary for numerous biomedical applications.

3.5 Figures

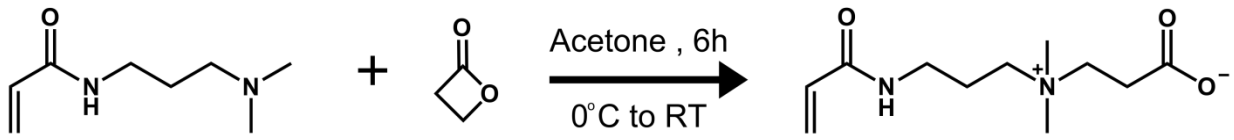

Figure 3.1. Synthesis of CB monomer.

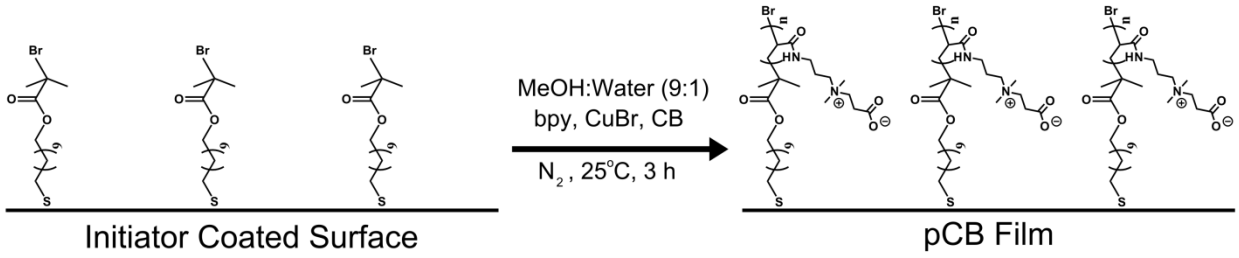

Figure 3.2. Preparation of pCB films.

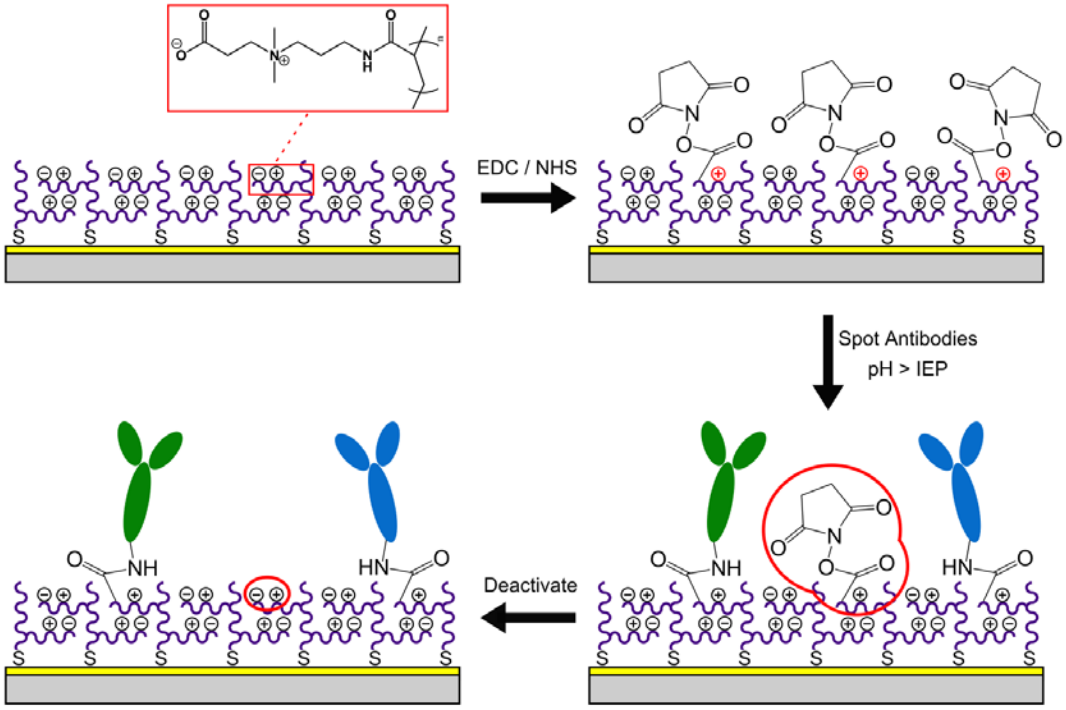

Figure 3.3. The immobilization strategy for the formation of antibody arrays on pCB coated substrates.

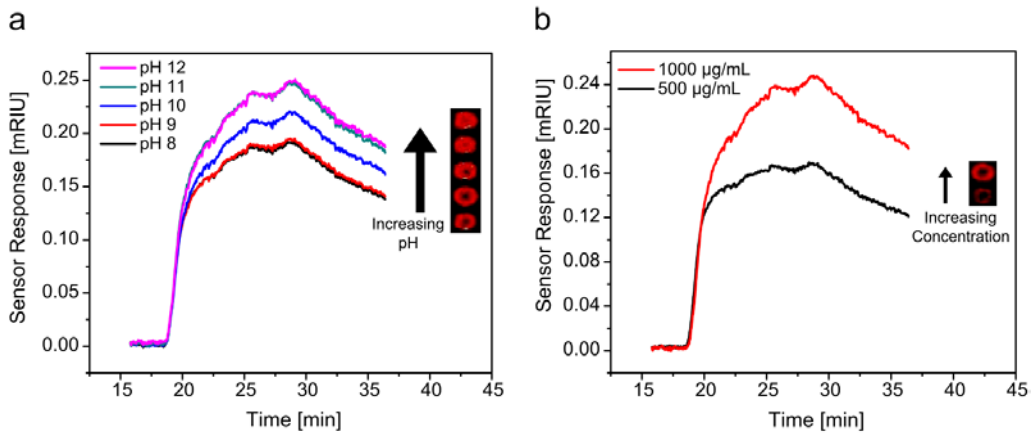

Figure 3.4. The effect of antibody solution pH (a) and concentration (b) on the immobilization level and the subsequent ability to detect antigen spiked into PBS (1 µg/mL). Here, increasing brightness corresponds to larger levels of covalent antibody attachment. Spot size is ~ 265 µm. Anti-hCG with a pI ~6.8 was used for these studies. The time-dependent behavior exhibited in (a) and (b) is described as follows: after establishing a baseline using running buffer, a solution of antigen spiked PBS was flowed over the surface. Antigens were then specifically captured by the immobilized antibody resulting in an increase in the sensor response. Upon injecting running buffer, antigen is dissociated from the antibody and the response decreases.

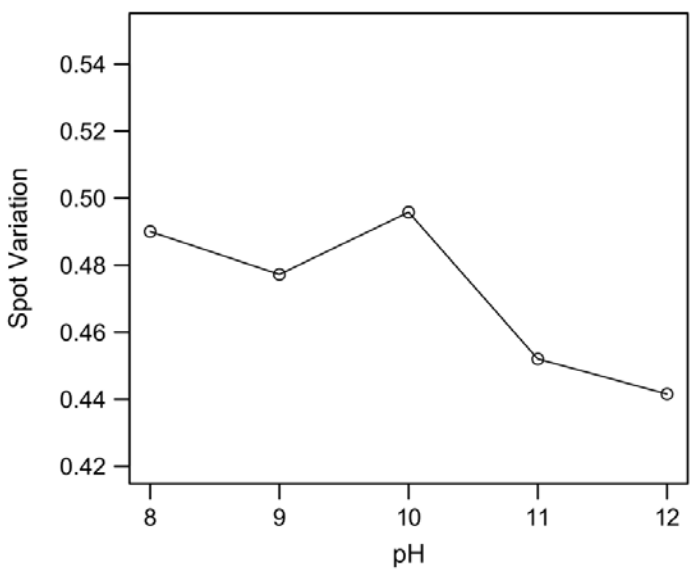

Figure 3.5. Spot variation of printed antibodies on pCB films as a function of the antibody solution pH used for immobilization. "Spot variation" is a variable used to represent the antibody spot uniformity/morphology. Spot variation is defined as the standard deviation in intensity of a spot divided by the mean of the spot. A larger value corresponds to poor spot morphology (e.g., the presence of holes, bright spots, etc. within the spot) and vice versa. Here, anti-hCG (pI ~6.8) was printed onto pCB films using 100 mM sodium carbonate buffer at several pH values. As the pH increased from 8 – 12, anti-hCG became increasingly more negative. As a positive charge is introduced onto the pCB film following the activation step, increasing the solution pH used for immobilization should lead to an increase in antibody spot uniformity due to favorable electrostatic interactions. As shown here, increasing the immobilization pH generally improved the antibody spot variation with the best spot morphology found at pH 11 and 12.

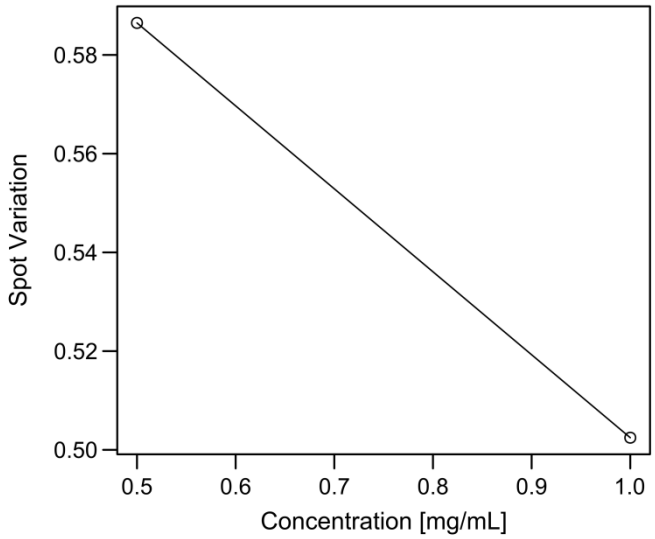

Figure 3.6. Spot variation of printed antibodies on pCB films as a function of the antibody concentration in the solution used for immobilization. “Spot variation” is a variable used to represent the antibody spot uniformity/morphology. Spot variation is defined as the standard deviation in intensity of a spot divided by the mean of the spot. A larger value corresponds to poor spot morphology (e.g., the presence of holes, bright spots, etc. within the spot) and vice versa. Here, anti-hCG was immobilized at 0.5 and 1.0 mg/mL using 100 mM boric acid buffer at a pH of 10. As shown, increasing the antibody concentration improved the antibody spot variation leading to better morphology.

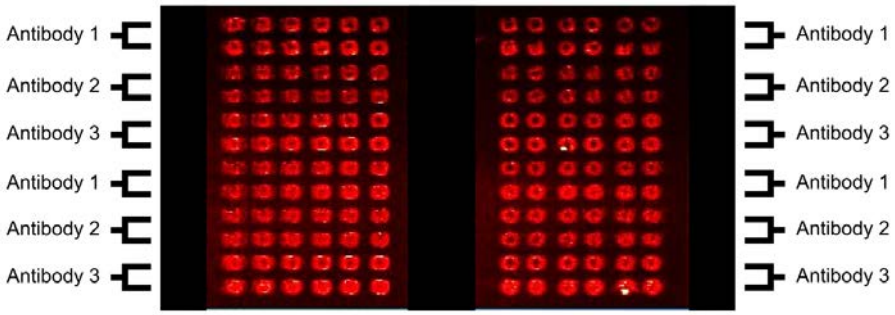

Figure 3.7. A typical SPR image consisting of 144 spots (~265 µm diameter) made with three antibodies printed onto a pCB sensor chip. The proteins (750 µg/mL) were spotted using 100 mM sodium carbonate buffer pH 11 and 12 for the top and bottom rows, respectively, for each indicated antibody. The spots were allowed to react for 1 hour at 70% humidity and room temperature before deactivating the entire chip with SCNa. The SPR image shows two channels (left and right) which are identical replicates.

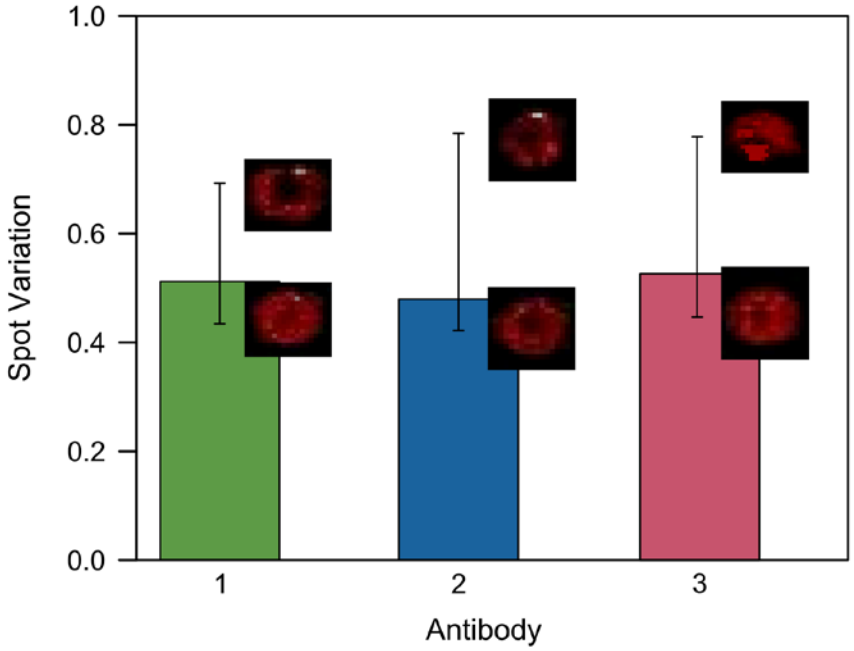

Figure 3.8. Spot variation for three antibodies printed on pCB films using 100 mM sodium carbonate buffer pH 11 and 12 with an antibody concentration of 0.75 mg/mL. “Spot variation” is a variable used to represent the antibody spot uniformity/morphology. Spot variation is defined as the standard deviation in intensity of a spot divided by the mean of the spot. A larger value corresponds to poor spot morphology (e.g., the presence of holes, bright spots, etc. within the spot) and vice versa. This analysis shows the median spot variation with error bars representing the 95% confidence interval, each maximum and minimum with representative antibody images. The asymmetric error bars are due to the skewed distribution of spot variation. As shown, the median variation for all three antibodies fell near the lower confidence interval indicating that most antibody spots have consistently good morphology, but also with outliers of poor morphology due in part to image artifacts (see image insets at top of bars). Achieving similar spot variation amongst all three antibodies demonstrates that the spotting is consistent even amongst different ligands.

Top of Substrate

6.1	5.3	5.3	5.5	5.3	6.1
16.5	11.9	11.5	11.4	12.4	11.6
13.7	8.8	8.2	8.5	8.3	9.4
11.2	9.4	9.0	10.2	16.7	20.2
10.4	7.9	8.0	7.9	19.2	31.0
10.0	8.5	7.7	7.6	10.4	12.1
10.8	9.4	8.4	7.6	14.7	27.6
8.6	6.6	7.0	8.0	9.4	13.1
7.0	6.0	6.0	5.9	7.3	9.3
7.8	5.6	5.5	5.6	6.2	9.0
6.7	5.1	4.7	4.7	5.2	6.4
6.5	4.6	4.5	5.8	6.0	7.8
7.4	5.0	5.0	4.7	5.8	8.0

Bottom of Substrate

Figure 3.9. The non-fouling raw data (ng/cm^2) for antibody arrays printed on pCB films being exposed to undiluted human plasma (flowed from the top to the bottom of the substrate). Each number outside the red box indicates the fouling level for an individual antibody spot. The red box represents the non-functionalized pCB background. The averaged post-functionalized antibody spots and the non-functionalized pCB background had fouling levels of ~9 ng/cm^2 and ~6 ng/cm^2, respectively.

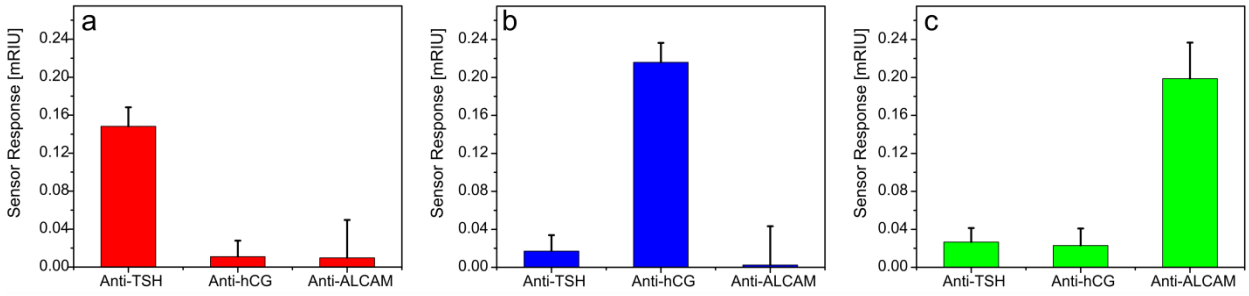

Figure 3.10. The sensor response to the corresponding antigen spiked into undiluted human plasma (1 μg/mL) for three antibodies immobilized on a pCB substrate. (a) The response from TSH spiked plasma. (b) The response from hCG spiked plasma. (c) The response from ALCAM spiked plasma. These results are the average across six different spots for each individual antibody (with all three antibodies being present the pCB substrate) and are relative to a blank plasma injection due to the natural presence of ALCAM in human blood (~84 ng/mL). A low level of cross-reactivity was observed, an analysis enabled by the low post-functionalized non-fouling properties of the pCB array. Error bars represent one standard deviation.

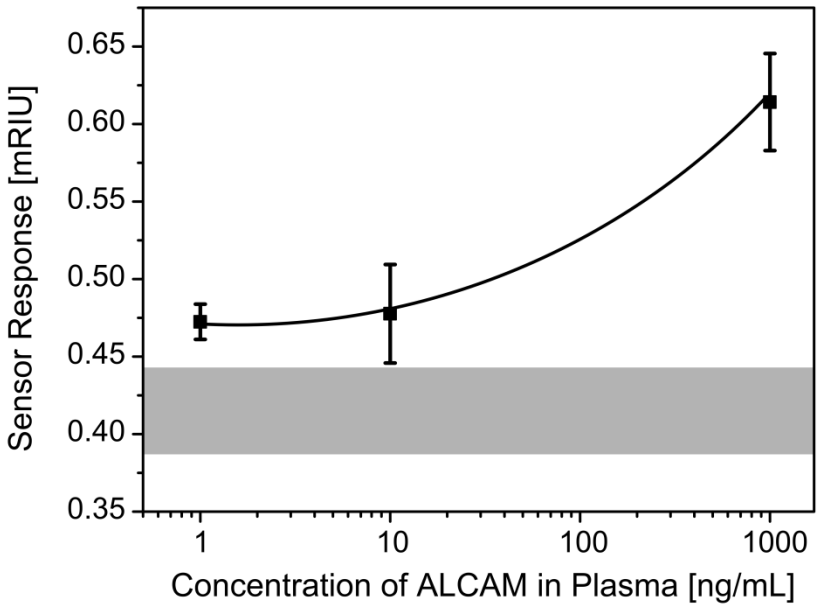

Figure 3.11. The detection curve for the *direct* detection of ALCAM spiked into undiluted human plasma using antibody arrays on pCB films, indicating a limit of detection (LOD) of ~10 ng/mL. The grey box represents the response to un-spiked plasma. The grey box and error bars for each concentration represent one standard deviation which was used to determine the LOD. The blank plasma response was relatively high due to the natural presence of ALCAM in human blood (~84 ng/mL). The curve was added to guide the eye.

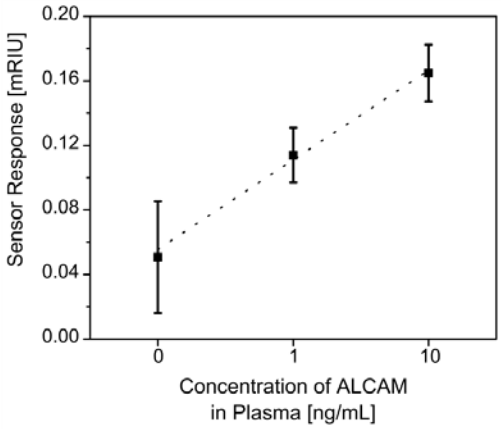

Figure 3.12. The sandwich assay sensor response for ALCAM spiked into undiluted human plasma. Polyclonal anti-ALCAM was used for amplification resulting in a limit of detection of 1 ng/mL. A linear plot was fitted to the data to serve only as a guide. Error bars represent one standard deviation which was used to determine the LOD.

Chapter 4

Two Layer Architecture using Atom Transfer Radical Polymerization for Enhanced Sensing and Detection in Complex Media

A novel two-layer hierarchical architecture based on surface-initiated atom transfer radical polymerization was investigated. It combines a thin and highly dense first layer, for non-fouling properties, with a loose second layer, for high immobilization levels of active biomolecules. Sodium azide treatment, to reduce the concentration of macro-initiators on the first layer for re-initiation, and by controlling the polydispersity allowed one to achieve three polymer architectures with low, moderate, or high azide substitution. Moderate substitution enabled the highest immobilization levels with a non-fouling background. Integration with dual-functional zwitterionic poly(carboxybetaine) made this platform suitable for applications in undiluted complex media such as blood. It was demonstrated via a surface plasmon resonance biosensor that antigen accessibility and antibody loading were greatly improved. These results indicate the two layer strategy as a generic concept suitable for applications from diagnostics to medical coatings in order to maximize and minimize specific and non-specific responses, respectively.

4.1 Introduction

The development and implementation of new point-of-care diagnostic devices, drug delivery platforms, and therapeutics has the potential to offer significant benefits to the health of society.[62-64] However, the realization of this concept relies on both the discovery of biomarkers, which allow a given disease to be identified and monitored, as well as the development of assays which can be used for actual detection. Due to the ease of accessibility as well as the ability to represent dynamic physiological and

abnormal processes, human plasma and serum are the most common sources for biomarker analysis.[6] However, the lack of a means to sensitively detect these target analytes, at or below nanogram/milliliter quantities, buried in the comprehensive proteome of human blood (thousands of core proteins which span more than 10 orders of magnitude in concentration) has severely hindered the biomarker development process due to the inability to fully verify the analyte as being clinically relevant.[65-67]

The two major short comings which limit biomarker validation include high rates of false-positives and a lack of sensitivity.[7,8] False-positives are typically a result of the inability to prevent non-specific protein adsorption thereby resulting in a high background noise leading to an incorrect diagnosis.[10] The lack of sensitivity arises from the limited immobilization capacity of molecular recognition elements (e.g., antibodies) which can bind the target of interest. The combined result of these two factors is the inability to achieve a high signal to noise ratio (S/N) which is necessary for detection. While protein resistant materials have been utilized to aid in the reduction of background noise, attempts to circumvent the lack of sensitivity have almost solely relied on signal amplification.[17,68] However, this methodology requires the use of two antibodies or ligands (e.g., ELISA) per target analyte. The expense and difficulty of manufacturing large amounts of high affinity and specific antibodies (or ligands), in addition to their limited stability, make this a non-viable approach for detection of analytes.[8]

Surface grafted polymer films composed of zwitterionic carboxybetaine (CB) have been shown to be highly attractive materials for protein resistant applications.[17] These films exhibit ultra low fouling properties to undiluted human serum and plasma (i.e., < 5 ng/cm^2 of non-specific protein adsorption) and possess abundant functionalizable groups which enable antibody immobilization via amino-coupling chemistry. Following deactivation, poly(CB) (pCB) returns to its original zwitterionic state and allows for the sensitive detection of target analytes from undiluted complex media.[20,63] However, such 2-dimensional (2D) films have the limitation of a low ligand immobilization capacity (i.e., only an effective monolayer of protein ($\sim$ 250 ng/cm^2) can be achieved).[20,57] Substrates based on carboxymethylated-dextran commonly used on Biacore sensor chips have been shown to enable more than 1000 ng/cm^2 of antibody immobilization due to a "loose" 3-dimensional (3D) polymer structure.[69] However, such a loose

architecture is naturally susceptible to large amounts of non-specific adsorption from undiluted complex media, such as human plasma and serum, thereby severely limiting its use in real-world applications.[70]

An additional approach to improve antibody grafting mobility, density, and activity has focused on developing a living radical photo-polymerization surface chemistry with acrylated whole antibodies. In these works, substrates were first photo-polymerized from a mixture of urethane and triethylene glycol diacrylates, initiator, and deactivator and then re-initiated in the presence of acrylated antibody and a poly(ethylene glycol) (PEG) monoacrylate, which was necessary to resist non-specific protein adsorption. The mobility and surface coverage of the grafted antibody could be controlled by adjusting the concentration of re-initiating species on the substrate or the antibody polymerization solution composition. This platform was shown to increase accessibility of the antigen binding sites and enhance detection. However, this approach achieved only low levels of covalently attached antibody (1 – 2 ng/cm^2) and could only undergo detection using diluted complex media at 20% (v/v).[71,72]

We have recently demonstrated a novel two layer architecture with pCB as shown in **Figure 4.1**.[73] This hierarchical architecture involves the combination of a thin and highly dense first layer to provide ultra low fouling properties from undiluted human plasma with a loose and controlled second layer to enable high levels of antibody immobilization (i.e., multiple monolayers) and improved antigen detection. This integration of the 2D with the 3D to create a novel yet generic approach to biosensing can be used to achieve high sensitivity without the need for signal amplification. These initial experiments (**Figure 4.1**) utilized the controlled radical polymerization, surface initiated atom transfer radical polymerization (SI-ATRP). For proof-of-concept experiments, only one single condition was chosen in order to illustrate the two layer concept.

Here, a systematic investigation of the individual parameters associated with the SI-ATRP approach was performed. As this method relies on azide treatment of the bottom layer for controlling the second layer graft density, this work investigated the effect of azide treatment (i.e., looseness of the top layer), the second layer polymerization rate (i.e., the polydispersity or polymer density), as well as alternative conditions for growing the initial bottom layer, as a function of the antibody immobilization

capacity, antigen binding, and non-fouling properties to undiluted human serum using a surface plasmon resonance (SPR) biosensor. While SPR with pCB was chosen here, due to the ideal dual-functional properties of pCB for sensing and detection in complex media, the conclusions of this work can be readily applied to many other platforms and surface chemistries.

4.2 Experimental Section

4.2.1 Materials

Copper(I) bromide (99.999%), 2,2'-bipyridine (bpy, 99%), tetrahydrofuran (THF), methanol, 4-(2-hydroxyethyl)-1-piperazineethanesulfonic acid (HEPES), phosphate buffered saline (PBS, 0.01 M phosphate, 0.138 M sodium chloride, 0.0027 M potassium chloride, pH 7.4), anhydrous acetone, and triethylamine were purchased from Sigma-Aldrich (St. Louis, MO). Ethanol (200 Proof) was purchased from Decon Laboratories (King of Prussia, PA). Sodium carbonate anhydrous and sodium azide were purchased from EMD Chemicals (Darmstadt, Germany). Sodium chloride (NaCl) and ether were purchased from J.T. Baker (Phillipsburg, NJ). Sodium acetate anhydrous was purchased from Fluka (subsidiary of Sigma Aldrich, St. Louis, MO). 1-Ethyl-3-(3-dimethylaminopropyl) carbodiimide hydrochloride (EDC) and N-hydroxysuccinimide (NHS) were purchased from Acros Organics (Geel, Belgium). β-propiolactone was purchased from Alfa Aesar (Ward Hill, MA). N-[3-(Dimethylamino)propyl] acrylamide (DMAPA, 98%) was purchased from TCI America (Portland, OR). Pooled human serum was purchased from Biochemed Services (Winchester, VA). Water was purified using a Millipore water purification system with a minimum resistivity of 18.2 MΩ cm. Mercaptoundecyl bromoisobutyrate (SI-ATRP initiator) was synthesized as described previously.[51]

Monoclonal antibody to human thyroid stimulating hormone (anti-TSH) and recombinant human TSH antigen were purchased from ThermoFisher Scientific (Waltham, MA). According to the manufacturer, anti-TSH is an IgG antibody produced in mice whose specificity was verified using ELISA,

a radio-immuno-assay, and an immuno-precipitation assay while also showing reactivity with human samples. The concentration of TSH in normal human serum is ~0.1 ng/mL.[74]

4.2.2 Synthesis of Carboxybetaine Acrylamide Monomer

(3-Acryloylamino-propyl)-(2-carboxy-ethyl)-dimethyl-ammonium (CB) was synthesized by reacting 48 mL of DMAPA with 25 g of β-propiolactone in 400 mL of anhydrous acetone at 0°C under nitrogen. After removing the ice bath at 20 min, the solution was allowed to warm up to room temperature. After 6 h, the product was filtered, washed with ether, and dried under vacuum. The rough product was re-dissolved in a 30% (v/v) triethylamine in methanol solution and stirred overnight. After concentrating the solution, the CB was precipitated with acetone and filtered. The white solids were suspended in acetone and ether, for 1 h each, filtered, dried under vacuum, and stored at 4°C. Yield: 61%. H'NMR (Bruker 500MHz, DMSO-d6): 8.61 (t, 1H,N-H), 6.28 (t, 1H, CHH=C*H*), 6.13 (t, 1H, CH*H*=CH), 5.61 (t, 1H, C*H*H=CH), 3.44 (t, 2H, N-CH_2-CH_2-COO), 3.21 (m, 4H, NH-CH_2-CH_2-CH_2), 2.97 (s, 6H, N-(CH_3)2), 2.25 (t, 2H, CH_2-COO), 1.87 (t, 2H,NH-CH_2-CH_2- CH_2).

4.2.3 Preparation of Two Layer pCB Films

SPR chips coated with initiator self-assembled monolayers were prepared by soaking the gold-coated substrates in 0.1 mM mercaptoundecyl bromoisobutyrate in pure ethanol for overnight. The chips were then removed, rinsed with ethanol, THF, and ethanol, and blown dry using filtered compressed air and placed into a custom glass tube reactor. In a separate glass tube, 8.86 mg CuBr, 57.87 mg bpy, and 600 mg of CB were added. Both tubes were then placed under nitrogen protection. Nitrogen purged methanol (4 mL) was then added to the solids. Once everything completely dissolved (~ 15 min), the mixture was then transferred to the reactor and allowed to react for 24 h at 25°C in a shaker. The reaction

was removed and quenched with a solution containing methanol (4 mL) and $CuBr_2$ (275.87 mg). The chips were then rinsed with methanol, water, and submerged in PBS.

To adjust the concentration of bromine groups and replace them with non-reactive azide moieties, the chips were submerged in an aqueous solution of sodium azide (6.5 mg/mL) and mixed at room temperature. After a specific time, the chips were removed, dipped in PBS, rinsed with water, dried, and the placed into the glass reactor for re-initiating ATRP. The second layer was then grown by repeating the above protocol and adjusting only the solvent ratio between nitrogen purged methanol and water. For example, a water content of 20% consisted of 0.8 mL of water and 3.2 mL of methanol. The re-initiated polymerization was allowed to react for 3 h at 25°C in a shaker. Following the reaction the chips were rinsed with copious amounts of water and then submerged overnight in PBS.

4.2.4 SPR Sensor, Chips, and Calibration of the Surface Sensitivity

A laboratory SPR sensor developed at the Institute of Photonics and Electronics, Prague, Czech Republic was used as described previously.[57] This custom built SPR is based on the attenuated total reflection method and wavelength modulation. It is equipped with a four-channel flow-cell, temperature control, and uses a peristaltic pump for delivering samples. SPR sensor chips were made of a glass slide coated with titanium film (∼2 nm) followed by a gold film (∼48 nm) using an electron beam evaporator. Since the SPR sensitivity depends on the distance of the binding event from the SPR active surface, the sensor response due to the polymer films had to be calibrated. This was done using previously described methods.[20]

4.2.5 Determination of Polymer Film Thickness, Refractive Index, and Polymer Density

Film thicknesses and refractive index measurements were determined using a multi-wavelength ellipsometer (J. A. Woollam Co., Inc., Model alpha-SE). A liquid cell with a volume of 0.5 mL supplied

by the manufacturer was used for obtaining the liquid measurements. The data was analyzed via fitting a Cauchy model for a bare SPR substrate which enabled the film thickness and refractive index to be simultaneously determined. The wet and dry refractive index measurements were then used with the effective medium approximation for calculating the polymer volume fraction (i.e., the polymer density) as described previously.[52] The data presented are the average values and one standard deviation of three independent measurements.

4.2.6 Measurements of Non-specific Protein Adsorption

The non-specific protein adsorption of the pCB films was determined with a SPR biosensor using a flow rate of 50 μL/min at 25°C. After first establishing a baseline using PBS, undiluted human serum was flowed for 10 min, followed by buffer to reestablish the baseline. Protein adsorption was quantified as the difference between buffer baselines and converted to a surface coverage using the appropriate sensitivity factor.

4.2.7 In situ Functionalization of pCB Polymer Surfaces

The functionalization procedure was monitored step-by-step in real time using an SPR sensor at 25°C. Sodium acetate buffer (10 mM) at pH 5.0 (SA) was first injected at 30 μL/min to obtain a stable baseline. Carboxylate groups of the polymer surface were then activated by flowing a solution of 0.05 M NHS and 0.2 M EDC in water for 7 min. Followed by a brief injection of SA buffer, anti-TSH (50 μg/mL) in HEPES buffer (pH 7.5) was flowed for 20 min at 20 μL/min. Subsequent washing for 10 min with 10 mM sodium carbonate (pH 10) containing 0.3 M NaCl (SC) at 30 μL/min removed non-covalently bound ligands and deactivated residual NHS-esters. SA buffer was then used to reestablish a

stable baseline. The amount of immobilized antibody was determined as the difference between the SA injection following EDC/NHS activation and the final baseline. The data representing antibody surface coverage as a function of the azide exposure time show the average values and one standard deviation of three independent measurements.

4.2.8 Measurements of Post-Functionalized Non-fouling and Specific Protein Activity

Following antibody immobilization, the pCB surface was washed with PBS until a steady baseline was established at 50 μL/min and 25°C. For post-functionalized non-fouling, undiluted human serum was injected for 10 min followed by PBS. The net adsorption was calculated as the difference between buffer baselines and converted to a surface coverage. Antigen detection for each polymer film was compared by measuring the maximum sensor response achieved for a fixed injection time. After establishing an initial buffer baseline, PBS spiked with TSH at 1000 ng/mL was flowed through the sensor for 10 min followed by buffer. The antigen binding was calculated as the difference between the original buffer baseline and the maximum signal observed, which was then converted to a surface coverage using the appropriate sensitivity factor. The data representing antigen detection as a function of the azide exposure time show the average values and one standard deviation of three independent measurements.

4.3 Results and Discussion

The strategy for developing the novel two layer architecture via SI-ATRP for sensing and detection in complex media as well as the polymerization scheme is shown in **Figure 4.2**. SI-ATRP was used due to its ability to provide excellent control over polymer growth. Additionally, the “living” characteristic enabled by the reversible equilibrium between active and dormant species allows for the formation of block copolymers due to the presence of initiating species which cap the chain ends upon

stopping the polymerization.[75] The use of this hierarchical architecture enables one to achieve a thin and highly dense first layer to provide ultra low fouling properties with a loose second layer for high levels of antibody immobilization. The combined result of these two factors enables the high S/N necessary for enhanced detection sensitivity.

As shown in **Figure 4.2A**, the concentration of re-initiating groups (i.e., bromines) on the surface is vital for controlling the second layer graft density. The bromine end groups can be reduced by reacting with an aqueous sodium azide solution to elicit a dramatic effect on the architecture of the subsequent two layer film as well as its biosensing performance. This termination forms a stable azide group which remains dormant and non-reactive as the second polymerization takes place.[76,77] Both the concentration and reaction time of sodium azide can affect the degree of termination resulting in surfaces which are low, moderately, or highly substituted with azide moieties. A low degree of substitution will result in most chains being re-initiated thus maintaining a relatively high polymer density and allowing for only monolayer antibody immobilization. For polymer chains to grow vertically, they require a certain graft density to stretch away from the surface. However, if they are too dilute then the chains will preferentially grow laterally in a mushroom configuration or along the surface.[78] In this highly substituted and very dilute case, the second layer will be thin, consisting of a small number of long chains with minimal surface area for antibody immobilization, also resulting in a low loading capacity. Therefore, in order to achieve high antibody loading, a moderate amount of substitution is desired. In this scenario, the chains will be close enough to be obliged to grow vertically but dilute enough so as to maximize the polymer surface area for achieving high protein functionalization and enable sufficient diffusion of the ligand to reactive NHS-esters. It is also important to note that a second layer grown from a moderately substituted bottom layer can grow longer (i.e., thicker) than from a low azide substituted film. This is due to a reduction in bimolecular termination as a result of more space between the growing polymer chains in addition to the polymerization rate.[39]

In this work, a systematic investigation of the individual parameters associated with the SI-ATRP approach was performed. In order to achieve the best control over the second layer graft density,

conditions for growing the bottom layer which maximized the number of re-initiating sites and enabled ultra low fouling polymer brushes were first investigated. Next, the effect of azide treatment (i.e., looseness of the top layer) and the second layer polymerization rate (i.e., the polydispersity or polymer density) were studied as a function of the antibody immobilization capacity, antigen binding, and non-fouling properties to undiluted human serum using a SPR biosensor.

4.3.1 First Layer Growth Conditions

It was previously shown that thin (~ 10 nm) and highly dense pCB films made via SI-ATRP from pure methanol as the solvent can maintain ultra low fouling properties to undiluted human serum.[52] The ability to minimize the final overall thickness of the two layer film is also crucial for SPR detection among other sensing platforms. For SPR, this is due to a rapid decrease in sensitivity as the measured biomolecular interaction gets further from the SPR active gold surface.[79] Hence, pure methanol, due to its ability to obtain ultra low fouling thin films while minimizing chain-chain termination events, was also used in this work. This, when combined with the use of quenching (i.e., spiking the reaction solution with a high concentration of deactivator (e.g., $CuBr_2$)) to stop the polymerization, was vital for providing the maximum number of re-initiating sites and controlling the second block graft density.[80]

The effect of polymerization times (0.5 – 24 hrs) for the bottom layer was first investigated. It was found that 24 hrs resulted in the thickest second layer, the highest antibody immobilization, and excellent functionalized and non-functionalized protein resistance to undiluted human serum (**Table 4.1** and **Figure 4.3**). The response to antigen was similar for all first layer polymerizations greater than or equal to 1 h, with bioactivity ratios (i.e., the molar ratio of antigen to antibody) of 0.98, 0.92, and 0.82 for reaction times of 1, 2, and 24 h, respectively. The similar antigen responses combined with the 24 h result having the lowest bioactivity ratio, even though it had the highest antibody loading, illustrates that both antibody immobilization as well as antigen accessibility are important for achieving the high S/N necessary for sensitive detection. The 24 h reaction enabled the same level of antibody immobilization on

the two layer film as that achieved from a single layer grown using a 50% water content (~290 ng/cm^2). A first layer made using a 50% water content was also explored (**Figure 4.4**). However, this condition was very difficult to control, even with short reaction times on the order of just a few min, resulting in the final two layer polymer structure being mostly determined by the rapid polymerization of the bottom layer. Furthermore, simply spiking solutions grown from a first layer of either 50% water or pure methanol with a high concentration of monomer dissolved in pure nitrogen purged water was also not found to be effective. Due to the ability to achieve ultra fouling properties for the two layer films with a 24 hr first layer polymerization time, such conditions were then used throughout the remainder of this work.

4.3.2 Azide Treatment and Antibody Immobilization

As shown in **Figure 4.2A**, the use of azide substitution can result in three hierarchical architectures. The effect of azide treatment on the second layer polymer thickness and corresponding antibody immobilization for two different second layer solvent conditions is shown in **Table 4.2** and **Figure 4.5**, respectively. Due to the significant influence of water on the polymer density of SI-ATRP films,[52] two concentrations were used. A 10% and 50% water content was chosen for slower (more controlled) and faster (less controlled but more polydisperse) polymerizations, respectively.[36,52] As shown in **Table 4.2** and **Figure 4.5**, both conditions resulted in the expected trends as discussed above for **Figure 4.2A**. A reduction in the concentration of re-initiating species generally lead to an increase in the film thickness which then decreased as the chains became more dilute. It was also observed that as the second layer thickness increased, the antibody immobilization also increased. As a moderately diluted second layer should result in the thickest film, this indicates that such films have more surface area (i.e., more accessible NHS-esters) available for protein attachment and hence azide treatment can be used to maximize antibody immobilization due to its effect on both the thickness (i.e., the chain length) and chain density of the second layer. However, as the chains became more dilute (i.e., more azide substitution), the

available surface area decreased along with the immobilization. As shown in **Figure 4.5**, the highest level of immobilization achieved was ~ 440 ng/cm^2, which was significantly more than that achieved for a single layer film grown from pure methanol (~210 ng/cm^2) or a 50% water content (~290 ng/cm^2).[73] While the ability to achieve high levels of antibody loading is important, it must also be balanced with the ability to allow sufficient diffusion of the desired target analyte into the film for providing a large sensor response as well as the ability to reduce background noise arising from non-specific adsorption.

4.3.3 Azide Treatment and Antigen Response

The antigen response for azide exposure times of 0, 60, and 120 min for films made using second layer water contents of 10% and 50% is shown in **Figure 4.6**. For second layers grown using 10% water content, an effective monolayer of antibody was achieved for all exposure times and hence all films gave similar antigen responses. The two layer film made from 50% water content and a 0 min azide exposure time exhibited the smallest level of immobilization and hence provided the smallest amount of antigen binding. Interestingly, the antigen binding for the 60 min exposure time was significantly less than that for 120 min despite the higher level of antibody loading for the former (i.e., a lower bioactivity ratio). For these experiments, PBS spiked with 1 µg/mL TSH was flowed over the surface for a fixed time of 10 min. For all experiments except the 60 min exposure time with a 50% second layer water content, the 10 min time period was sufficient to nearly saturate antigen binding. Thus, while the result for the 60 min case shown in **Figure 4.6** does not represent the fully saturated value, which would be larger, it does imply that the polymer density of the second block is higher relative to the 120 min exposure time. This indicates that the ability of the antigen to diffuse through the film was more restricted compared to the 120 min film which would be expected as the azide substitution reaction time increased. As a reference, a single layer pCB film made via pure methanol with ~ 210 ng/cm^2 of antibody immobilization gave a response of ~39 ng/cm^2.[73]

Importantly, a comparison of **Table 4.2** with **Figure 4.5 and 4.6** reveal that while the thickest film did enable the highest degree of antibody immobilization, it did not enable the best detection due to the inability of the target analyte to rapidly diffuse through the film. Hence, these results indicate that there must be a balance between azide treatment, second layer thickness (i.e., chain length), and antibody immobilization level in order to achieve the best detection. While antibody immobilization and antigen accessible are important for achieving a high sensor signal, the amount of sensor noise or protein fouling can significantly influence the limit of detection. Thus, the non-fouling properties of the two layer films were subsequently investigated.

4.3.4 Azide Treatment and Fouling to Undiluted Human Serum

The non-specific protein adsorption from undiluted human serum as a function of azide exposure time is shown in **Figure 4.7**. All cases except the 60 min azide time with a second layer grown from 10% water content resulted in excellent functionalized and non-functionalized protein resistant properties with most being at or below ultra low fouling levels. This also indicates that the azide moiety itself does not affect the protein resistant properties of the film. Due to the natural concentration of TSH in human serum being very low, ~0.1 ng/mL,[74] the low post-functionalized serum fouling results (typically < 5 ng/cm^2) shown in **Figure 4.7** also demonstrates that the response to 1 μg/mL of TSH spiked into PBS (up to 75 ng/cm^2, **Figure 4.6**) was due to only specific binding with the immobilized antibody.

However, a relatively high fouling result achieved with a second layer water content of 10% following a 60 min azide treatment was observed. This can be simply explained as a highly azide substituted film with long and dilute second layer polymer chains. Evidence for this explanation is provided by the SPR sensor-grams (**Figure 4.8**) which compare this film with a typical response (**Figure 4.8**, 50% water) which was observed for all but one other two layer films in this work. As shown in **Figure 4.8**, the film made from 10% water content revealed both faster binding during the antibody immobilization step as well as a larger decrease in response upon the injection of deactivation buffer.

Zwitterionic pCB films take on a slight positive charge following EDC/NHS activation.[20] This forces the long and dilute chains for the 10% water condition to extend from the surface due to charge-charge repulsion. Using an immobilization buffer pH of 7.5, anti-TSH maintains a partial negative charge. Thus, the charge interaction between the surface and protein will result in a rapid accumulation of antibody near the surface due to easily accessible and dilute polymer chains. These two effects are illustrated in **Figure 4.9**. However, for the 10% water condition, the limited accessible polymer surface area of these chains prevents most of the protein from being covalently bound. Upon deactivation, the surface regains its zwitterionic backbone and as a result the proteins are washed away which can be seen as a large drop in the SPR response upon injection of the deactivation buffer (**Figure 4.8**). It is believed that this particular conformation of collapsed polymer chains may increase the hydrophobicity of the surface by exposing more of the polymer backbone and thereby lead to the observed increase in fouling.

It is important to note that due to the combination of abundant carboxylate groups in pCB films which become activated with NHS-esters and the presence of numerous primary amines on antibodies, there is the potential for cross-linking between polymer chains to occur via binding to multiple sites on the protein, if the chains are too close together (i.e., not “loose” enough). A significant amount of cross-linking would drastically reduce antibody immobilization levels and also worsen the ability to detect antigen, due to fewer antibody receptors being present as well as restricted diffusion throughout the film. This was resolved with the two layer approach via reducing the density of the second layer so as to achieve far enough spacing between polymer chains which minimizes the potential for cross-linking while maximizing the surface area available for immobilization. Due to achieving high immobilization levels for both second layer films made using 50% water content for azide exposure times of 60 and 120 min as mentioned above for **Figure 4.6**, it is unlikely that a significant amount of cross-linking occurred. Hence, the significant increase in the antigen response combined with ultra low fouling properties indicates that this novel architecture has the potential to dramatically enhance diagnostic device performance. The ability of the azide group to react with terminal bromines was important for controlling

the “looseness” of the two layer films. However, adjusting the second layer polymerization rate (i.e., the polydispersity or polymer density) also influenced the film properties.

4.3.5 Effect of Second Layer Polymerization Rate

Due to the ability of the water concentration to significantly affect the rate of the ATRP reaction and the subsequent polymer density, the amount of water for the second layer polymerization was varied from 0 – 90% using a 60 min azide treatment time as this condition enabled the highest antibody immobilization.[52] The functionalized and non-functionalized serum fouling, antibody immobilization, and antigen response are shown in **Figure 4.10**. A peak of the antibody immobilization was found for the 50% water condition. Further investigation of these films by calculating the polymer volume fraction (PVF) in PBS (i.e., the wet polymer density) found that this particular condition had an effective PVF of ~ 25% where as all others films except for those made using a 0% water content second layer, had a PVF of ~ 43% (**Figure 4.11**). A lower value for PVF indicates a more dilute polymer film. Hence, based on PVF alone, the film made using a 50% water content would be expected to yield the highest level of immobilization due to having the most “loose” structure. All second block thicknesses for each condition are shown in **Table 4.3**. Note that the film made using a 0% water second layer condition resulted in a lower thickness in PBS than in air which could be indicative of its slightly hydrophobic character and explain the correspondingly high fouling result.

The two layer films made from 20-50% water all resulted in excellent non-fouling properties, had the highest level of immobilization, and also had the highest second layer thickness, again illustrating the trend from **Figure 4.2A**. It is believed that the two layer films made from 0% water content grew a very small second layer due to the limited solubility of the highly dense first layer polymer brush in pure methanol, resulting in few polymer chains actually being reinitiated. Additionally, the significantly low level of immobilization (~100 ng/cm^2) indicates that very few functionalizable groups were accessible. This could interpreted as laterally grown polymer chains covering the surface, interacting via ion-pairing

intermolecular interactions, thereby resulting in the presence of the hydrophobic acrylamide backbone being exposed on the surface thus resulting in high fouling.

Beyond the 50% water condition, the films appear to be much more affected by the balance between the improved solubility at higher water concentrations, which improves accessibility of the terminal ends of the bottom layer, with the loss of control in the ATRP reaction.[39] The 60% water condition resulted in a similar SPR response during immobilization as for the 10% water case and thus it is probable that a similar phenomenon, long and dilute chains, occurred as illustrated by its SPR sensorgram (**Figure 4.8**). However, increases in chain-chain termination reactions as a result of the loss of control are likely to have further reduced the effective area for immobilization. The 90% water result was attributed to a significant presence of radical recombination reactions with the same but more pronounced negative consequences as for the film made using 60% water. With an exception of the two extreme endpoints (films made using 0% and 90% water contents), the similar antigen response corresponds with the expected result for 2D surfaces (~ 39 ng/cm^2), with the 50% case simply having a low rate of diffusion as discussed above.

4.4 Conclusions

The two major short comings which severely limit biomarker validation and the advancement of personalized medicine include high occurrences of false-positives, from non-specific binding, and a lack of sensitivity, due to low ligand loading. In this work, a unique two layer architecture made via SI-ATRP with zwitterionic dual-functional pCB was investigated. This strategy consists of a highly dense and ultra low fouling bottom layer with a loose second layer to enable high antibody immobilization. In this work it was found that the polymerization of the bottom layer had a significant effect on the final film structure and conditions to maximize the number of re-initiating terminal sites was vital for control over the second layer graft density. For SI-ATRP with pCB, this was accomplished using pure methanol as the solvent. Using azide treatment to adjust to the polymer density of the second block resulted in three distinct

conformations of the polymer architecture (i.e., with low, moderate, and high substitution). Moderate substitution enabled the highest antibody immobilization, twice that compared to single layer films, with excellent non-fouling properties to undiluted human serum. The results also indicated that antibody immobilization in addition to accessibility is vital for detecting the target analyte and hence for providing the highest possible S/N. The second layer film structure could be further modified by adjusting the water content in the SI-ATRP reaction hence providing more control over the film architecture. The ideal properties of pCB integrated with this novel architecture offer the ability to significantly improve detection abilities from undiluted complex media. In summary, these results indicate the two layer strategy as a generic concept suitable for applications from diagnostics to medical coatings in order to maximize and minimize specific and non-specific responses, respectively.

4.5 Tables

Table 4.1. Effect of the first layer SI-ATRP reaction time using pure methanol as the solvent on the corresponding second layer thickness achieved using a 50% water content. The data presented are the average values and one standard deviation of three independent measurements.

Reaction Time [hr]	**Second Layer Thickness [nm]**
0.5	0.10 ± 0.09
1.0	2.92 ± 0.40
2.0	3.54 ± 0.90
24.0	5.61± 1.08

These results show that the largest second layer thickness can be achieved via a bottom polymer layer made by reacting in pure methanol for 24 hours. This condition provides a sufficiently dense first layer with the maximum number of terminal bromines available for the subsequent second block polymerization.

Table 4.2. Affect of azide exposure time on the second layer polymer thickness for second blocks grown using SI-ATRP water contents of 10% and 50% (v/v).

Azide Exposure Time [min]	**Second Layer Thickness [nm] (10% Water)**[a]	**Second Layer Thickness [nm] (50% Water)**[a]
0	4.6 ± 1.7	5.6 ± 1.1
15	8.8 ± 1.5	3.4 ± 0.4
30	3.1 ± 0.5	6.8 ± 0.1
60	1.7 ± 0.1	13.8 ± 0.4
120	2.5 ± 0.5	9.9 ± 0.7

[a]The thickness of the first layer was ~6 nm.

Table 4.3. Second layer film thicknesses as a function of the SI-ATRP water concentration using 60 min azide treated films. The data presented are the average values and one standard deviation of three independent measurements.

ATRP Water Content [%]	**Second Layer Thickness [nm]** **(1 hr Azide)**
0	0.9 ± 0.3
10	1.7 ± 0.1
20	13.2 ± 1.0
40	11.8 ± 1.0
50	13.8 ± 0.4
60	2.9 ± 1.3
90	1.1 ± 0.1

4.6 Figures

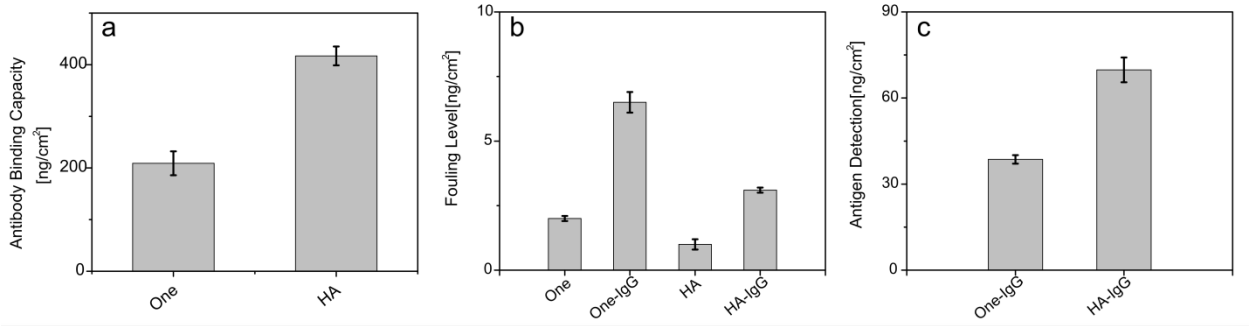

Figure 4.1. (a) Antibody binding capacity for films with one-layer (One) and hierarchical (HA) structures prepared via SI-ATRP. (b) Fouling levels in the presence of undiluted human plasma, before and after IgG immobilization. (c) Antigen detection from PBS.

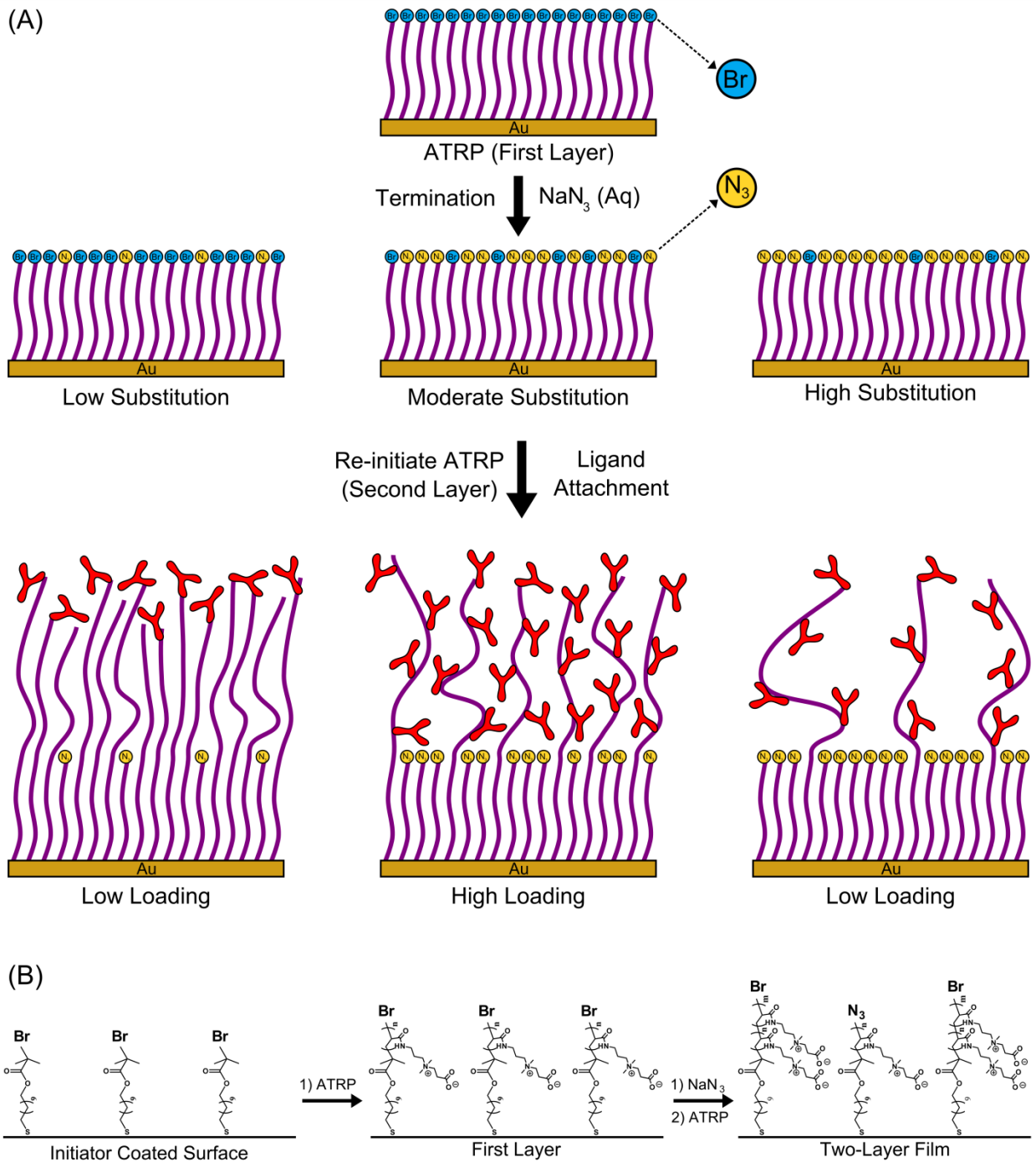

Figure 4.2. (A) A novel strategy for improving sensing and detection from undiluted complex media using unique "two layer" architecture integrated with zwitterionic dual-functional pCB via SI-ATRP. (B) The polymerization scheme for the "two layer" pCB films.

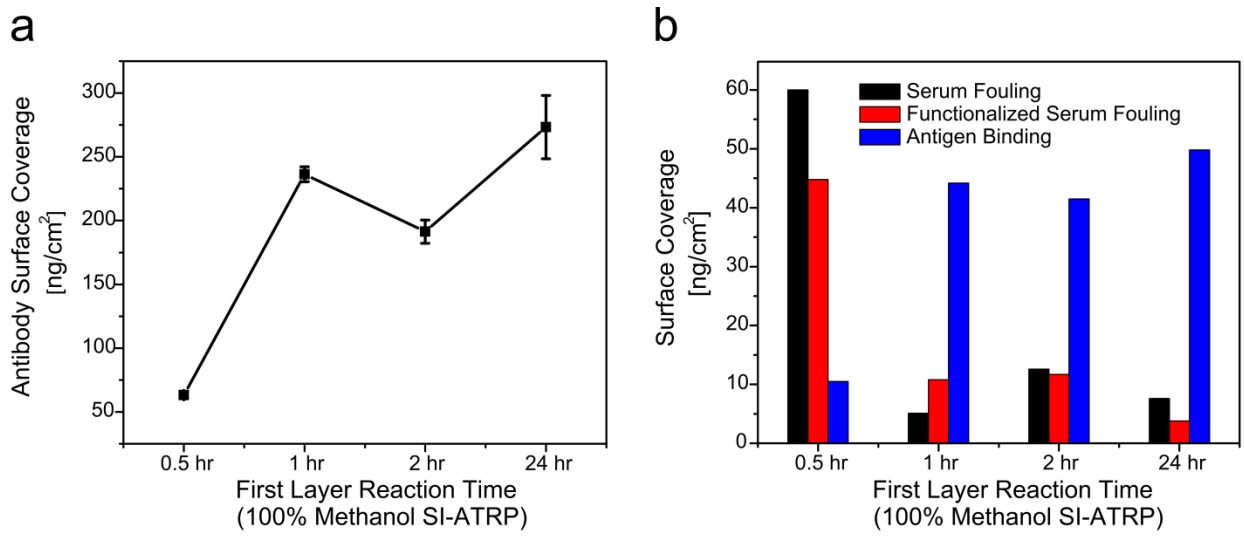

Figure 4.3. (a) The antibody immobilization as a function of the first layer reaction time using pure methanol as the polymerization solvent and a 50% water content for the second layer. The data presented are the average values and one standard deviation of three independent measurements. (b) The corresponding fouling data to undiluted human serum and antigen response. These results indicate that the best immobilization and fouling results were obtained using a first layer reaction time of 24 hours. For comparison, a single layer made using pure methanol achieved an immobilization level of ~ 210 ng/cm^2 with similar fouling levels. The 24 hour condition enabled the formation of a dense bottom layer (to resist protein adsorption) followed by a polydisperse second layer to achieve the highest level of immobilization which is almost identical to that achieved with a single layer film made using 50% water content. The response to antigen was similar for all reactions greater than or equal to 1 hour, with bioactivity ratios (i.e., the molar ratio of antigen to antibody) of 0.98, 0.92, and 0.82 for reaction times of 1, 2, and 24 hours, respectively. The similar antigen responses combined with the 24 hour result having the lowest bioactivity ratio (even though it had the highest antibody loading) illustrates that both antibody immobilization as well as antigen accessibility is important for achieving highly sensitive detection.

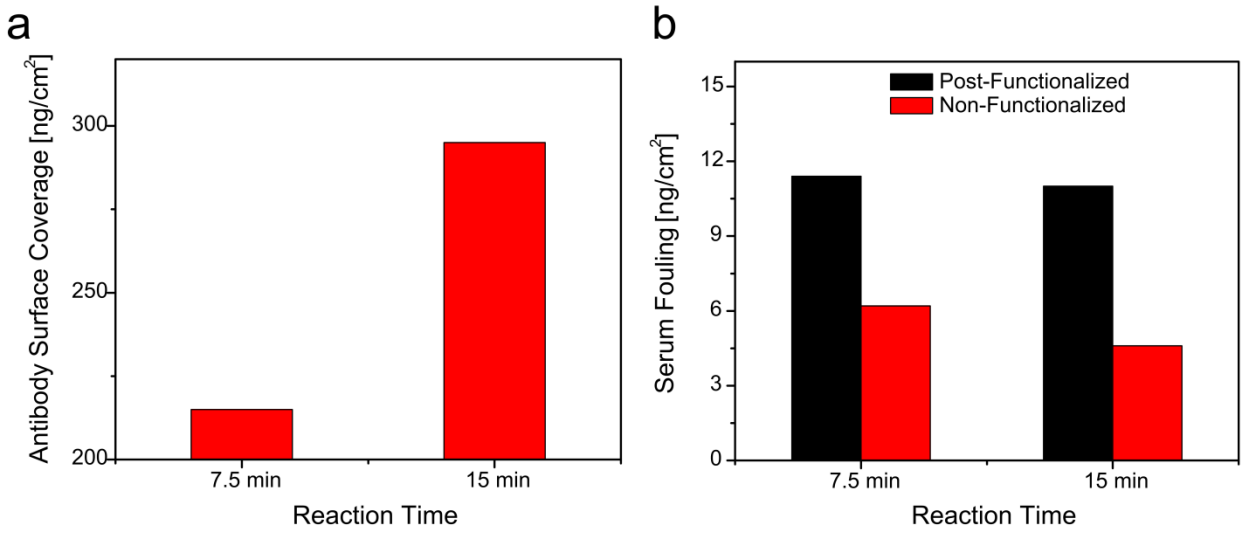

Figure 4.4. (a) The antibody immobilization for two layer films grown using a first layer SI-ATRP water content of 50% for 7.5 and 15 minutes. These films had second layers grown using 80% and 90% water contents, respectively. (b) The corresponding fouling to undiluted human serum for the functionalized and non-functionalized films. For comparison, a single layer made using a 50% water content achieved an immobilization level of ~ 290 ng/cm^2, ~14 ng/cm^2 of post-functionalized fouling and ~2.0 ng/cm^2 of non-functionalized fouling to undiluted human serum. These results indicate that the 50% water content of the first layer mostly determines the final polymer structure of the two layer film due to the very fast rate of polymerization under this condition.

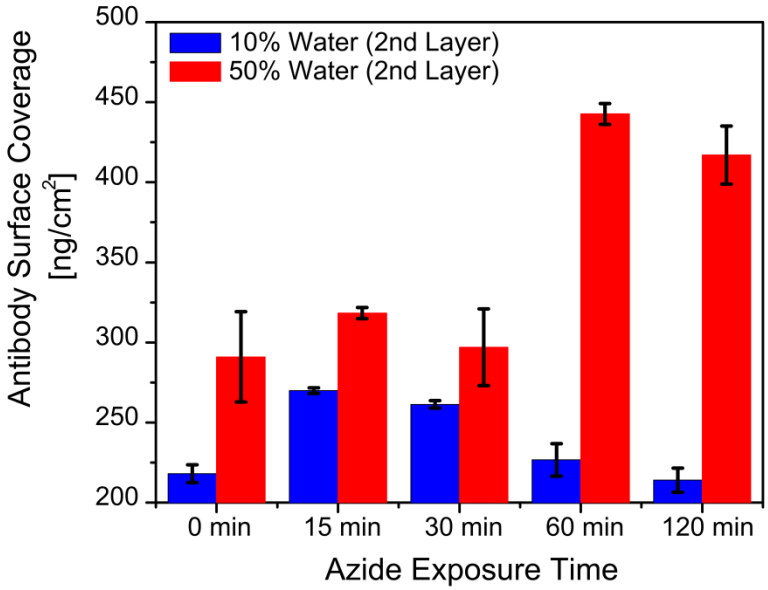

Figure 4.5. Antibody immobilization versus azide exposure time for two layer pCB films grown using SI-ATRP water contents of 10% and 50%.

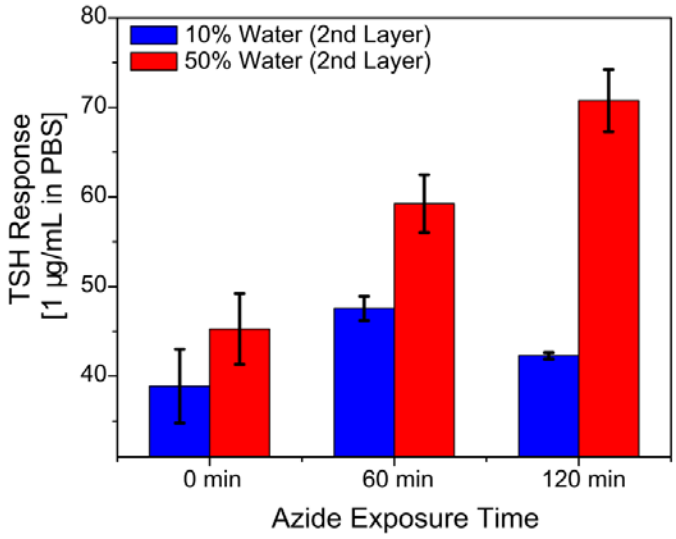

Figure 4.6. A comparison of the antigen responses versus azide exposure time for second layers made using 10% and 50% water contents. PBS spiked antigen (1 µg/mL) was flowed for a fixed time of 10 min.

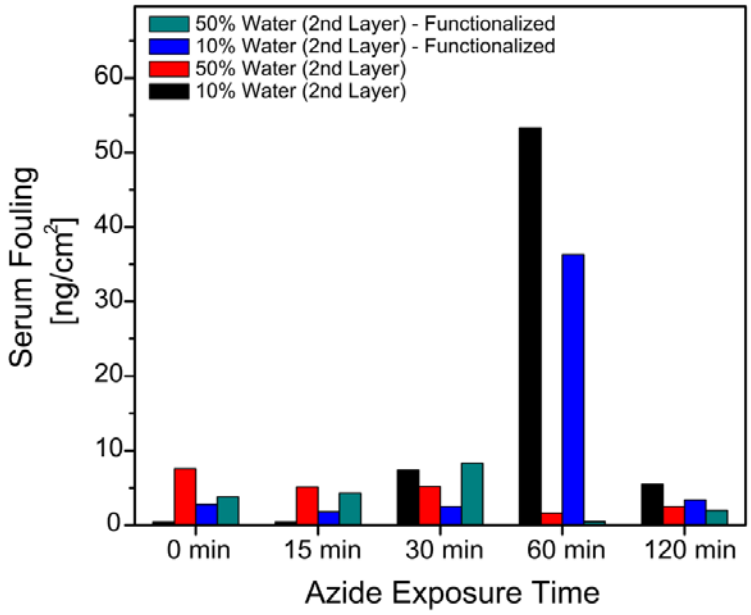

Figure 4.7. Fouling to undiluted human serum versus azide exposure time for second layer films made using 10% and 50% water content.

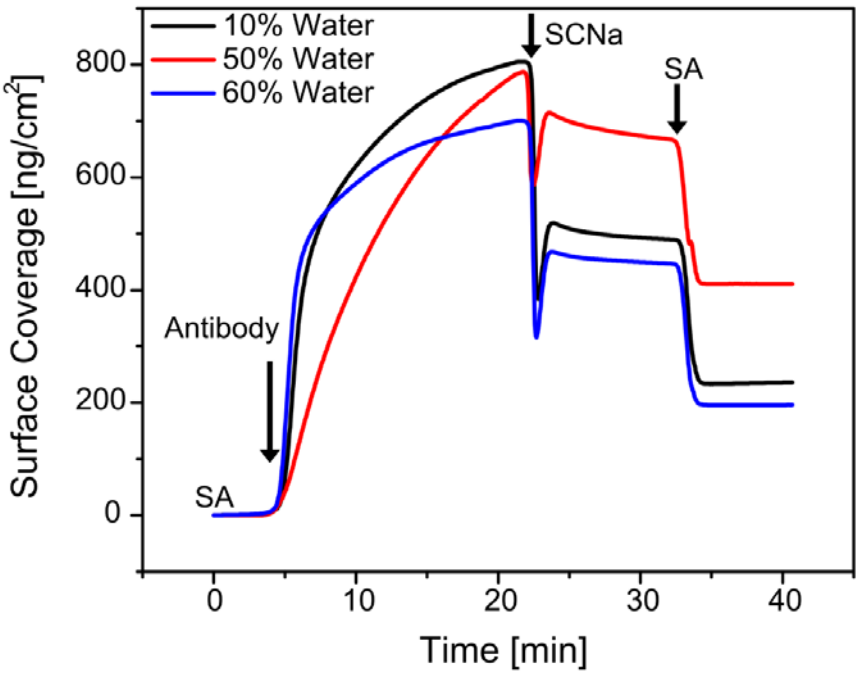

Figure 4.8. Representative SPR sensor-grams for two-layer films grown using 10%, 50% and 60% water content following a 60 min azide exposure time. Antibody immobilization was calculated as the difference between the SA buffer baselines. Two key differences were observed when comparing the unique 10% and 60% water content results with a typical sensor-gram (50% water) which was observed for all other experiments in this work. The former two show faster antibody binding kinetics which quickly saturate. Furthermore, upon injection of the deactivation buffer, a much larger drop in the SPR response was also observed. Such characteristics are indicative of long and dilute polymer chains making up the second layer for these two conditions. Following EDC/NHS activation, the surface takes on a slight positive charge forcing the "loose" chains to extend. Upon deactivation of the surface, which returns the polymer to its original zwitterionic state, a large amount of attracted but non-covalently bound antibody is washed away as the chains collapse due to the small surface area of polymer available for attachment, thus resulting in a larger drop in the SPR response and lower immobilization levels.

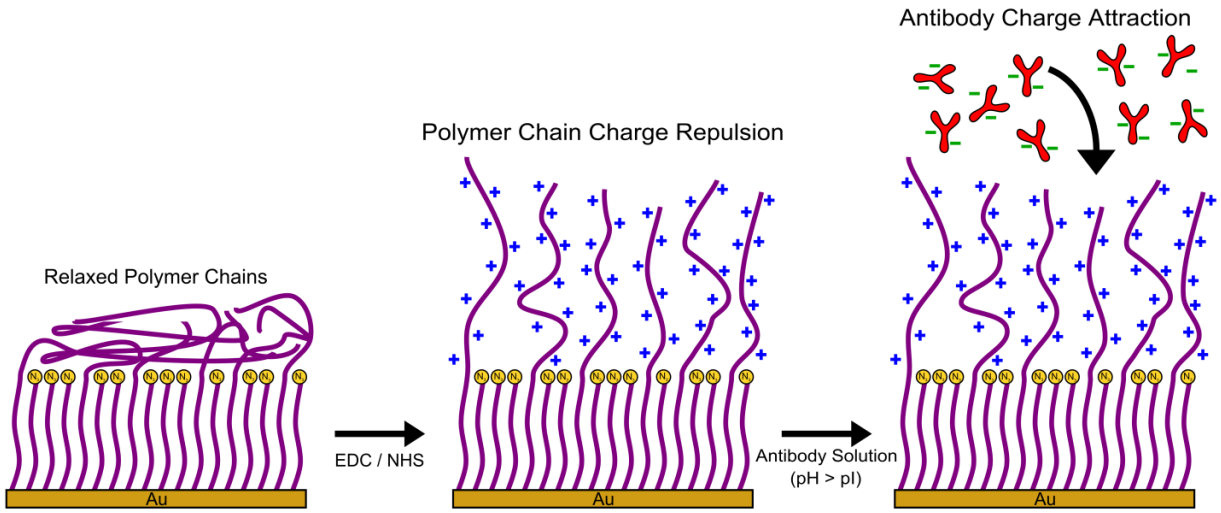

Figure 4.9. The influence of EDC/NHS coupling chemistry on "two layer" pCB films. Activation of the carboxylate groups of the relaxed polymer chains into NHS-esters leads to a net positive charge on the polymer chains which forces them to extend due to charge repulsion. The addition of antibody at a pH greater than the isoelectric point of the protein permits rapid accumulation of the negatively charged antibody to the positively charged polymer chains thus enabling immobilization.

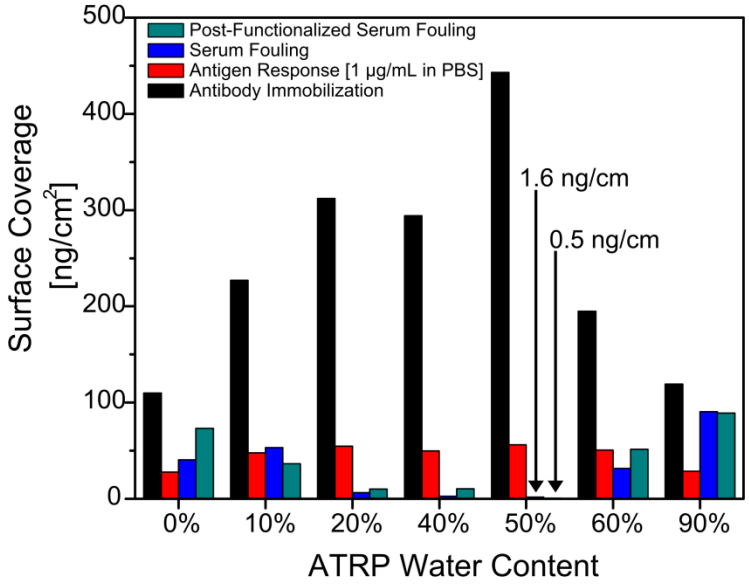

Figure 4.10. The effect of water concentration on the second layer polymerization for 60 min azide treated films and the subsequent antibody immobilization level, antigen response, and non-fouling properties.

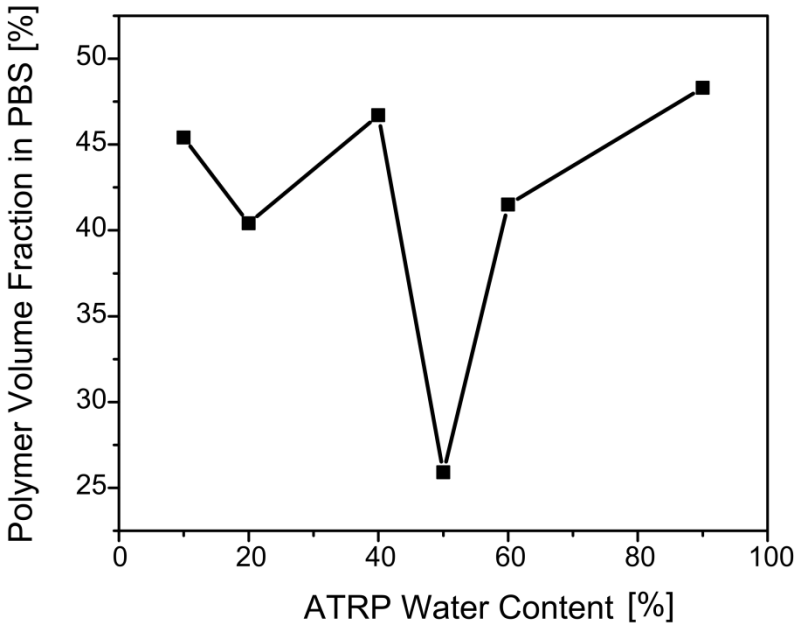

Figure 4.11. The polymer volume fraction in PBS (i.e., the wet polymer density) for two layer films as a function of the water content of the second layer ATRP reaction following a 60 min azide exposure. The film obtained using 50% water had the lowest polymer volume fraction indicating that this film has the "loosest" polymer structure and should thus enable the highest level of immobilization (which was observed). The film obtained using a pure methanol second layer (data not shown) resulted in a lower wet thickness than in air thus indicative of a slightly hydrophobic structure.

Chapter 5

Ultra-Low Fouling and Functionalizable Zwitterionic Coatings Grafted onto SiO_2 via a Biomimetic Adhesive Group for Sensing and Detection in Complex Media

Non-specific protein binding from human plasma and serum has severely hindered the full capabilities of biosensors concerned with cancer biomarker detection. Currently, there is a strong desire for developing new materials which allow for the convenient attachment of an ultra-low fouling and functionalizable surface coating which can be used for highly sensitive and label-free detection of target analytes directly from complex media. In this work, a short 20 minute *in-situ* "graft to" protocol using Tris pH 8.5 buffer was developed for zwitterionic carboxybetaine methacrylate (CBMA) polymer conjugates containing the adhesive biomimetic moiety, 3,4-dihydroxy-L-phenylalanine (DOPA), on SiO_2 substrates. Using a surface plasmon resonance (SPR) biosensor, different buffers, pH values, salt concentrations, and temperatures were investigated for determining the "graft to" conditions that yield dense polymer films which both minimize non-specific protein adsorption and maximize antibody immobilization. The optimized surface coatings were shown to be highly protein resistant to 100% human blood plasma and serum. Subsequent antibody functionalized surfaces without any blocking agents enabled the specific detection of the cancer biomarker ALCAM directly from undiluted human serum down to 64 ng/mL. The successful use of this zwitterionic surface coating for detection from complex media on SiO_2 surfaces indicates its potential for broad impacts in the development of implantable medical devices, *in-vivo* diagnostics, and nano-scale biosensors.

5.1 Introduction

The inability to identify and verify suitable biomarkers using various sensing devices has been the major shortcoming in cancer diagnostics [6,67,81]. As many of these low concentration proteins are found in

complex bodily fluids (e.g. plasma, serum, urine, etc.) [82,83] the culprit underlying detection using biosensors is the overwhelming background noise as a result of non-specific protein adsorption [84-87].

Recent studies have shown the ability of polymers containing the carboxybetaine (CB) moiety, formed via surface initiated atom transfer radical polymerization (SI-ATRP), to outperform commonly used protein resistant ethylene glycol (EG) based coatings. These polyCB (pCB) films were shown to be ultra-low fouling to 100% human plasma and serum [19,20,29]. It has been hypothesized that the surface hydration formed via ionic solvation due to the zwitterionic groups is primarily responsible for the ability of CB polymers to prevent protein adsorption [88]. Subsequent functionalization with antibodies using the abundant carboxylic acid groups and convenient N-hydroxysuccinimide (NHS) / *N*-ethyl-*N*'-(3-diethylaminopropyl) carbodiimide (EDC) chemistry enabled sensitive and specific detection of analytes directly from undiluted human plasma [20].

However, many biosensors today incorporate the use of a variety of nanomaterials with differing geometries into their design [22,23]. The dimensions of the sensing surface have also been decreasing to the nanometer length scale [89]. Therefore, other methods for creating a bifunctional coating on such devices, capable of highly sensitive detection from complex media, need to be developed.

As an alternative to SI-ATRP, there has been much attention focusing on developing "graft to" technologies due to their simplicity and convenience [90]. However, this technique requires a method for chemically attaching the non-fouling material "to" the substrate via some form of an adhesive moiety. During a study of surface modification strategies which could be applied to a variety of materials [91] it was found that the compound 3,4-dihydroxy-L-phenylalanine (DOPA) could strongly adhere to numerous substrates (noble metals, native oxides, ceramics, etc.).

Several studies on the ability of PEG polymers containing DOPA anchors for forming protein resistant coatings on oxide surfaces have been performed [24]. It was found that the number of residues in the DOPA anchor significantly affected the surface density of the grafted polymer and its subsequent ability to resist protein adsorption. In previous work [92], a single DOPA anchor conjugated to polymers composed of zwitterionic sulfobetaine methacrylate (SBMA) was shown to form protein resistant

coatings on various surfaces. To increase the surface density of the grafted zwitterionic polymers and provide for functionalization capabilities, two linked DOPA-poly(carboxybetaine methacrylate) ($DOPA_2$-$pCBMA_2$) polymer conjugates was synthesized and grafted to gold substrates [93]. Following antibody immobilization, the detection of a target protein directly from undiluted human plasma was demonstrated using a SPR biosensor.

Conventional SPR sensor chips are composed of a top layer of gold (~ 48 nm) for which many surface chemistries have been developed. However, many other materials are incorporated into the design of biosensors today which include silica, titanium, platinum, among others [22,23,94,95]. Thus, there has been a push to use available sensing platforms as tools for developing new surface chemistries for these materials. Silica is an attractive material for many biosensor platforms due to the widely established use of silicon (from which SiO_2 is formed) in the semiconductor industry which has enabled the development of convenient micro-fabrication methods. Silicon is currently used in many microelectromechanical system (MEMS) devices [96] and has since been applied to developing nanoelectromechanical system (NEMS) based biosensors with recent advances in nanotechnology [21]. Hence, new surface chemistries for this material need to be developed.

In this work, the "graft to" behavior of novel $DOPA_2$-$pCBMA_2$ polymer conjugates onto silica substrates was studied using a SPR sensor. The grafting conditions were investigated in order to both minimize biofouling and maximize protein immobilization efficiency. The ability of the $DOPA_2$-$pCBMA_2$ surface functionalized with antibodies to detect analytes directly from undiluted human blood serum was demonstrated using the cancer biomarker, activated leukocyte cell adhesion molecule (ALCAM, CD 166). Using a simple 20 minute *in-situ* attachment protocol, the detection of ALCAM at concentrations down to ~64 ng/mL was enabled.

5.2 Experimental Section

5.2.1 Materials

$DOPA_2$-pCBMA polymer conjugates were synthesized as described previously [93]. Sodium hydroxide (99.998%), tetrahydrofuran (THF, HPLCgrade), N-hydroxysuccinimide (NHS), and *N*-ethyl-*N*'-(3-diethylaminopropyl) carbodiimide hydrochloride (EDC) were purchased from Sigma-Aldrich (Milwaukee, WI). Tris, crystallized free base, (molecular biology grade) was purchased from Fisher Scientific. Fibrinogen (fraction I from bovine plasma), lysozyme (from chicken egg white), and 3-(N-morpholino)propanesulfonic acid (MOPS, minimum 99.5%), and phosphate-buffered saline (PBS, 0.01M phosphate, 0.138 M sodium chloride, 0.0027 M potassium chloride, pH 7.4) was purchased from Sigma Chemical Company. Sodium chloride and sodium phosphate were purchased from J.T. Baker (Phillipsburg, NJ). Anhydrous sodium acetate was purchased from Fluka BioChemika. Pooled human plasma and serum were purchased from BioChemed Services (Winchester, VA). Human monoclonal antibodies against the activated leukocyte cell adhesion molecule (anti-ALCAM) and human recombinant ALCAM/Fc chimera were purchased from R&D Systems (Minneapolis, MN). Rabbit polyclonal biotinylated antibody to Salmonella sp.was purchased from Meridian Life Science Inc. (Saco, MA). Ethanol (200 proof) was purchased from Decon Laboratories. The water used was purified using a Millipore water purification system with a minimum resistivity of 18.0 MΩ·cm.

5.2.2 SPR Sensor and Substrates

A laboratory SPR sensor developed at the Institute of Photonics and Electronics, Prague, Czech Republic was used [95] as described previously [20]. This custom built SPR is based on the attenuated total reflection method and wavelength modulation. It is equipped with a four-channel flow cell, temperature control, and uses a peristaltic pump for delivering samples.

SPR sensor chips were made of a glass slide coated with an adhesion-promoting titanium film (~ 2 nm), a gold film (~ 48 nm), and an additional titanium film, for promoting the adhesion of the SiO_2 film (~1 nm), by an electron beam evaporator. The substrates were then immediately coated with ~20 nm of SiO_2 by plasma enhanced chemical vapor deposition (PECVD). Prior to being mounted on the SPR sensor, the chips were rinsed with ethanol, placed in a UV ozone cleaner for 20 minutes, rinsed with Millipore water and ethanol, and then blown dry with filtered air.

5.2.3 Calibration of the SPR Sensor Response

The sensitivity of a SPR sensor depends on the distance of the binding event from the SPR active surface [95]. Since an additional 1 nm titanium film and ~20 nm SiO_2 film were coated on top of the regular SPR chips, the sensitivity had to be calibrated. The sensitivity calibration factor was determined experimentally and found to be 1.40 (i.e. a 1 nm wavelength shift on the silica substrates is equivalent to a 1.4 nm shift on the standard SPR substrates).

A theoretical model for the silica coated SPR substrate was also developed to predict the change in surface sensitivity. The model revealed a calibration factor of 1.33, which was in good agreement with the experimental measurement (within 5.3%). The difference is mostly caused by the accuracy of the dielectric constants used in the theoretical calculation. Therefore, a calibration factor of 1.37, an average of the experimental and theoretic results, was used for this study. Hence, for the SPR sensor used with the silica coated SPR chips, a 1 nm shift in resonant wavelength corresponded to a change in protein surface coverage of ~23 ng/cm^2 [97].

5.2.4 Grafting $DOPA_2$-$pCBMA_2$ to the Substrates

$DOPA_2$-$CBMA_2$ polymer was grafted to the silica substrate *in-situ* by flowing the polymer solution over the sensor chip using Tris buffer (2.5 mg/mL) for 20 minutes at a flow rate of 40 μL/min.

After injecting the polymer solution, the surface was then rinsed with water followed by PBS before quantifying the net surface coverage.

5.2.5 Surface Functionalization

The functionalization procedure was monitored step by step in real-time using the SPR sensor at a flow rate of 40 µL/min and 25°C. Following polymer attachment, the carboxylate groups were activated by injecting a solution consisting of 0.1 M NHS and 0.4 M EDC in water for 7 minutes. After briefly flowing 10 mM sodium acetate buffer (SA, pH 5.0), a solution of antibody dissolved in 10 mM Tris-HCl (pH 9.0, 50 µg/mL) was flowed for 11 minutes. A buffer solution containing 10 mM sodium phosphate and 0.3 M NaCl (PBNa, pH 8.2) was subsequently injected for 10 minutes to wash the surface followed SA buffer to reestablish the baseline for quantifying the antibody surface coverage.

5.2.6 Measurements of Non-specific Protein Adsorption

The non-specific protein adsorption for the polymer conjugate attached to the silica substrate was determined by flowing PBS buffer and then protein solutions consisting of 1 mg/mL of fibrinogen and lysozyme in PBS, 100% human plasma, and 100% human serum in four separate flow channels followed by PBS.

5.2.7 Measurements of Specific Protein Binding

ALCAM was selected to demonstrate the specific protein biomarker detection abilities of antibody functionalized $DOPA_2$-$pCBMA_2$ surfaces in both buffer and in undiluted human serum. For the detection in buffer, both anti-ALCAM and reference anti-Salmonella were immobilized using the above protocol. After establishing a stable baseline with PBS buffer, PBS spiked with ACLAM at increasing

concentrations (26, 64, 160, 398, and 1000 ng/mL) was then subsequently injected for 10 minutes followed by rinsing with buffer for 10 minutes between samples. The net specific (or non-specific in the case of anti-Salm.) protein binding for each concentration was taken as the difference between the initial and incremental PBS baselines. For the detection in undiluted human serum, only anti-ALCAM was immobilized on all four channels using the above protocol. After establishing a stable baseline with PBS, samples of ALCAM spiked 100% human serum at six concentrations (26, 64, 160, 280, 398, and 1000 ng/mL) were then flowed through three channels and un-spiked serum was flowed through the fourth channel followed by PBS for an additional 15 minutes.

5.3 Results and Discussion

5.3.1 SiO_2 Coated SPR Chips

In order for the SiO_2 thin film coated onto the SPR chips to serve as a model system for developing new surface chemistries for biosensing applications, it must be compatible to a variety of conditions (i.e. various temperatures, pH's, solvents, etc.) and maintain its stability during detections. Prior to grafting $DOPA_2$-$pCBMA_2$ onto the substrates, the stability of the SiO_2 layer was tested under a variety of pH values (1-10) and solutions / organic solvents (e.g. 3 M NaCl in PBS, DMF/water, THF, ethanol, and acetone) . It was found that the SiO_2 layers formed on conventional SPR chips mediated with 1 nm of titanium were very stable. However, when the film was formed directly on the gold surface of the chip, it was washed away during experiments (data not shown). Furthermore, the change in SPR surface sensitivity due to both the titanium interlayer and SiO_2 film was found to be minor from both experimental measurements and theoretical calculations. Little variation in the characteristics of the SPR wavelength dips was also observed. Therefore, substrates composed of 20 nm of SiO_2 and 1 nm of titanium on conventional SPR chips were used for the remainder of the study.

Several attempts for making SiO_2 coated SPR chips were reported previously. Some of them used a thin titanium interlayer between the silica and gold films to promote adhesion [98,99] but some did not [100]. The SiO_2 thin film deposited directly on a gold surface via PECVD was demonstrated to be stable in both acidic and basic solutions as well as organic solvents [100]. However, our results showed that the SiO_2 thin film formed via this method was very unstable just after a few days and was easily removed by water or organic solvents alike. While PECVD is a common method for the formation of silica films, little variation in the experimental parameters can cause significant differences in the quality of the layer formed (e.g. silanol and water impurities, porosity, etc.) which may explain the different resulting film characteristics [101,102].

5.3.2 $DOPA_2$-$pCBMA_2$ Grafted to SiO_2 Substrates and Non-specific Protein Adsorption

As shown in **Figure 5.1a**, the first step for obtaining sensitive and specific detection is to achieve a high surface coverage of pCBMA polymer which can minimize non-specific protein adsorption. In order to maximize the surface density of the non-fouling and functionalizable CB groups on silica substrates using the "graft to" method, the $DOPA_2$-$pCBMA_2$ structure shown in **Figure 5.1b** was used.

Previous investigations of the adhesive mechanism for DOPA have been conducted [103]. It was found that under non-oxidizing conditions (e.g. neutral pH) a strong metal-oxygen coordination complex can form between catecholic DOPA and an oxide surface thereby creating an adhesive interaction with high dissociation energy. As oxidation of the side chains occur, DOPA cross-linking reactions begin to take place. This was found to be an important mechanism for forming dense films using DOPA polymer conjugates [93]. Therefore, a variety of grafting conditions were studied in order to optimize the surface coverage onto the silica substrates.

Tris buffer was selected due to its ability to allow a strong attachment of DOPA onto a variety of surfaces [103]. The polymer surface coverage under different pH values, salt concentrations, and

temperatures for a fixed flow time of 20 minutes and the protein fouling properties of these films are summarized in **Table 5.1**. The conditions of high salt (~ 1 M) and temperature (40°C) were tested because it was reported that $DOPA_3$-PEG conjugates were able to form dense polymers on TiO_2 substrates in such an environment [24]. The results indicated that the amount of bound polymer was the largest in the range of pH values of 8 – 10, decreased with decreasing pH and high ionic strengths, and was not affected by temperature over the range tested (as limited by the SPR equipment). The optimal "graft to" condition was 10 mM Tris buffer pH 8.5 at 25°C, in which the $DOPA_2$-$pCBMA_2$ surface coverage was found to be 260.1 ± 18.1 ng/cm^2. As shown in **Figure 5.2**, very little polymer was removed during the washing steps indicating a strong and mostly permanent attachment of polymer on the SiO_2 surface. The adsorption of 1 mg/mL fibrinogen and lysozyme on the optimized polymer surfaces was undetectable (data not shown). The protein fouling to undiluted human plasma and serum were 6.3 ± 0.9 ng/cm^2 and 11.7 ±3.0 ng/cm^2, respectively. The sensor-gram for a typical fouling experiment using undiluted human plasma and serum is shown in **Figure 5.3**.

The observation that the polymer surface coverage was decreased under low pH conditions (pH ≤ 7) could be attributed to the ionizable carboxylate groups present in the pCBMA chains (pKa ~3.5) [104] and the working range of Tris buffer (pH 7 – 9.2). When the pH of the original Tris solution (without polymer) approaches the lower limit of the working range, there is minimal buffering capacity. Upon dissolution of $DOPA_2$-$pCBMA_2$, the pH of the solution drops due to the release of protons from the ionizable carboxylate groups. As this occurs, the decreasing pH causes the polymer to take on a slight positive charge as a result of approaching the pKa of the CB groups. Additionally, the lower pH also creates a slight positive charge on the silica surface [105]. The resulting effect is charge-charge repulsion which reduces the overall polymer surface coverage. However, for all pH values tested, low fouling to 100% human plasma was obtained indicating that despite the decrease in coverage, enough of the polymer conjugate was still adsorbed in order to make the surface protein resistant. Since the attachment of the polymer in Tris pH 8 – 10 buffer at 25°C was shown to offer the best surface coverage and subsequent non-fouling properties, a pH of 8.5 was used for all further experiments.

As shown in **Table 5.1**, high ionic strength also reduced the polymer surface coverage. Water soluble amphoteric polymers are known to exhibit the anti-electrolyte effect at their isoelectric point (IEP). This means that the polymer will unfold from a compact formation upon the addition of salts. However, for uniformly charged polyelectrolytes, when the polymer is present in acidic or basic conditions relative to its IEP, the addition of salt causes the formation of a more compact structure to form, which is more pronounced at higher ionic strengths [106]. The formation of this more compact structure may have reduced the ability of $DOPA_2$-$pCBMA_2$ to adsorb to the silica surface by forcing the slightly hydrophobic DOPA residues inside the hydrophilic polymer chains thereby decreasing the ability to react with the substrate and anchor the polymer.

Other "graft to" solutions were also tested in an effort to increase the polymer surface coverage. These solutions include water, PBS (pH 7.4) and MOPS cloud point buffer (pH 6, 3 M NaCl). However, none of the above media resulted in any noticeable improvement in terms of surface coverage or non-fouling.

Recently, our group also studied the "graft to" behavior of $DOPA_2$-$pCBMA_2$ onto gold substrates. It was found that dense polymer films could be formed under cloud point conditions in a THF/pH 3 water mixture [93]. The resulting surface was shown to be highly protein resistant. This condition was also tested for grafting to silica substrates. While this solution also resulted in low fouling properties using the 20 minute attachment protocol (6.3 ng/cm^2 adsorption of protein for undiluted blood plasma) the polymer surface coverage was lowered (233.6 ng/cm^2). This indicates that the attachment mechanism for gold and silica substrates could be different. Catechol groups are capable of four different energetic reactions: hydrogen bonding, metal-ligand complexes, Michael-type additions, and charge-transfer complexes [107]. Considering the chemical composition and molecular structure of the two substrates, different binding mechanisms would be expected thus requiring different grafting conditions.

5.3.3 Antibody Immobilization

In order to obtain highly sensitive detection, as shown in **Figure 5.1a**, the grafted polymer coating must be able to efficiently immobilize molecular recognition elements. Following polymer attachment, the $DOPA_2$-$pCBMA_2$ coated surface was subsequently immobilized with an antibody for the detection of the cancer biomarker, activated leukocyte cell adhesion molecule (ALCAM, CD 166). ALCAM is a 105 kDa protein with a normal presence in human blood serum (~84 ng/mL). Up-regulation of this protein in the range of ≥ 100 ng/mL has been shown to be indicative of various cancer types [55] indicating the importance for detection of small changes in concentration.

It was previously determined that a buffer solution with the pH value above the isoelectric point (IEP) of the antibody was necessary for efficient protein immobilization on pCB surfaces [57]. This is necessary because of the slight positive charge on the polymer which is created during activation. Therefore, several different solutions were tested as efficient buffers for this antibody immobilization step. These include sodium carbonate (pKa 10.25), boric acid (pKa 9.14), sodium tetraborate decahydrate (pKa 9.14), and tris (pKa 8.08). Sodium hydroxide (pH 10) was previously shown to work well for anti-ALCAM immobilization [29,93] and was also tested. Further optimization in terms of pH (8.5 – 10) and buffer concentration (10 – 100 mM Tris) revealed that 10 mM Tris pH 9.0 offered the best immobilization condition and subsequent activity for anti-ALCAM on the $DOPA_2$-$pCBMA_2$ coated surface. Using similar EDC/NHS activation conditions from previous work [29], the anti-ALCAM immobilization levels were 55.4 ± 20.0 ng/cm^2. The results for the four other buffers tested were all less than 20 ng/cm^2. A typical sensor-gram for the antibody immobilization step can be found in **Figure 5.4**.

The previous antibody immobilized levels for the pCB films made via SI-ATRP and for the attachment of $DOPA_2$-$pCBMA_2$ onto gold substrates were found to be 220 – 330 ng/cm^2 and 100 – 130 ng/cm^2, respectively [20,29,93]. The primary reason for the difference amongst the three surfaces could arise from the amount of available pCB groups as a result of both the different surface densities and thicknesses of the polymers. Based on this comparison, the amount of pCB groups available has the

following order: pCB by SI-ATRP, $DOPA_2$-$pCBMA_2$ on gold, and $DOPA_2$-$pCBMA_2$ on silica and thus the immobilization levels would likely follow the same trend.

The antibody to Salmonella (anti-Salm.) was tested to determine the effect of immobilization of different proteins under identical conditions. The immobilization amount of anti-Salm. was found to be ~116 ng/cm^2. This indicates that in cases where an effective monolayer of antibody is not obtained, different antibodies will likely have different immobilization amounts which can likely be attributed to the different IEP's of the proteins. This property results in varying degrees of attraction between the antibody and the activated pCB surface and thus can significantly affect the total amount functionalized.

5.3.4 Detection of Target Analytes in Buffer

The ability of the immobilized antibody to specifically detect low concentrations of target protein was first tested using buffer. **Figure 5.5** shows the cumulative detection curve for ALCAM spiked into PBS at concentrations from 26 ng/mL to 1.0 µg/mL (the raw sensor response converted to protein surface coverage is shown in **Figure 5.6**). The results indicate that the level of anti-ALCAM immobilization was sufficient enough to detect ALCAM in PBS at concentrations down to 26 ng/mL. In order to verify the target specificity of the functionalized surface, the same experiment was performed using the reference antibody, anti-Salm. The results for the highest concentration tested (1 µg/mL) shown in **Figure 5.7** indicate that despite a higher surface coverage of anti-Salm., there was no non-specific binding of ALCAM, while there was a large specific response on the anti-ALCAM functionalized surface. This indicates that the immobilized anti-ALCAM can specifically bind to the target analyte from buffer while preventing non-specific adsorption.

5.3.5 Detection of Target Analytes Directly from Undiluted Human Serum

After grafting the polymer to the silica surface and subsequent protein immobilization, the last step as shown in **Figure 5.1a**, is to detect target analytes from complex media. The resulting detection curve from 100% human serum is shown in **Figure 5.8**. The unblocked $DOPA_2$-$pCBMA_2$ functionalized surface was shown to detect ALCAM directly from undiluted human serum down to concentrations as low as 64 ng/mL. This offers an improvement over the thoroughly blocked OEG COOH/OH alkane thiol-based surface which had a ALCAM limit of detection of >100 ng/mL from human plasma [20]. A comparison of the detection curve obtained from serum to that obtained from buffer reveals, that for the same concentration of ALCAM, a larger specific response to the antigen is observed in the buffer solution. This is likely the result of two factors. First, the presence of numerous other proteins in the serum may interfere with the ability of the antigen to reach the surface where it can be detected. Secondly, the presence of non-specific binding on the functionalized surface may block some of the binding sites on the antibody which would further limit the response. In buffer solution, both of these effects do not exist.

Typical sensor responses for the direct detection of ALCAM from undiluted serum are shown in **Figure 5.9**. The difference between the two curves was caused by the additional specific binding of ALCAM in the spiked channel. This shows that the anti-ALCAM functionalized surface can recognize and bind to the target analyte with high specificity even from undiluted human serum. The typical background signal (i.e. the response of the anti-ALCAM functionalized surface to serum only) was found to be ~55 ng/cm^2.

We have previously shown pCB coatings made via SI-ATRP functionalized with an effective monolayer of antibody to sensitively detect spiked ALCAM directly from human plasma at concentrations down to ~10 ng/mL. Furthermore, the $DOPA_2$-$pCBMA_2$ polymer grafted to gold could detect spiked ALCAM down to ~30 ng/mL. Therefore, for $DOPA_2$-$pCBMA_2$ grafted silica to be effective in cancer diagnostics, the functionalized surface must be able to detect similar biomarker concentrations. In this work, the limit of detection of ALCAM directly from human serum was found to be 64 ng/mL,

which is of similar magnitude to the other two platforms. The differences likely arise from the different surface densities and total amount of non-fouling and functionalizable CB groups.

5.4 Conclusions

A novel polymer conjugate containing ultra-low fouling and functionalizable zwitterionic pCB polymers and two DOPA moieties (for increased polymer surface coverage) was successfully grafted to SiO_2 coated SPR chips. SiO_2 is being increasingly incorporated into the design of novel NEMS devices which emphasize the importance of developing new surface chemistries for this material. Subsequent antibody functionalization enabled the detection of a target analyte directly from undiluted human serum with high sensitivity and specificity using a SPR sensor.

The attachment of the polymer conjugate was tested under a range of pH values, temperatures, and ionic strengths. Using the optimal conditions, a straightforward and convenient “graft to” method in room temperature Tris pH 8.5 buffer enabled a strong and mostly permanent surface coating to form on the silica surface. Subsequent biofouling experiments yielded undetectable adsorption to single protein solutions and low-fouling to 100% human plasma and serum. The sensitivity of the $DOPA_2$-$pCBMA_2$ surface for the label-free detection of specific analytes directly from undiluted human serum was tested using the cancer biomarker ALCAM. Under optimized conditions, the detection limit of ALCAM spiked into whole human blood serum was found to be ~64 ng/mL. The successful demonstration of the *in-situ* attachment of $DOPA_2$-$pCBMA_2$ to SiO_2 coated SPR chips and subsequent detection abilities illustrate the potential this approach holds for development of nano-scale sensors for medical diagnostics. Furthermore, the unique ultra-low fouling and functionalizable properties make this zwitterionic polymer promising for applications in implantable medical devices and *in vivo* diagnostics.

5.5 Tables

Table 5.1. $DOPA_2$-$pCBMA_2$ Polymer Surface Coverage and Total Non-specific Protein Adsorption from 100% Human Blood Plasma under Different "Graft To" Conditions[a]

Condition	Polymer Surface Coverage [ng/cm^2]	Non-specific Protein Adsorption (100% human plasma) [ng/cm^2]
pH 3	212.9	10.5
pH 6	217.1	11.4
pH 7	223.8	6.5
pH 8	273.7	5.6
pH 8.5	283.2	5.4
pH 9	262.2	6.1
pH 10	265.0	6.8
pH 8.5 , 40°C	271.8	6.4
pH 8.5 + 10 mM NaCl	282.7	5.1
pH 8.5 + 1 M NaCl	212.4	7.9

[a] Polymer surface coverage and non-specific protein adsorption using 10 mM Tris-HCl. The polymer was dissolved in buffer at 2.5 mg/mL and flowed over the sensor chip for 20 minutes at a flow rate of 40 µL/min. Unless otherwise specified, each condition was run at 25°C. For protein fouling experiments, following polymer attachment, a stable PBS baseline was obtained. Undiluted human plasma was then flowed over the sensor surface for 10 minutes followed by rinsing with buffer for 10 minutes.

5.6 Figures

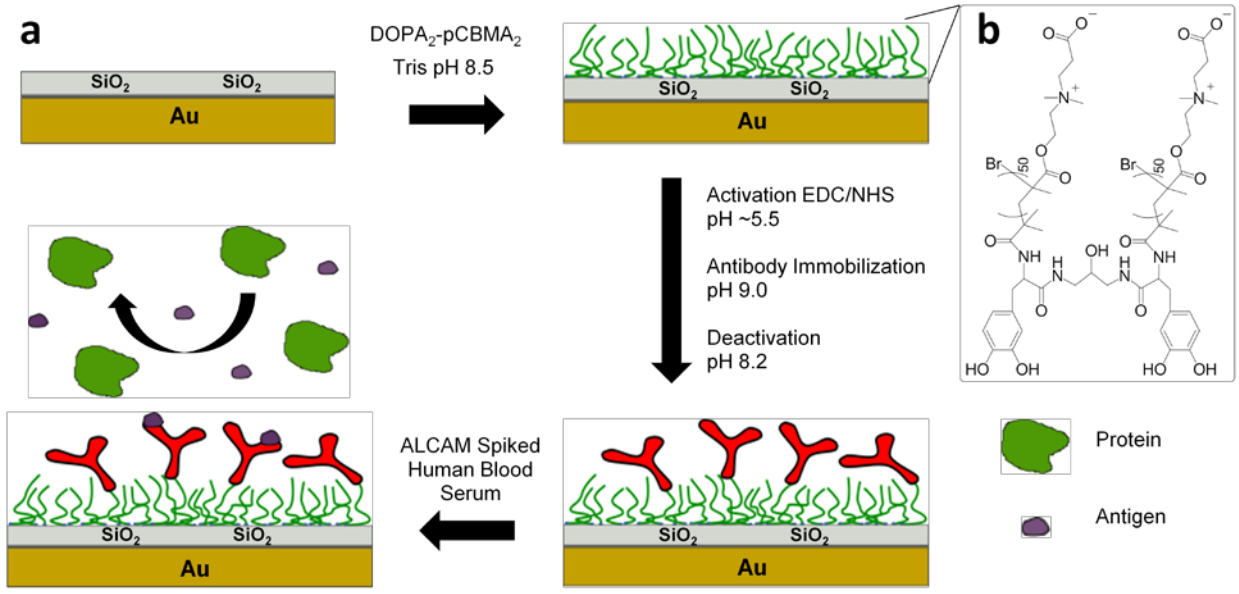

Figure 5.1. (a) The newly developed protocol for a novel "graft to" method which allows for highly sensitive detection from undiluted human serum on SiO_2 using a SPR biosensor. Starting with a cleaned silica substrate, the $DOPA_2$-$pCBMA_2$ polymer conjugate is grafted to the sensing surface. Carboxylic groups on the polymer are activated using EDC/NHS chemistry which can then react with primary amines on antibodies. Following deactivation of the residual activated groups, the functionalized surface is used for specific detection of a target analyte from human serum. The low fouling background combined with good immobilization efficiency allows for highly sensitive detection. (b) The $DOPA_2$-$pCBMA_2$ polymer conjugate. The two DOPA anchors combined with the two bifunctional CBMA polymer chains allows a high surface coverage of both non-fouling and functionalizable groups on silica substrates.

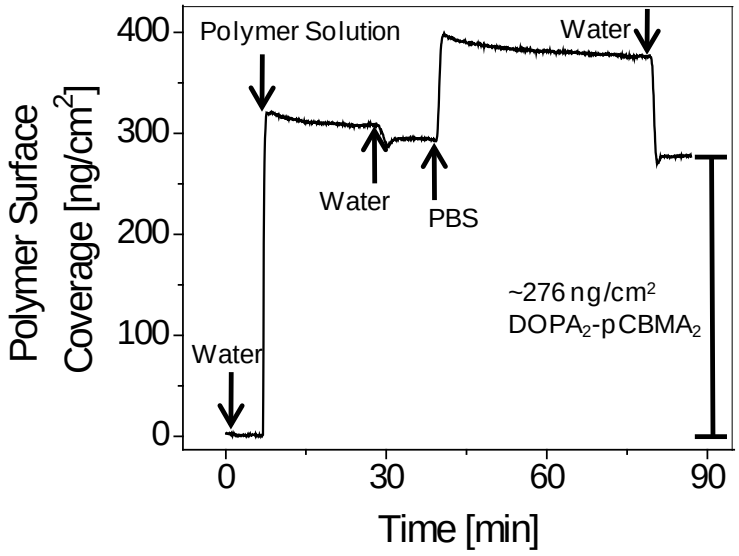

Figure 5.2. The typical sensor-gram for attaching $DOPA_2$-$pCBMA_2$ to silica. The polymer conjugate was first dissolved 10 mM Tris buffer pH 8.5 at 2.5 mg/mL. After establishing a baseline using water, the polymer solution was then injected into the SPR followed by washing with water and PBS. Here, ~276 ng/cm^2 of polymer was grafted to the silica substrate. The resonant wavelength shift conversion to surface coverage for proteins was also applied to the polymer conjugates due to their similar refractive indices [20,33].

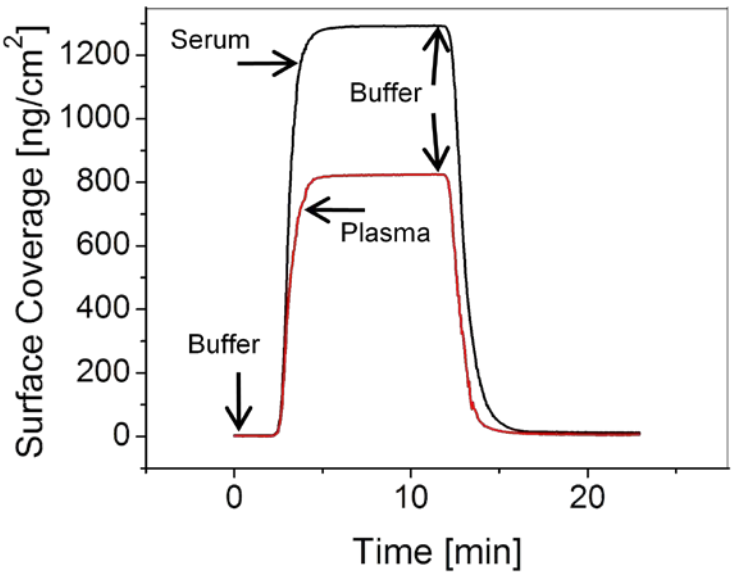

Figure 5.3. SPR response to flowing undiluted human plasma and serum over the $DOPA_2$-$pCBMA_2$ coated surface. After obtaining a stable baseline using buffer, each protein solution was flowed for 10 minutes at 40 µL/min followed by rinsing with PBS for an additional 10 minutes. The sensor response for determining the non-fouling properties of the surface coating was calculated as the difference between the starting and ending buffer baselines. Here, the total biofouling to human plasma and serum were 5.4 and 9.5 ng/cm^2, respectively.

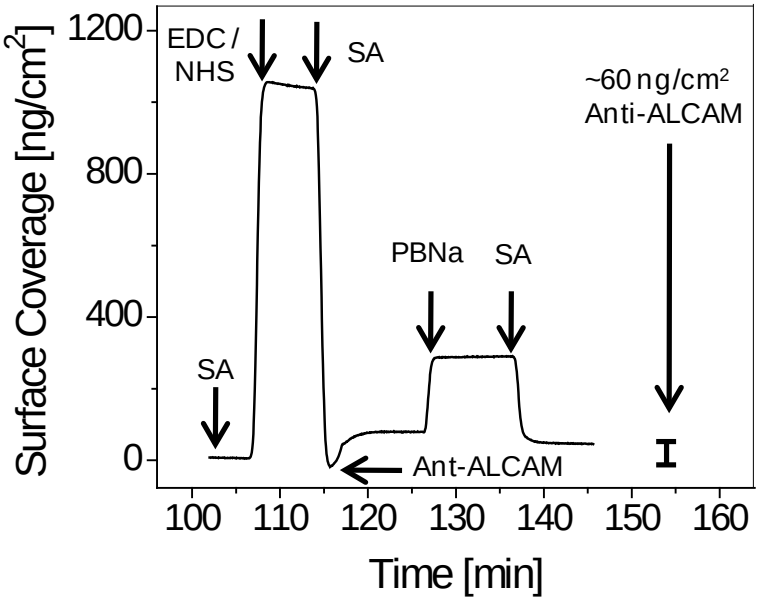

Figure 5.4. A typical functionalization sensor-gram for the immobilization of anti-ALCAM. A 10 mM sodium acetate (SA) solution at a pH of 5.0 was first used to establish a stable baseline. The carboxylate groups present on the attached polymer conjugate were then activated using 0.1 M NHS / 0.4 M EDC aqueous solution for 7 minutes at 40 µL/min and 25°C. After briefly flowing SA, an antibody solution consisting of 10 mM Tris pH 9.0 with 50 µg/mL of anti-ALCAM was flowed for 11 minutes followed by a 10 mM sodium phosphate, 0.3 M NaCl, pH 8.2 (PBNa) solution for 10 minutes. Flowing a solution with a pH > 8.2 over the activated surface for ~21 minutes was necessary to completely deactivate the residual carboxylic groups [57]. SA buffer was then used to re-establish the baseline in order to calculate the total amount of immobilized antibody. For this particular experiment, ~ 60 ng/cm^2 of anti-ALCAM was immobilized on the surface.

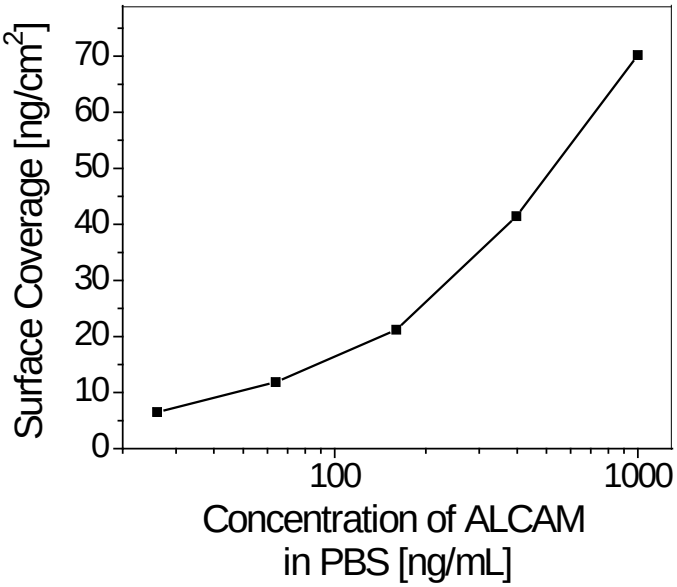

Figure 5.5. Cumulative ALCAM detection curve in buffer. After first attaching the polymer and subsequent functionalization with anti-ALCAM, a PBS baseline was obtained. Incremental samples of PBS spiked with ALCAM at known concentrations (26 – 1000 ng/mL) were then flowed over the surface and the sensor response was calculated. The data shown is the average result for two channels each functionalized with ~60 ng/cm^2 of anti-ALCAM. The results indicated that the level of immobilized antibody was sufficient to detect target proteins down to concentrations as low as 26 ng/mL from PBS.

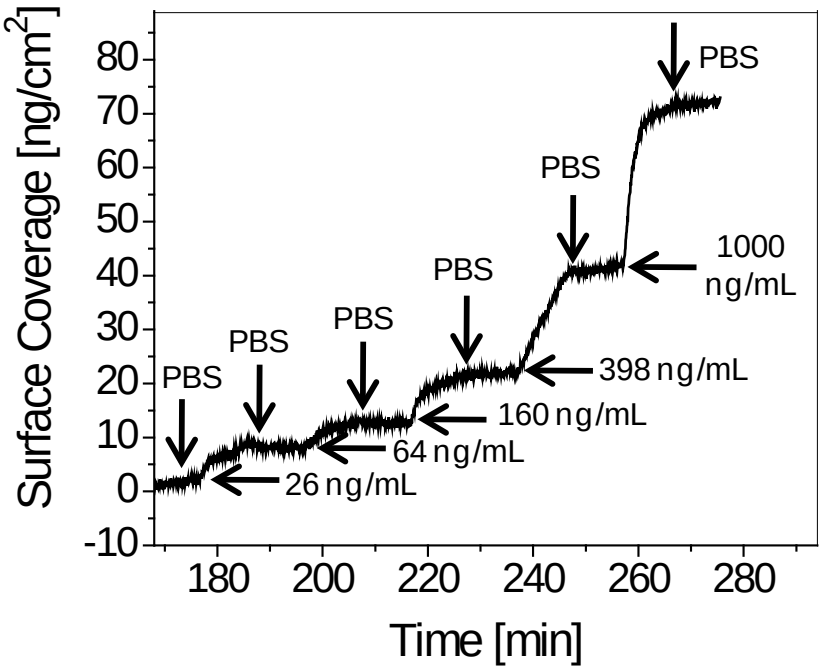

Figure 5.6. Raw sensor response for the cumulative detection of ALCAM in PBS.

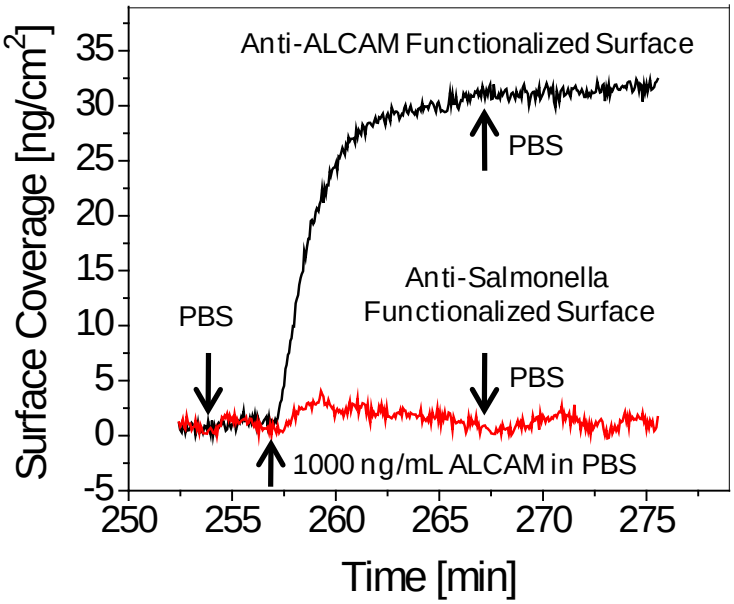

Figure 5.7. The specific detection of ALCAM from PBS. After establishing a stable baseline with buffer, PBS spiked with 1 ug/mL ALCAM was flowed over two surfaces. The top and bottom curves represent the responses of a surface functionalized with anti-ALCAM (~60 ng/cm^2) and anti-Salm.(~116 ng/cm^2), respectively. Large and purely specific protein binding is demonstrated by a net shift on the anti-ALCAM functionalized surface and a zero response for the control.

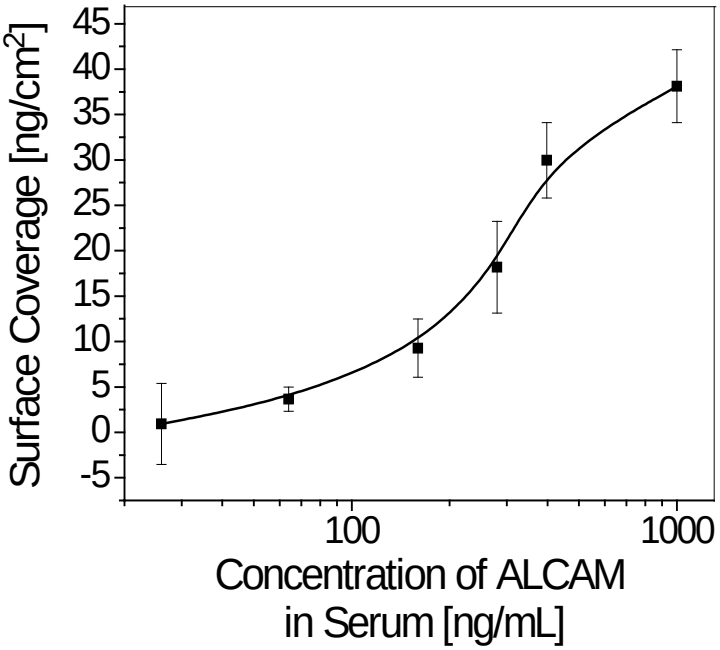

Figure 5.8. The detection curve of ALCAM from undiluted human serum. After attachment of the polymer and subsequent functionalization with anti-ALCAM on all four SPR channels (at levels of 55.4 ± 20.0 ng/cm^2) a PBS baseline was obtained. Serum spiked with ALCAM at known concentrations (26 – 1000 ng/mL) and un-spiked serum was flowed through the sensor. The buffer baseline was then reestablished. The net response for each data point was completed in triplicate using *de novo* functionalized surfaces and calculated by subtracting the reference response (i.e. un-spiked serum) from each measurement. The detection limit of the unblocked $DOPA_2$-$pCBMA_2$ surface was found to be ~64 ng/mL.

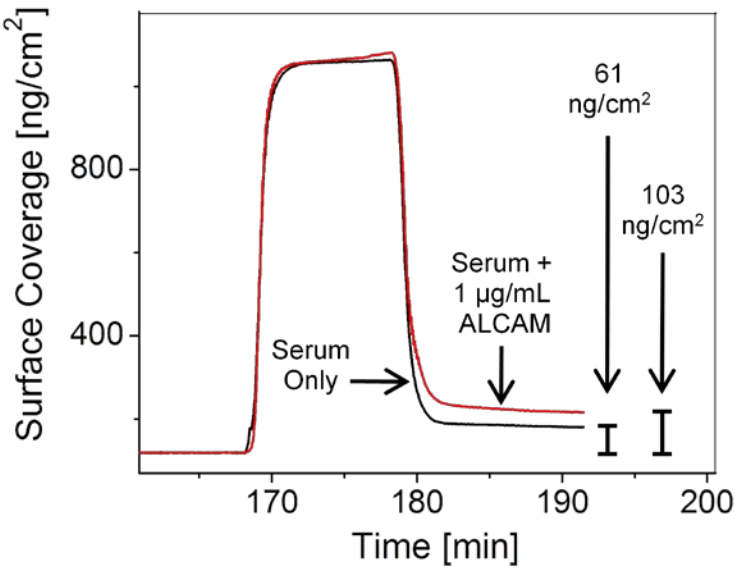

Figure 5.9. Specific detection of ALCAM directly from undiluted human serum. After obtaining a stable baseline using buffer, both spiked and un-spike human serum were flowed for 10 minutes at 40 µL/min followed by rinsing with PBS for an additional 15 minutes. The lower curve represents the typical response for flowing unspiked serum over the anti-ALCAM functionalized surface. The net response for this curve is due to both specific (ALCAM) and non-specific protein adsorption. The upper curve represents the response for flowing serum spiked with 1 µg/mL ALCAM, which causes additional specific protein binding of the target antigen. Both channels were functionalized with ~80 ng/cm^2 of anti-ALCAM.

Chapter 6

Novel Zwitterionic Carboxybetaine Immobilization Strategy for Basic Proteins

Zwitterionic poly(carboxybetaine) (pCB) is ideally suited for overcoming the difficulties associated with detection from undiluted complex media using biosensors due to its ability to achieve ultra low fouling properties all while presenting abundant functionalizable groups for covalently coupling. Traditionally restricted to ligands with isoelectric points less than pH ~7.5, the use of citraconic anhydride (CA) for protecting primary amines on the basic protein, lysozyme (pI ~11) was used to demonstrate a novel approach for covalent coupling onto a pCB surface. The zeta potential of the protein conjugate, CA-Lysozyme, was found to be highly negatively charged and rapidly became positive following exposure to acidic solution. Such properties enabled electrostatic attraction and efficient covalent coupling to the positively charged EDC/NHS activated pCB surface. Subsequent removal of the remaining protecting groups using an acidic solution at 37°C revealed a biologically active ligand, which was verified via the detection of monoclonal anti-Lysozyme. This protection strategy is amenable to many other proteins thereby extending the functionalization capabilities of pCB to ligands with isoelectric points spanning nearly the entire pH range to further advance applications involving undiluted complex media.

6.1 Introduction

Applications of biosensors are vast and include numerous fields such as medicine, agriculture, food safety, homeland security, bio-processing, and environmental and industrial monitoring. In its simplest form, a biosensor can be defined as a self-contained device consisting of a recognition element in close proximity with a transducer.[108] Recently, a sensing configuration was shown to enable the real-time detection of target analytes *in vivo* from whole blood.[109] The detection of biomarkers and therapeutics from blood plasma highlights the push towards the analysis of crude complex matrices, a phenomenon

highly prevalent in the paradigm of personalized medicine.[108-110] This has created the need for surface chemistries which are capable of maintaining high signal to noise (S/N) ratios in samples such as undiluted human plasma,[110] which consists of thousands of core proteins spanning more than 10 orders of magnitude in concentration.[6]

A high S/N ratio is accomplished by (1) a reduction in background effects associated with non-specific adsorption and (2) enabling the convenient immobilization of a large variety of high-affinity molecular recognition elements (MREs) to capture the largest amount of target analytes as possible. Significant reduction or elimination of background noise from undiluted human blood plasma has almost solely been achieved by either ethylene glycol-based or zwitterionic carboxybetaine surface chemistries.[16,17] However, oligo- or poly(ethylene glycol) (OEG or PEG) films have major limitations. Short OEG self-assembled monolayers end terminated with carboxylic groups enable functionalization of MREs but offer only a minor reduction in fouling from undiluted human plasma.[20] Longer PEG-based chains, while exhibiting improved non-fouling performance, are very difficult to functionalize all while maintaining the non-fouling properties on the post-functionalized film.[16,18]

Zwitterionic poly(carboxybetaine) (pCB) has been shown to be highly attractive for protein resistant applications. These films exhibit ultra low fouling properties to undiluted human serum and plasma (i.e., <5 ng/cm^2 of non-specific protein adsorption) and possess abundant functionalizable groups to enable ligand immobilization via amino-coupling chemistry. Importantly, following deactivation, pCB returns to its original zwitterionic non-fouling state, thus allowing for the sensitive detection of target analytes from undiluted complex media due to the ability to significantly reduce background noise on the functionalized film without the use of blocking agents.[20] While the development of a 3-dimensional pCB hierarchical architecture has significantly improved immobilization levels,[73] is it still difficult to functionalize highly basic protein ligands.

As shown in **Figure 6.1**, the activation of pCB using 1-Ethyl-3-(3-dimethylaminopropyl) carbodiimide hydrochloride (EDC) and N-hydroxysuccinimide (NHS) results in a slight positive charge on the surface which can be used to take advantage of electrostatic effects for coupling negatively charged

analytes to the film.[20,57] Such electrostatic effects facilitate immobilization by attracting a high local concentration of analytes near the surface.[111] However, if the pH of the immobilization buffer is too high (e.g. larger the pH ~8.5) rapid hydrolysis of NHS-esters occurs which decreases the coupling levels.[57] Thus, this approach works well for proteins with an isoelectric point (pI) less than pH ~7.5 in which the ligand will be negatively charged using typical pCB immobilization buffers (e.g. TAPS pH 8.2). While many proteins fall into this category, there are several ligands with larger pI values whose immobilization levels on pCB are reduced due to electrostatic repulsion from the surface. The engineering of high-affinity MREs remains a major challenge for biosensing as a large variety of ligands are being designed and synthesized.[110] Thus, it is important to develop a coupling strategy for pCB to include the total range of protein isoelectric points all while maintaining the bioactivity of the attached ligand, to further advance detection capabilities from undiluted complex media.

In this work, a reversible protein modification strategy based on citraconic anhydride (CA) was demonstrated with lysozyme (pI ~11)[112] for immobilization onto pCB films. Protein conjugation methods with CA as well as the study of the reversible nature of the modification were investigated. Subsequent immobilization conditions onto pCB were developed to enable detection of a monoclonal antibody to lysozyme. This demonstration significantly expands the range of protein ligands which can be immobilized onto pCB and further advances the utility of pCB for analysis of crude sample matrices.

6.2 Experimental Section

6.2.1 Materials

Copper(I) bromide (99.999%), 2,2'-bipyridine (bpy, 99%), tetrahydrofuran (THF), methanol, N-[Tris(hydroxymethyl)methyl]-3-aminopropanesulfonic acid (TAPS), 2-(N-Morpholino)ethanesulfonic acid (MES), boric acid, glycine, citraconic anhydride, citric acid, phosphate buffered saline (PBS, 0.01 M phosphate, 0.138 M sodium chloride, 0.0027 M potassium chloride, pH 7.4), lysozyme from chicken egg

white, anhydrous acetone, and triethylamine were purchased from Sigma-Aldrich (St. Louis, MO). Ethanol (200 Proof) was purchased from Decon Laboratories (King of Prussia, PA). Sodium chloride (NaCl) and ether were purchased from J.T. Baker (Phillipsburg, NJ). Sodium acetate anhydrous was purchased from Fluka (subsidiary of Sigma Aldrich, St. Louis, MO). 1-Ethyl-3-(3-dimethylaminopropyl) carbodiimide hydrochloride (EDC) and N-hydroxysuccinimide (NHS) were purchased from Acros Organics (Geel, Belgium). β-propiolactone was purchased from Alfa Aesar (Ward Hill, MA). N-[3-(Dimethylamino)propyl] acrylamide (DMAPA, 98%) was purchased from TCI America (Portland, OR). Water was purified using a Millipore water purification system with a minimum resistivity of 18.2 MΩ cm. Mercaptoundecyl bromoisobutyrate (SI-ATRP initiator) was synthesized as described previously.[51] Monoclonal antibody to hen egg lysozyme (anti-Lys) were purchased from RayBiotech (Norcross, GA).

6.2.2 Modification of Lysozyme using Citraconic Anhydride

All seven primary amine residues on lysozyme were blocked with citraconic anhydride (CA) using the following method. Lysozyme was dissolved (10 mg/mL) in a buffer containing 300 mM TAPS, 150 mM NaCl and citraconic anhydride adjusted to pH 9 using 1 M NaOH. The molar ratio of CA to primary amines was 10 to 1. The reaction was mixed overnight at room temperature to ensure complete protection of all seven available amines on lysozyme. The solution was then passed through a 0.2 μm cellulose filter and dialyzed against 20 mM boric acid containing 20 mM NaCl at pH 9 for 3 days. The final product was obtained via lyophilization using a Labconco FreeZone 2.5 liter freeze dry system and then stored at -20°C.

6.2.3 Solution Hydrolysis of Citraconic Anhydride Protected Lysozyme (CA-Lysozyme)

The solution hydrolysis of the protecting groups on citraconic anhydride modified lysozyme (CA-Lysozyme) was analyzed using a Malvern Zetasizer Nano Series for the determination of protein size and

zeta potential (ZP). It was important to maintain an alkaline pH prior to that start of the hydrolysis characterization so as to minimize any loss of the protecting groups. First, CA-Lysozyme (20 mg) was dissolved in 5 mM TAPS pH 9 buffer (4 mL) and underwent a buffer exchange using an Amicon Ultra-4 Centrifugal Filter unit (3,000 NMWL) from Millipore. The end protein concentration was adjusted to 10 mg/mL using TAPS pH 9 buffer to yield a final volume of ~2 mL. A 1 mL sample of the solution was then passed through a 0.2 µm cellulose filter and analyzed with the Zetasizer. After measuring the size and ZP, the sample was added back into the original solution. Next, 100 µL of 480 mM sodium acetate pH 5 buffer was spiked into the protein solution which was then stirred continuously at room temperature. At intervals of 30, 60, 90, 180, and 1200 minutes a 1 mL sample was removed, filtered through a 0.2 µm cellulose filter, analyzed for size and ZP, and then added back into the original solution. The ZP and size of unmodified lysozyme was determined after performing buffer exchanges using 5 mM sodium acetate pH 5 and 5 mM TAPS pH 9, to serve as a comparison.

6.2.4 Synthesis of Carboxybetaine Acrylamide Monomer

(3-Acryloylamino-propyl)-(2-carboxy-ethyl)-dimethyl-ammonium (CB) was synthesized by reacting 48 mL of DMAPA with 25 g of β-propiolactone in 400 mL of anhydrous acetone at 0°C under nitrogen. After removing the ice bath at 20 min, the solution was allowed to warm up to room temperature. After 6 h, the product was filtered, washed with ether, and dried under vacuum. The rough product was re-dissolved in a 30% (v/v) triethylamine in methanol solution and stirred overnight. After concentrating the solution, the CB was precipitated with acetone and filtered. The white solids were suspended in acetone and ether, for 1 h each, filtered, dried under vacuum, and stored at 4°C. Yield: 61%. H'NMR (Bruker 500MHz, DMSO-d6): 8.61 (t, 1H,N-H), 6.28 (t, 1H, CHH=C*H*), 6.13 (t, 1H, CH*H*=CH), 5.61 (t, 1H, C*H*H=CH), 3.44 (t, 2H, N-CH_2-CH_2-COO), 3.21 (m, 4H, NH-CH_2-CH_2-CH_2), 2.97 (s, 6H, N-(CH_3)2), 2.25 (t, 2H, CH_2-COO), 1.87 (t, 2H,NH-CH_2-CH_2- CH_2).

6.2.5 Preparation of pCB Films by Surface-Initiated Atom Transfer Radical Polymerization

SPR chips coated with initiator self-assembled monolayers were prepared by soaking the gold-coated substrates in 0.1 mM mercaptoundecyl bromoisobutyrate in pure ethanol for overnight. The chips were then removed, rinsed with ethanol, THF, and ethanol, and blown dry using filtered compressed air and placed into a custom glass tube reactor. In a separate glass tube, 8.86 mg CuBr, 57.87 mg bpy, and 600 mg of CB were added. Both tubes were then placed under nitrogen protection. Nitrogen purged methanol (2 mL) and water (2 mL) was then added to the solids. Once everything completely dissolved (~ 15 min), the mixture was then transferred to the reactor and allowed to react for 3 h at 25°C in a shaker. The chips were removed, rinsed with water, and submerged in PBS prior to analysis. Film thicknesses were determined using a Cauchy model with a multi-wavelength ellipsometer (J. A. Woollam Co., Inc., Model alpha-SE).

6.2.6 SPR Sensor, Chips, and Calibration of the Surface Sensitivity

A laboratory SPR sensor developed at the Institute of Photonics and Electronics, Prague, Czech Republic was used as described previously.[57] This custom built SPR is based on the attenuated total reflection method and wavelength modulation. It is equipped with a four-channel flow-cell, temperature control, and uses a peristaltic pump for delivering samples. SPR sensor chips were made of a glass slide coated with titanium film (~2 nm) followed by a gold film (~48 nm) using an electron beam evaporator. Since the SPR sensitivity depends on the distance of the binding event from the SPR active surface, the sensor response due to the polymer films had to be calibrated. This was done using previously described methods.[20]

6.2.7 In situ Immobilization of CA-Lysozyme onto pCB Surfaces, Protein Deprotection, and Analyte Detection

CA-Lysozyme was dissolved in 5 mM TAPS pH 9 buffer at 1 mg/mL. Next, 120 µL of the solution was added to an Amicon Ultra-0.5 mL Centrifugal Filter unit (3,000 NMWL) followed by 380 µL of TAPS pH 9 buffer. Following the buffer exchange, the collected sample was stored at room temperature prior to being analyzed.

The functionalization procedure was monitored step-by-step in real time using an SPR sensor at 25°C. Sodium acetate buffer (10 mM) at pH 5.0 (SA) was first injected at 30 µL/min to obtain a stable baseline. Carboxylate groups of the polymer surface were then activated by flowing a solution of 0.05 M NHS and 0.2 M EDC in water for 7 min. After briefly injecting SA buffer, the collected CA-Lysozyme sample from the buffer exchange was diluted in either 10 mM Sodium acetate pH 5, 10 mM MES pH 6, or 10 mM TAPS pH 8.2 at 50 µg/mL and injected into the sensor for 60 min. Subsequent washing for 10 min with 10 mM boric acid (pH 9) containing 0.3 M NaCl (BANa) followed by 10 min of 10 mM glycine pH 3 removed non-covalently bound protein and deactivated residual NHS-esters. SA buffer was then used to reestablish a stable baseline. The amount of immobilized protein was determined as the difference between the SA injection following EDC/NHS activation and the final baseline and then converted into a surface coverage. In situations where unmodified lysozyme was used, the protein was dissolved in the corresponding immobilization buffer at the necessary concentration prior to injecting the solution into the sensor.

The immobilized CA-Lysozyme was completely deprotected by flowing 10 mM citric acid pH 4 buffer at 37°C for 7 hours followed by rinsing with SA. In order to test for the bioactivity of the immobilized protein and the efficiency of hydrolysis of the CA groups, the detection of monoclonal anti-Lys was performed before and after deprotection. Here, PBS was injected into the SPR at 50 µL/min to establish a stable baseline. Anti-Lys (1 µg/mL in PBS) was then injected for 10 minutes followed by

washing with buffer. The amount of anti-Lys detected was calculated as the different between buffer baselines and converted into surface coverage units.

6.3 Results and Discussion

6.3.1 CA-Lysozyme Characterization

The reaction chemistry of citraconic anhydride (CA) is shown in **Figure 6.2**. CA was chosen due to its ability for reacting with primary amines under alkaline conditions, temporarily blocking them via the creation of an amide linkage and a terminal carboxylate, and due to its amenability to numerous proteins. The blocking leads to a -2 change in charge per primary amine thus enabling highly negatively charged proteins to be formed (i.e. it decreases the pI of a given protein ligand). The CA-protein modification is stable under neutral to basic conditions but the reaction can be reversed to yield the original primary amine and citraconic acid under acidic conditions and room temperature (or higher).[113,114] In this work, the CA protection was allowed to go overnight to ensure all seven amines of lysozyme were blocked thus yielding a highly negatively charged ligand with favorable electrostatic conditions for being coupled to activated pCB films.[115]

After protecting lysozyme with CA, the zeta potential (ZP) of the purified conjugate was characterized as a function of hydrolysis time using pH 5, as shown in **Figure 6.3** (squares). The initial measurement of CA-Lysozyme at a time of zero and pH 9 was found to be about -24 mV, thus being highly negatively charged, as expected, due to the net -2 change in charge which accompanied the modification of each primary amine on lysozyme. As a reference, unmodified lysozyme had a ZP of about +5 mV at pH 9 (**Figure 6.3**, star, 0 min). **Figure 6.3** further revealed an initial rapid increase in ZP for CA-Lysozyme, which then slowed as time elapsed. For example, lysozyme became only slightly negative at 30 min and even positive after only 60 min. However, it took more than 3 hours to become fully deprotected, as indicated by the overlapping signals of the CA-Lysozyme at 1200 min (**Figure 6.3**,

square) to that of unmodified lysozyme at pH 5 (star, 1200 min). The size measurements as determined by DLS for both CA-Lysozyme and the unmodified protein were 1 – 2 nm, consistent with other studies.[116]

There are two important observations which can be made from these results. First, the highly negative charge of CA-Lys at pH 9 indicates that electrostatic adsorption to the activated and positively charged pCB surface would occur, as hypothesized. Second, the relatively quick increase in ZP with time indicates that the protected amines rapidly become free and subsequently available to react with NHS esters. Furthermore, since the rate of hydrolysis is pH dependent, the increase is zeta potential can be further controlled by adjusting the pH of the immobilization buffer used during pCB functionalization, which was investigated next.

6.3.2 Immobilization and Biological Specificity

Figure 6.4 shows the SPR sensor-gram results for the immobilization of CA-Lysozyme as a function of pH on activated pCB films. Following the injection of SA running buffer after EDC/NHS activation, aqueous CA-Lysozyme solutions were injected, followed by surface deactivation and washing. These latter two steps are responsible for removing non-covalently modified protein and deactivating residual NHS esters into the original zwitterionic background. While all pH values enabled similar immobilization levels for CA-Lysozyme (~90 ng/cm^2), the results revealed two distinct kinetic behaviors. First, the use of pH 6 and pH 8.2 led to a very rapid and large attraction to the surface as indicated by the initial large increase in signal. This was attributed to desirable electrostatic interactions with the positively charged surface. The plateau in the response for pH 6 is indicative of a saturated surface and is comparable to what is typically achieved for antibody immobilization on pCB films. The rapid increase, decrease, and then increase in surface coverage at pH 8.2 was attributed to the high negative charge which still persisted on the modified lysozyme under this condition. Even so, a sufficient number of protecting groups were still removed to enable efficient coupling to the surface under this slightly basic condition. The second distinct behavior is shown by the linear result for pH 5 and is representative of mass transport

limitations. Here, it is likely that the hydrolysis of the protecting groups happened very rapidly, perhaps even faster than the 30 min indicated by **Figure 6.3**, thus leading to a nearly neutral charged protein that can only diffuse to the surface rather than being attracted (or repulsed) electrostatically. Due to the desirable kinetic profile being demonstrated by the pH 6 immobilization condition, this pH was used for the remainder of studies involving CA-Lysozyme coupling.

In order to demonstrate the benefit of the citraconic anhydride protection approach for coupling basic proteins to pCB, a comparison of the pCB immobilization kinetics for CA-Lysozyme and the unmodified protein is shown in **Figure 6.5**. This figure reveals the sensor-grams for the initial part of the immobilization step in which the protein solutions were injected following the SA wash after EDC/NHS activation. The clear difference between the two curves is due to the advantageous electrostatic attraction enabled by the citraconic anhydride protection of the amine groups for CA-Lysozyme making the protein conjugate negatively charged. The initial increase and then nearly flat response for lysozyme is simply due to only the bulk solution sensor response, representing an increase in the refractive index of the solution compared to the running buffer, rather than any attraction to the activated pCB surface. This was further confirmed by the negligible immobilization level for unmodified lysozyme (~0 ng/cm^2).

While the citraconic anhydride modification method enabled sufficient immobilization, it was important confirm that the protection strategy does not lead to degradation of the original protein. In order to verify the biological specificity of immobilized CA-Lysozyme, a monoclonal antibody to lysozyme (anti-Lys) was used. When performing detection (1 ug/mL anti-Lys in PBS) immediately following the pCB functionalization procedure, a very small response (~ 3 ng/cm^2) was observed. It was hypothesized that such a low response was due to the presence of remaining CA protecting groups which were not initially removed, as indicated by **Figure 6.3**. Thus, in order to expedite the removal of the remaining groups, the functionalized surface was exposed to a pH 4 solution at an elevated temperature of 37°C for seven hours. Detection following this hydrolysis step resulted in an anti-Lys response of ~110 ng/cm^2. These results are shown in **Figure 6.6** and indicate that, upon the hydrolysis of the remaining groups, the immobilized protein maintains significant biological specificity. This has been confirmed by previous

reports that indicated citraconic anhydride reaction chemistry to cause minimal protein degradation and be fully reversible.[113,114]

6.4 Conclusions

The significant push for the application of biosensors in crude samples, and especially in personalized medicine for the detection of biomarkers and other therapeutics from blood plasma, has created a need for surface chemistries which can achieve high signal to noise (S/N) ratios in such challenging environments. Zwitterionic poly(carboxybetaine) is best suited for overcoming these difficulties due to its ability to achieve ultra low fouling properties all while presenting abundant functionalizable groups for covalently coupling. As demonstrated in this work, the use of citraconic anhydride to protect the primary amine groups enabled the immobilization of a highly basic protein onto pCB all while maintaining biological specificity. This protection strategy is amenable to many other proteins thereby extending the functionalization capabilities of pCB to ligands with isoelectric points spanning nearly the entire pH range to further advance applications involving undiluted complex media.

6.5 Figures

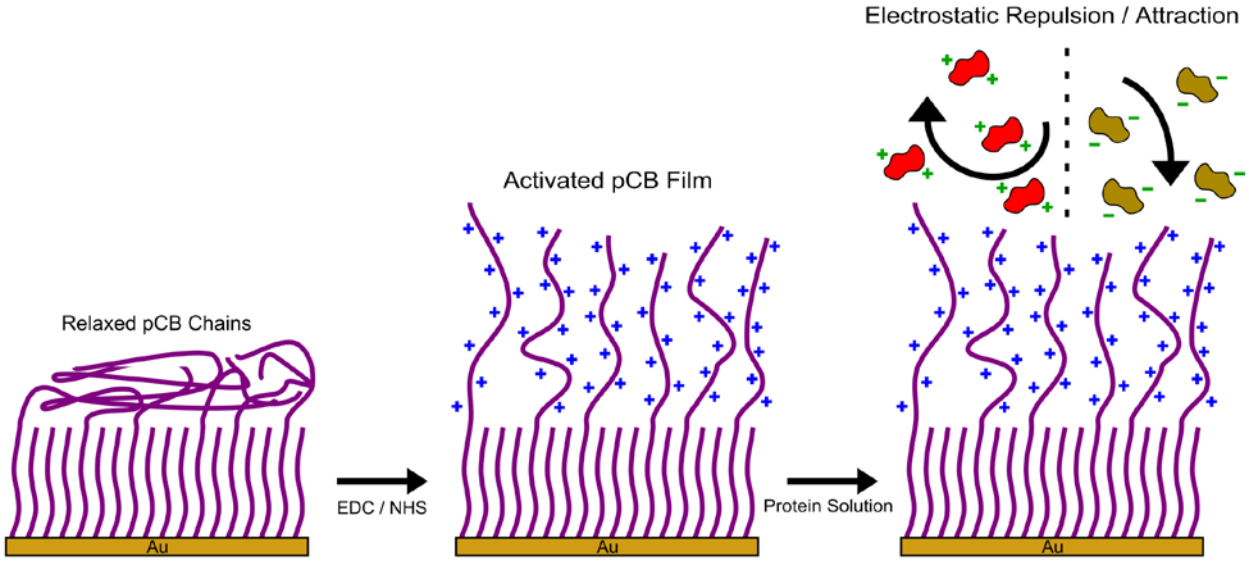

Figure 6.1.

The activation of pCB using EDC/NHS leads to a net positive charge on the surface which is advantageous for the coupling of negatively charged analytes to the film via achieving a high local concentration due favorable electrostatic interactions. However, if the pH of the immobilization buffer is too high, rapid hydrolysis of NHS-esters occurs, decreasing coupling levels. Thus, this approach works well for proteins with an isoelectric point (pI) less than pH ~7.5, which will be negatively charged using typical immobilization buffer pH values. While many proteins fall into this category, there are several ligands with larger pI values whose immobilization levels on pCB are reduced due to electrostatic repulsion from the surface.

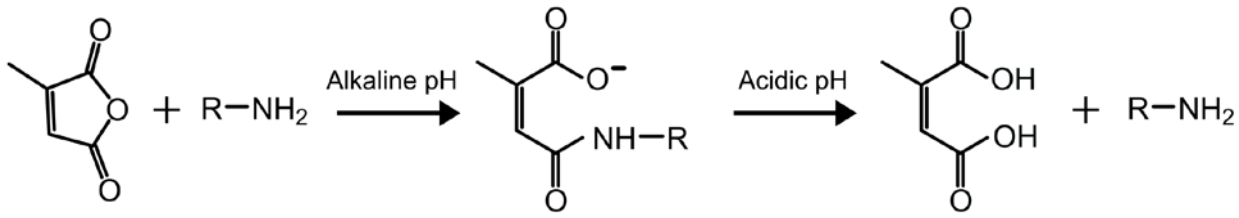

Figure 6.2.

The reaction chemistry of citraconic anhydride (CA). CA reacts with primary mines under alkaline conditions, temporarily blocking them via the creation of an amide linkage and a terminal carboxylate. This results in a -2 change in charge per amine modified thereby significantly decreasing the pI of protein ligands. The CA-protein modification is stable under neutral to basic conditions but the reaction can be reversed to yield the original primary amine and citraconic acid using acidic conditions and temperature.

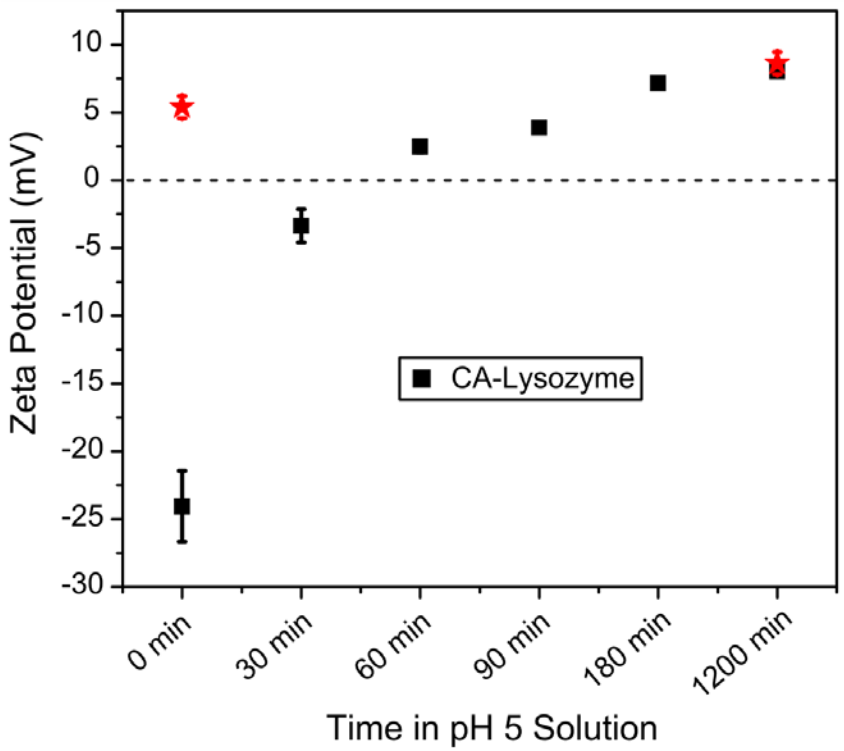

Figure 6.3.

The zeta potential of citraconic anhydride-lysozyme (CA-Lysozyme) as a function of hydrolysis time in pH 5 buffer (squares). The initial measurement at 0 min was performed in pH 9 buffer. The zeta potential for unmodified lysozyme (stars) at pH 5 and pH 9 is shown at 1200 min and 0 min, respectively, and was used as a reference. More than 3 hours was required to fully deprotected CA-Lysozyme as indicated by the overlapping signals at 1200 min. The size measurements as determined by DLS for both CA-Lysozyme and the unmodified protein were 1 – 2 nm.

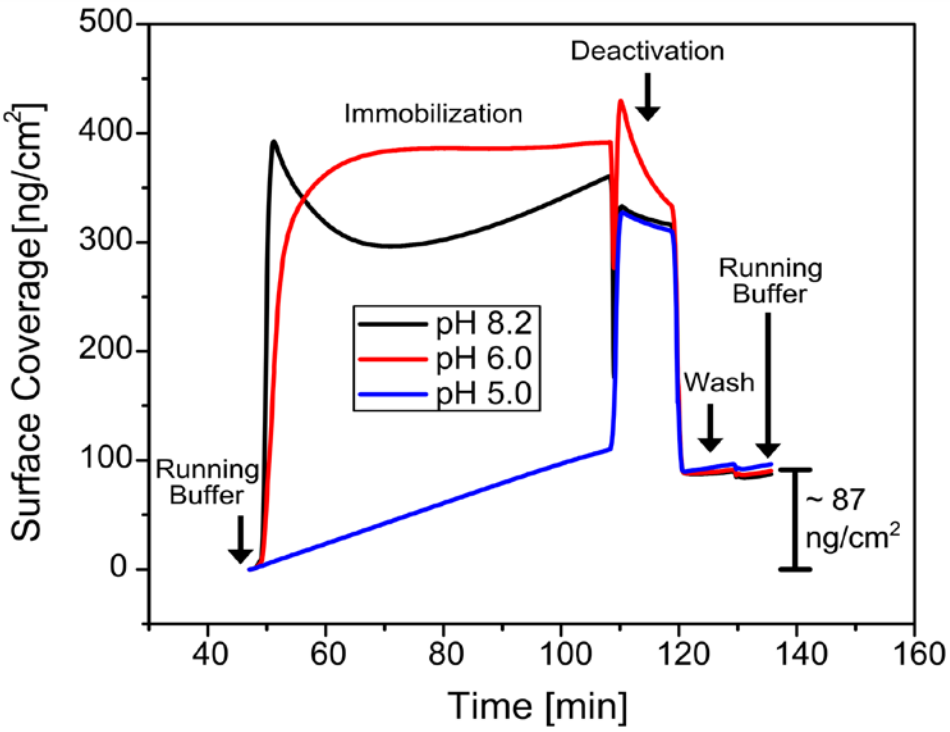

Figure 6.4.

The SPR sensor-gram results for the immobilization of CA-Lysozyme as a function of pH on activated pCB films. Following EDC/NHS activation and the injection of running buffer, the immobilization response for CA-Lysozyme (50 µg/mL) at three different pH values was monitored. Subsequent deactivation and washing removed non-covalently attached protein and deactivated residual NHS-esters. All three results led to similar immobilization levels but with two distinct kinetic behaviors. First, the rapid initial response for pH 6 and pH 8.2 was the result of electrostatic attraction to the surface where as the linear response for pH 5 was likely the result of mass transport limitations in which a neutral analyte could only diffuse to the surface without favorable electrostatic interactions. As a reference, unmodified lysozyme achieved negligible immobilization levels (~ 0 ng/cm^2).

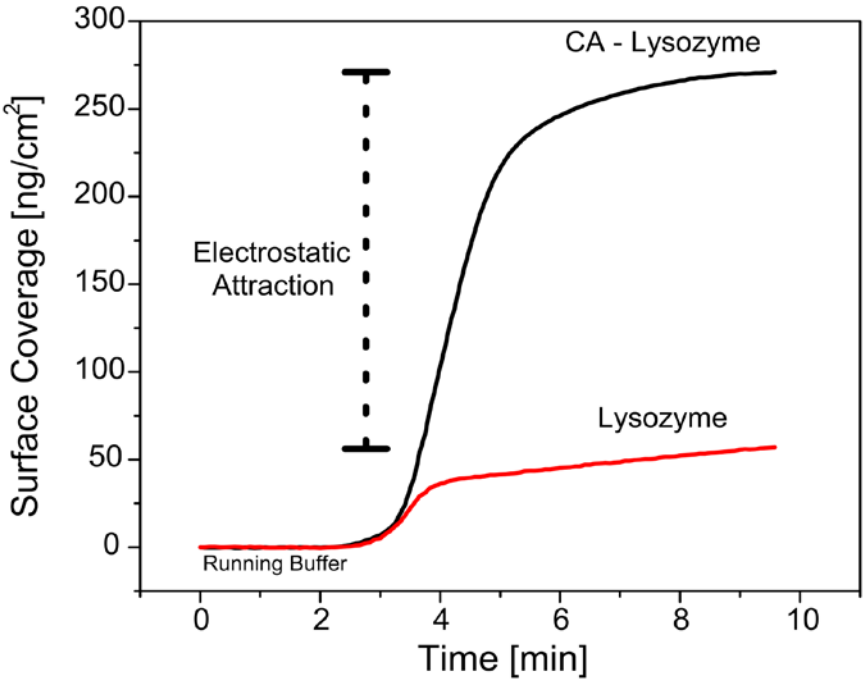

Figure 6.5.

A comparison of the pCB immobilization kinetics for CA-Lysozyme and the unmodified protein. This sensor-gram reveals the initial part of the immobilization step in which the protein solutions were injected following the SA wash after EDC/NHS activation. The clear difference between the two curves is due to the advantage of electrostatic attraction enabled by the citraconic anhydride protection of the amine groups on lysozyme making the protein conjugate negatively charged. The initial increase and then nearly flat response for unmodified lysozyme is simply due to the bulk solution sensor response, representing mostly an increase in the refractive index of the solution compared to the running buffer.

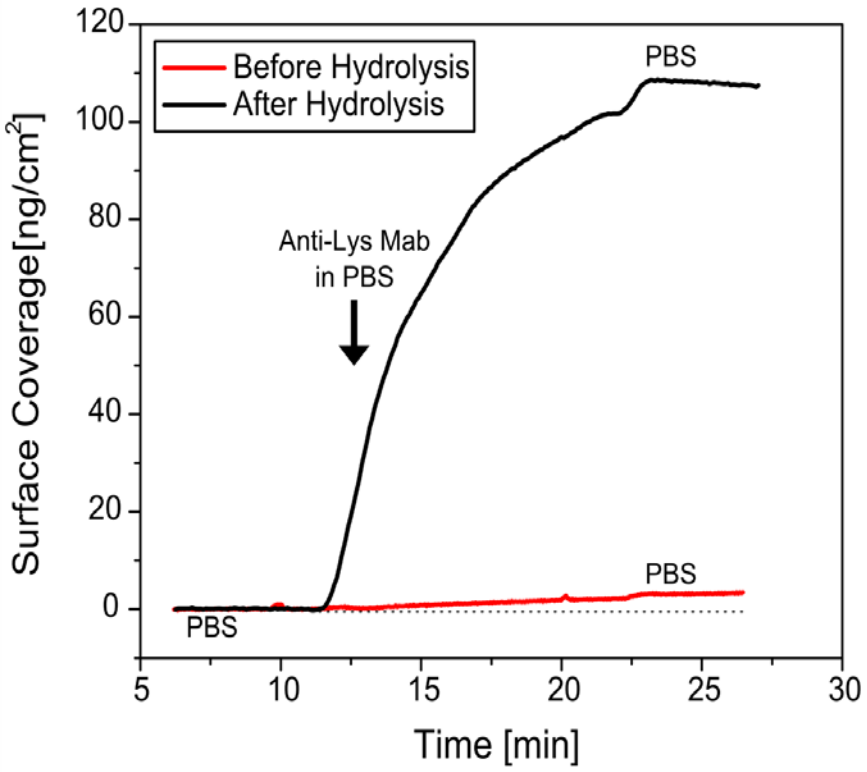

Figure 6.6.

The detection of monoclonal anti-Lys on CA-Lysozyme functionalized pCB films. Here, 1 µg/mL of anti-Lys was injected for 10 min followed by rinsing with buffer. The red sensor-gram shows the response immediately following the immobilization procedure. The black sensor-gram represents the response following the hydrolysis of residual CA protecting groups by injecting a 37°C and pH 4 solution over the surface for 7 hours. These results reveal that, upon complete hydrolysis of the protecting groups, lysozyme retains its biological specificity.

Chapter 7

Immobilization of Basic Proteins using a Switchable Zwitterionic Polymer with Ultra Low Fouling Properties

Zwitterionic carboxybetaine (CB) polymer films have been shown to enable convenient immobilization of protein ligands using standard amino-coupling chemistry all while maintaining ultra low fouling properties to undiluted complex media. However, due to CB containing a permanently positively charged quaternary amine which makes the surface slightly positive following EDC/NHS activation, primarily only proteins with an isoelectric point less than pH ~ 7.5 can be efficiently coupled to the surface using electrostatic attraction. The use of a new switchable polymer material containing a tertiary amine and a carboxylic acid, tertiary amine carboxybetaine methacrylate (TA-CBMA), offers a potential solution. It is proposed that activating polymer films composed of TA-CBMA using sulfo-NHS will result in a net negatively charged surface under neutral pH immobilization conditions, where sulfo-NHS is not prone to hydrolysis. This is based on the observed drop in pKa of the tertiary amine to ~5.5 upon esterification of the carboxylate group. The window created in which the surface will be negatively charged all while containing a stable amine reactive agent will enable efficient immobilization of basic proteins via traditional electrostatic attraction. Following deactivation, the surface will return to its original zwitterionic non-fouling background.

7.1 Introduction

Protein resistance to complex media has been achieved by few materials, prominently, zwitterionic carboxybetaine (CB) polymers. Such films exhibit ultra low fouling properties to undiluted human serum and plasma (i.e., < 5 ng/cm^2 of non-specific protein adsorption) and possess abundant functionalizable groups for enabling protein immobilization via amino-coupling chemistry.[17] Following

EDC/NHS activation of pCB films, the presence of a permanently charged quaternary amine on carboxybetaine results in a net positive charge on the surface. Under these conditions, the most efficient protein immobilization occurs when ligands are attached using a solution with a pH greater than their corresponding isoelectric point (pI), thus enabling favorable electrostatic interactions to increase the local concentration of analytes near the surface and significantly improve the coupling efficiency.[20,57,111] Upon deactivation, pCB returns to its original zwitterionic state allowing for the sensitive detection of target analytes from undiluted complex media. While this approach works well for numerous proteins, there is one difficulty. Due to the rapid hydrolysis of NHS esters in basic pH (pH > ~8.5)[115] which significantly decreases immobilization levels, the higher end of protein isoelectric points which can be accommodated using pCB films is around pH 7.5. As mentioned in the previous chapter, a pH less than the pI for a given ligand results in low immobilization levels due to charge-charge repulsion. Here, a novel approach was investigated in which the modification of a basic ligand using citraconic anhydride may not be practical.

Recently, a single material containing a tertiary amine and a carboxylic acid separated by a single carbon spacer has been introduced.[25] The tertiary amine can exist in both positive and neutral states while the carboxylic acid can exist in anionic and neutral forms, as shown in **Figure 7.1a**. Surface grafted polymers composed of this material, tertiary amine carboxybetaine methacrylate (TA-CBMA), subsequently revealed distinct charge switching properties. For example, at pH < 4 the polymer films were found to be positively charged; at pH > 8 the films were negatively charged; at pH values between 4 and 8 the film was zwitterionic and demonstrated ultra low fouling properties to undiluted human serum and plasma. However, the key property of this material which makes it amenable to the immobilization of basic ligands is shown in **Figure 7.1b**. The tertiary amine component on the unmodified TA-CBMA monomer has a pKa of ~8.7. Upon the esterification of the carboxylic acid, the pKa drops to ~5.5.[25] Lacking a net charge on the attached R-group, the esterification results in a neutral (non-ionic) material at pH > ~6.0.

However, if a negatively charged and amine reactive agent is chosen as the R-group, such as N-hydroxysulfosuccinimide (sulfo-NHS, **Figure 7.1c**) whose esters hydrolyze at pH values similar to those

of NHS, there exists an immobilization pH window in which the surface would theoretically be negatively charged without risking the rapid loss of the amine reactive agent. Raising the pH during surface deactivation could then subsequently be used to hydrolyze the residual sulfo-NHS groups, as with traditional pCB, resulting in the original zwitterionic background. Thus, polymers composed of TA-CBMA have the potential to be used for the immobilization of highly basic proteins all while maintaining the low fouling zwitterionic background following functionalization. Here, this hypothesis was investigated.

7.2 Experimental Section

7.2.1 ^{1}H NMR Characterization of Solution Activated TA-CBMA

The tertiary amine carboxybetaine methacrylate monomer (TA-CBMA) was synthesized as described previously.[25] Solution activation of TA-CBMA was then studied using a 300 MHz ^{1}H NMR. First, TA-CBMA (15 mg), 1-Ethyl-3-(3-dimethylaminopropyl) carbodiimide hydrochloride (63 mg, EDC), and N-hydroxysuccinimide (38 mg, NHS) was each dissolved in 0.5 mL of deuterated chloroform and then combined and allowed to react overnight at room temperature with mixing. TA-CBMA (15 mg) dissolved in 1.5 mL of deuterated chloroform was used as the control. The next day, the pure monomer sample as well as the crude mixture was analyzed using ^{1}H NMR.

7.2.2 Surface Initiated Photoiniferter-Mediated Polymerization (SI-PIMP)

The monomer solution was prepared by weighing out the appropriate amount of monomer and adding solvents to achieve the desired monomer concentration and solvent composition (methanol:water = 90:10) all under nitrogen protection. A gold coated substrate prepared with a dithiocarbamate photo-iniferter self-assembled monolayer (SAM) was placed in a quartz reaction tube. The test tube was sealed

with a rubber septum and placed under nitrogen protection. The degassed monomer solution was then transferred to the reaction tube using a syringe, under nitrogen protection. A stream of nitrogen was allowed to pass through the monomer solution in the reaction tube for 1-2 min before removing and wrapping with parafilm. In order to prevent the cleavage of the thiol-gold bond of the photo-iniferter SAM, a 280 nm cutoff filter was mounted to the outside of the reaction tube. Samples were then irradiated with 302 nm-centered UV light (UVP, model UVM-57) for the desired reaction time. Following the polymerization, the substrates were removed from the reactor, washed with PBS, and then stored in PBS overnight.[25]

7.3 Results and Discussion

As the investigation of surface grafted polymer films is traditionally more difficult, the solution activation properties of TA-CBMA were first investigated as a simplified approach to determine the feasibility of our hypothesis. The ^{1}H NMR results for the solution activation of TA-CBMA using EDC/NHS in deuterated chloroform is shown in **Figure 7.2**. **Figure 7.2a** shows the control spectrum of monomer in only solvent while **Figure 7.2b** shows the crude mixture for the reaction of TA-CBMA with EDC and NHS. There are several key observations which indirectly but clearly reveal the presence of an activated TA-CBMA material being formed. First, a large chemical shift in the vinyl protons was observed (1 and 2 in **Figures 7.2a and 7.2b**). Here, peak 1 shifted from 6.14 ppm to 6.68 ppm and peak 2 shifted from 5.63 ppm to 6.04 ppm. The ratio of the integrations of peak 2 to peak 1 for **Figures 7.2a and 7.2b** also changed slightly, from 1.16:1 to 1.26:1, respectively. Another observation was the absence of the peak for proton 3 in **Figure 7.2b**, which was likely shifted up-field where it could not be easily observed due to peak overlapping. The last major observation indicative of an activated TA-CBMA material involves the presence of a single singlet for proton 4 in **Figure 7.2a** as opposed to the 3 singlets for proton 4 in **Figure 7.2b**. This group of three singlets for the latter is likely attributed to the presence of three different versions of the original starting material (TA-CBMA). These include TA-CBMA itself,

TA-CBMA-EDC, and TA-CBMA-NHS as shown in **Figure 7.2c**. Taken together, the differences observed in the two spectra strongly indicate the ability of TA-CBMA to be activated in solution.

The positive result from the NMR analysis led to an attempt at the synthesis of TA-CBMA-NHS. This was attempted to verify the further confirm the formation of the activated material and also to enable a better characterization of the charge switching properties of the TA-CBMA-NHS by verifying the shift in pKa for the amine group. Following the synthesis, the TLC plate (using DCM and methanol) revealed a near complete conversion of the starting material into a single spot containing the activated TA-CBMA. However, it was unfortunately observed that the activated product was unstable and slowly reverted back into the starting material over time, during the purification, as indicated by TLC analysis. A proposed mechanism for the instability of the activated TA-CBMA is presented in **Figure 7.3**, which involves the formation of a highly unstable aziridinone (i.e. a three-membered ring) which rapidly breaks down to yield the starting material and NHS. A subsequent attempt at the activation of a poly(TA-CBMA) brush made via surface initiated photo-iniferter mediated polymerization revealed the formation of a hydrophobic surface which rapidly transformed into a superhydrophilic surface upon rinsing with ethanol. It is likely that the activation of surface grafted polymer films will be the required route to enable functionalization of basic proteins using this material.

7.4 Conclusions

In this work, a novel zwitterionic material containing a tertiary amine and carboxylic group separated by a single carbon space (TA-CBMA) was investigated as an approach for immobilizing highly basic proteins onto an ultra low fouling background. ^{1}H NMR data strongly indicate the presence of an activated TA-CBMA during a solution characterization study. Further evidence which supports the ability to activate this material was provided by the formation of a hydrophobic film upon activating a polymer brush, which was quickly hydrolyzed back into a superhydrophilic surface upon washing with ethanol.

While the conditions for functionalizing poly(TA-CBMA) brushes were not yet determined, the promising evidence supports further investigation of this work.

7.5 Figures

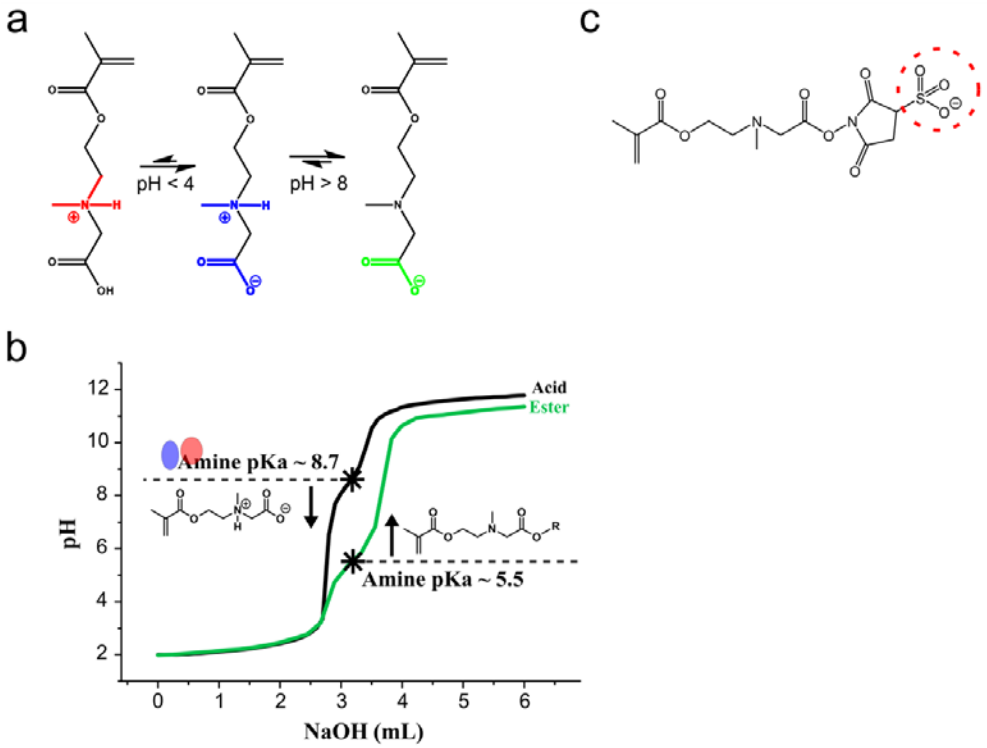

Figure 7.1.

The switchable zwitterionic material, TA-CBMA, contains a tertiary amine and a carboxylic acid separated by a single carbon spacer. (a) The three distinct charged states of TA-CBMA, corresponding to the pKa's of the tertiary amine and the carboxylic acid, 8.7 and 2.6, respectively. (b) Esterification of the carboxylate group leads to a decrease in the pKa of the tertiary amine. The pKa for the ester-derivative was observed ~5.5.[25] (c) It is hypothesized that if a negatively charged and amine reactive agent is chosen for the R-group, such as N-hydroxysulfosuccinimide (sulfo-NHS) shown here which is stable at pH < 8.5, there exists an immobilization pH window for which the surface would be negatively charged without risking the rapid loss of the amine reactive agent. Raising the pH during surface deactivation could then subsequently be used to hydrolyze the residual sulfo-NHS groups, as with traditional pCB, resulting in the original zwitterionic background. Thus, polymers composed of TA-CBMA have the potential to be used for the immobilization of highly basic proteins all while maintain the low fouling zwitterionic background following functionalization.

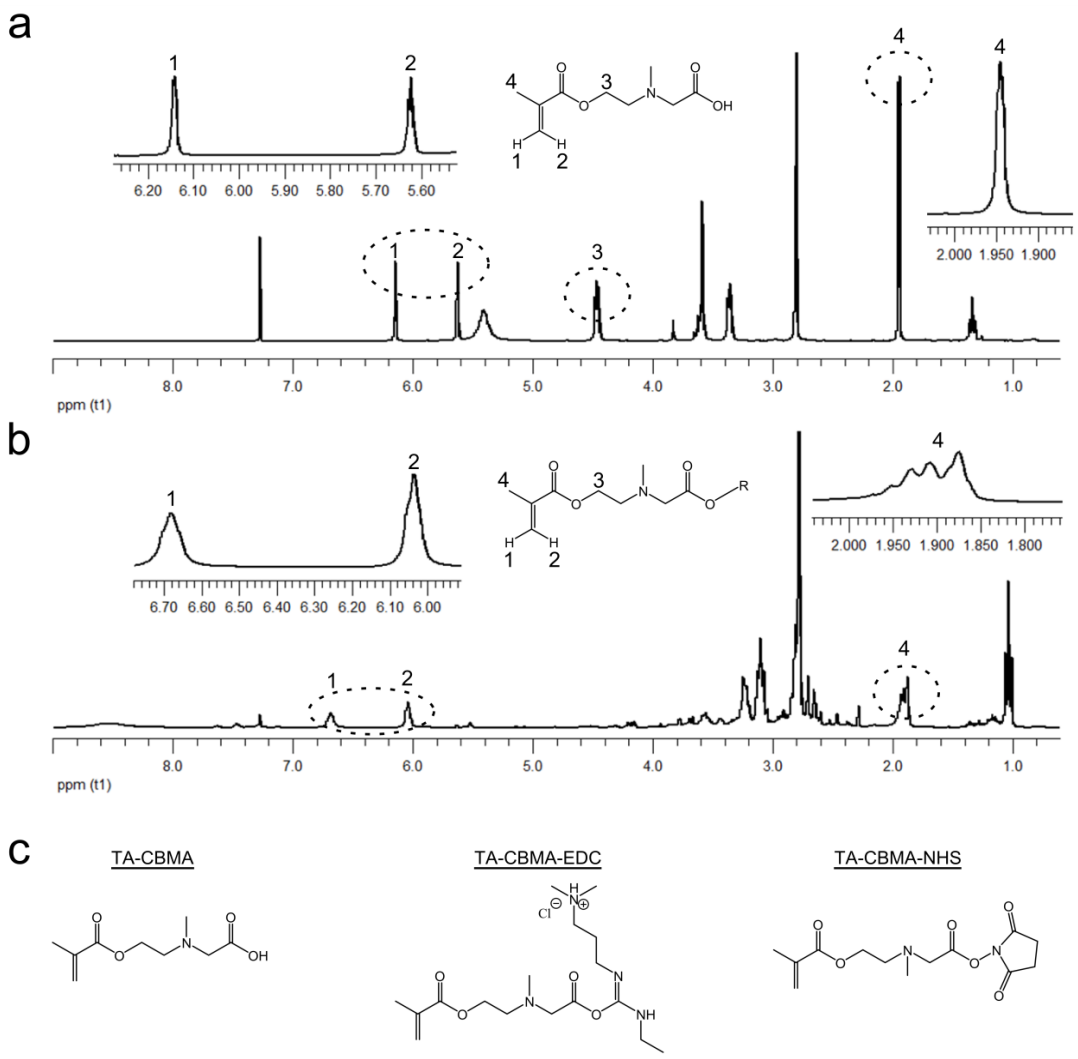

Figure 7.2.

The ^{1}H NMR results for the solution activation of TA-CBMA using EDC and NHS in deuterated chloroform. (a) The control spectrum of the TA-CBMA monomer. (b) The crude mixture for the reaction of TA-CBMA with EDC and NHS. Key observations include: a large chemical shift in the vinyl protons (1 and 2 in (a) and (b)): a slight change in the ratio of the integrations of peak 2 to peak 1 for the pure monomer and the reaction mixture, from 1.16:1 to 1.26:1, respectively: the absence of the peak for proton 3 in the reaction mixture spectrum: and the change of a single singlet for proton 4 in (a) to three singlets for proton 4 in (b), the latter which is likely attributed to the presence of three difference versions of the original starting material (c). Taken together, the difference between the two spectra strongly indicates the ability of TA-CBMA to be activated in solution.

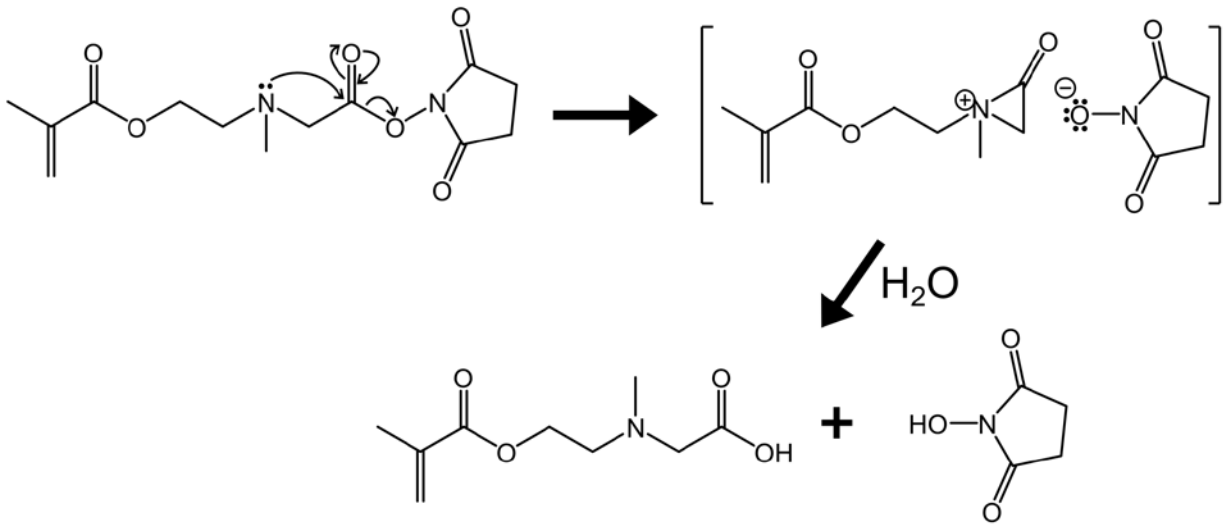

Figure 7.3.

A proposed mechanism of TA-CBMA-NHS instability involving the formation of a highly unstable aziridinone which can rapidly break down and reform the starting material.

Chapter 8

Conclusions

The two major short comings which severely limit the advancement and implementation of personalized medicine via biomarker-based diagnostics include high occurrences of false-positives, from non-specific binding, and a lack of sensitivity, due to low ligand loading. The significant push for the application of biosensors in crude samples, such as human blood plasma for biomarker detection, has created a need for surface chemistries which can meet the challenges of such complex environments. In this dissertation, these shortcomings were addressed using zwitterionic poly(carboxybetaine) (pCB) surface chemistry.

First and most importantly, a minimal surface density was found to be required to achieve ultra low fouling surface coatings. While previous literature had indicated the need for certain polymer thicknesses to be achieved for the best protein resistance, this work established a simple approach and pointed towards a single parameter which can be used to predict ultra low fouling polymer films. This knowledge was vital to the remainder of the dissertation as it served as a necessary benchmark which must be achieved to enable protein resistance from undiluted complex media. Next, the ability to reduce background fouling was then applied to protein arrays on pCB films. This work highlighted the difficulty in achieving both uniform spot morphology as well as excellent non-fouling properties following functionalization that, once achieved, could improve the sensitivity for multiplexed detection of target analytes directly from undiluted human plasma. The work also introduced a novel parameter which allows for the quantitative description of spot morphology.

Due to the limitations of relatively low signal to noise ratios of 2-dimensional films, two approaches were investigated to improve the “signal” component. The first led to the development of a hierarchical architecture. It was found that thin but highly dense pCB films, when grown under controlled polymerization conditions, could be manipulated and re-initiated to grow multiple layers, each exhibiting

a different functionality. By creating a thin and highly dense bottom layer, for ultra low fouling properties, with a loose top layer, for high ligand loading, this approach doubled both the antibody immobilization capacity and the corresponding response to antigen, compared to traditional 2-D polymer films. It also served as a generic model which can be applied to many other polymer systems.

While all of the above methods for improving S/N ratios were based on the "graft-from" approach, an additional challenge was investigated in which a "graft-to" based zwitterionic pCB surface chemistry was necessary. Such coating methods, while more difficult, offer the advantages of increased simplicity and convenience for more practical applications of biosensors, especially those sensors with unique and small geometries that are capable of increased theoretical sensitivities. Here, taking advantage of the larger signal (i.e. larger sensitivity) of such devices involved the synthesis of $DOPA_2$-pCB_2 to achieve ultra low fouling and functionalizable coatings via "grafting to" the biosensing surface. This method is also easily transferable to other sensor platforms. Furthermore, these studies highlighted the need to balance the activation and deactivation conditions with respect to pCB functionalization in order to achieve sensitive detection from undiluted complex matrices.

Two unique zwitterionic immobilization strategies for pCB, to enable the coupling of highly basic proteins to the ultra low fouling surface, were also explored. As new ligands are continuously being designed and engineered, this functionality must be developed for pCB to continue to advance applications in complex media. Due to the polymer containing a permanently positively charged quaternary amine, which makes the surface slightly positive following EDC/NHS activation, only proteins with an isoelectric point near neutral pH or lower can be efficiently coupled to the surface using electrostatic attraction. This increases the local concentration of analytes near the film and improves the coupling efficiency. The first solution to address this concern involved the use of a reversible blocking agent to temporarily modify the basic ligand and substantially reduce its isoelectric point. Subsequent functionalization of the basic ligand followed by deprotection of the blocking group revealed an immobilization strategy which, importantly, maintained biological specificity. The second approach involved a novel and fully switchable zwitterionic material containing a tertiary amine and carboxylic

acid in a single molecule. Importantly, this compound exhibits shifts in the pKa of the amine functional group upon esterification of the acid. Early studies to take advantage of these properties for immobilizing basic proteins indicated promising results.

References

[1] Bedard, P. L., et al. *Nature* 2013, *501*, 355-364.

[2] Brennan, D. J., et al. *Nat. Rev. Cancer* 2010, *10*, 605-617.

[3] Maliepaard, M., et al. *Nat. Rev. Drug Discov.* 2013, *12*, 103-115.

[4] Hartwell, L., et al. *Nat Biotech* 2006, *24*, 905-908.

[5] Maecker, H. T., et al. *Nat. Rev. Rheumatol.* 2012, *8*, 317-328.

[6] Hanash, S. M., et al. *Nature* 2008, *452*, 571-579.

[7] Arnaud, C. H. *Chem. Eng. News* 2011, *89*, 40-43.

[8] Giljohann, D. A.; Mirkin, C. A. *Nature* 2009, *462*, 461-464.

[9] Malekzadeh, A., et al. *Methods* 2012, *56*, 508-513.

[10] Vasilyeva, E., et al. *Angewandte Chemie-International Edition* 2011, *50*, 4137-4141.

[11] Gaster, R. S., et al. *Nat. Med.* 2009, *15*, 1327-1332.

[12] Liu, Y. S., et al. *Biomedical Microdevices* 2011, *13*, 769-777.

[13] Piliarik, M., et al. *Biosens. Bioelectron.* 2010, *26*, 1656-1661.

[14] Wellhausen, R.; Seitz, H. *Journal of Biomedicine and Biotechnology* 2012.

[15] Breen, E. C., et al. *Clin. Vaccine Immunol.* 2011, *18*, 1229-1242.

[16] Hucknall, A., et al. *Adv. Mater.* 2009, *21*, 2441-2446.

[17] Jiang, S. Y.; Cao, Z. Q. *Adv. Mater.* 2010, *22*, 920-932.

[18] Hucknall, A., et al. *Adv. Mater.* 2009, *21*, 1968-1971.

[19] Ladd, J., et al. *Biomacromolecules* 2008, *9*, 1357-1361.

[20] Vaisocherova, H., et al. *Anal. Chem.* 2008, *80*, 7894-7901.

[21] Burg, T. P., et al. *Nature* 2007, *446*, 1066-1069.

[22] Chen, J. R., et al. *Biotechnol. Adv.* 2004, *22*, 505-518.

[23] Zhang, X. Q., et al. *Sensors* 2009, *9*, 1033-1053.

[24] Dalsin, J. L., et al. *Langmuir* 2005, *21*, 640-646.

[25] Sundaram, H. S., et al. *Chemical Science* 2014, *5*, 200-205.

[26] VaisocherovaÌ, H., et al. *Anal. Chem.* 2008, *80*, 7894-7901.

[27] Ratner, B. D., et al. In *Biomaterials Science - An Introduction to Materials in Medicine (2nd Edition)*. 2nd ed.; Elsevier: 2004.

[28] Farokhzad, O. C.; Langer, R. *ACS Nano* 2009, *3*, 16-20.

[29] Yang, W., et al. *Langmuir* 2009, *25*, 11911-11916.

[30] Cheng, N., et al. *Macromol. Rapid Commun.* 2006, *27*, 1632-1636.

[31] Toomey, R.; Tirrell, M. In *Annu. Rev. Phys. Chem.*, 2008; Vol. 59, pp 493-517.

[32] Jordan, R. In *Surface-initiated polymerization I*. Springer: Berlin, 2006.

[33] Voros, J. *Biophys. J.* 2004, *87*, 553-561.

[34] Kim, B. S., et al. *Macromolecules* 2009, *42*, 368-375.

[35] Wang, X. J., et al. *Langmuir* 2006, *22*, 817-823.

[36] Pyun, J., et al. *Macromol. Rapid Commun.* 2003, *24*, 1043-1059.

[37] Braunecker, W. A.; Matyjaszewski, K. *Prog. Polym. Sci.* 2007, *32*, 93-146.

[38] Edmondson, S., et al. *Macromolecules* 2007, *40*, 5271-5278.

[39] Jones, D. M., et al. *Langmuir* 2002, *18*, 1265-1269.

[40] Krause, J. E., et al. *Macromolecules* 2011, *44*, 9213-9220.

[41] Homola, J.; Dostálek, J. In *Surface plasmon resonance based sensors*. Springer: Berlin; New York, 2006.

[42] Li, L. Y., et al. *J. Phys. Chem. B* 2005, *109*, 2934-2941.

[43] Turgman-Cohen, S.; Genzer, J. *Macromolecules* 2010, *43*, 9567-9577.

[44] Mendelsohn, J. D., et al. *Langmuir* 2000, *16*, 5017-5023.

[45] Aspnes, D. E. *Thin Solid Films* 1982, *89*, 249-262.

[46] Berrade, L., et al. *Pharm. Res.* 2011, *28*, 1480-1499.

[47] Hartmann, M., et al. *Anal. Bioanal. Chem.* 2009, *393*, 1407-1416.

[48] Huang, R. P., et al. *Curr. Proteomics* 2012, *9*, 55-70.

[49] Ligler, F. S. *Anal. Chem.* 2009, *81*, 519-526.

[50] Yu, X. B., et al. *Clin. Chem.* 2010, *56*, 376-387.

[51] Zhang, Z., et al. *Biomacromolecules* 2008, *9*, 2686-2692.

[52] Brault, N. D., et al. *Biomacromolecules* 2012, *13*, 589-593.

[53] Ladd, J., et al. *Anal. Chem.* 2008, *80*, 4231-4236.

[54] Chen, S., et al. *Langmuir* 2003, *19*, 2859-2864.

[55] Faca, V. M., et al. *PLos Med.* 2008, *5*, 953-967.

[56] Seurynck-Servoss, S. L., et al. *Anal. Biochem.* 2007, *371*, 105-115.

[57] Vaisocherova, H., et al. *Biosens. Bioelectron.* 2009, *24*, 1924-1930.

[58] Gutmann, O., et al. *Lab Chip* 2005, *5*, 675-681.

[59] Ressine, A., et al. *NanoBioTechnology* 2005, *1*, 93-103.

[60] Hara, I., et al. *The Journal of Urology* 2002, *167*, 1487-1491.

[61] Meyerovitch, J., et al. *Arch. Intern. Med.* 2007, *167*, 1533-1538.

[62] Gubala, V., et al. *Anal. Chem.* 2012, *84*, 487-515.

[63] Wang, A. Z., et al. In *Annu. Rev. Med.*, Caskey, C. T.; Austin, C. P.; Hoxie, J. A., Eds. Annual Reviews: Palo Alto, 2012; Vol. 63, pp 185-198.

[64] Whitehead, K. A., et al. *Nat. Rev. Drug Discovery* 2009, *8*, 129-138.

[65] Buchen, L. *Nature* 2011, *471*, 428-432.

[66] Rifai, N., et al. *Nat. Biotechnol.* 2006, *24*, 971-983.

[67] Sawyers, C. L. *Nature* 2008, *452*, 548-552.

[68] Thaxton, C. S., et al. *Proc. Natl. Acad. Sci. U. S. A.* 2009, *106*, 18437-18442.

[69] Lofas, S.; Johnsson, B. *Journal of the Chemical Society-Chemical Communications* 1990, 1526-1528.

[70] Masson, J. F., et al. *Talanta* 2005, *67*, 918-925.

[71] Hume, P. S.; Anseth, K. S. *Biomaterials* 2010, *31*, 3166-3174.

[72] Sebra, R. P., et al. *Langmuir* 2005, *21*, 10907-10911.

[73] Huang, C.-J., et al. *Adv. Mater.* 2012, *24*, 1834-1837.

[74] Demers, L. M. *Clin. Lab. Med.* 2004, *24*, 19-+.

[75] Matyjaszewski, K., et al. *Macromolecules* 1999, *32*, 8716-8724.

[76] Lee, B. S., et al. *Biomacromolecules* 2007, *8*, 744-749.

[77] Topham, P. D., et al. *Macromolecules* 2008, *41*, 9542-9547.

[78] Jordan, R., *Surface-initiated polymerization I*. Springer: Berlin, 2006.

[79] Homola, J. In *Surface Plasmon Resonance Based Sensors.* Springer-Verlag: Berlin, Germany, 2006.

[80] Barbey, R., et al. *Chem. Rev.* 2009, *109*, 5437-5527.

[81] Benson, J. D., et al. *Nature* 2006, *441*, 451-456.

[82] Feng, B., et al. In *Advances in Clinical Chemistry, Vol 47*, Elsevier Academic Press Inc: San Diego, 2009; Vol. 47, pp 45-57.

[83] Radpour, R., et al. *Genet. Test. Mol. Biomark.* 2009, *13*, 565-571.

[84] Ullah, M. F.; Aatif, M. *Cancer Treat. Rev.* 2009, *35*, 193-200.

[85] Ferrari, M. *Nature Reviews Cancer* 2005, *5*, 161-171.

[86] Cheng, M. M. C., et al. *Curr. Opin. Chem. Biol.* 2006, *10*, 11-19.

[87] Paulovich, A. G., et al. *Proteomics Clinical Applications* 2008, *2*, 1386-1402.

[88] Chen, S. F., et al. *J. Am. Chem. Soc.* 2005, *127*, 14473-14478.

[89] Kim, S. K., et al. *Nanotechnology* 2009, *20*, 7.

[90] Ryu, D. Y., et al. *Science* 2005, *308*, 236-239.

[91] Lee, H., et al. *Science* 2007, *318*, 426-430.

[92] Li, G. Z., et al. *Biomaterials* 2008, *29*, 4592-4597.

[93] Gao, C., et al. *Biomaterials* 2010, *31*, 1486-1492.

[94] Archakov, A. I.; Ivanov, Y. D. *Molecular Biosystems* 2007, *3*, 336-342.

[95] Homola, J. *Chem. Rev.* 2008, *108*, 462-493.

[96] Zhu, Z. Q., et al. *Sensor Lett.* 2005, *3*, 71-88.

[97] Homola, J. In *Surface plasmon resonance based sensors*. Springer: Berlin; New York, 2006; Vol. 4, p 251.

[98] Glasmastar, K., et al. *J. Colloid Interface Sci.* 2002, *246*, 40-47.

[99] Graneli, A., et al. *Langmuir* 2003, *19*, 842-850.

[100] Szunerits, S., et al. *Langmuir* 2006, *22*, 10716-10722.

[101] Adams, A. C., et al. *J. Electrochem. Soc.* 1981, *128*, 1545-1551.

[102] Ceiler, M. F., et al. *J. Electrochem. Soc.* 1995, *142*, 2067-2071.

[103] Lee, H., et al. *Proc. Natl. Acad. Sci. U. S. A.* 2006, *103*, 12999-13003.

[104] Wielema, T. A.; Engberts, J. *Eur. Polym. J.* 1990, *26*, 415-421.

[105] Bousse, L., et al. *J. Colloid Interface Sci.* 1991, *147*, 22-32.

[106] Ibraeva, Z. E., et al. *Macromol. Chem. Phys.* 2004, *205*, 2464-2472.

[107] Waite, J. H. *Int. J. Adhes. Adhes.* 1987, *7*, 9-14.

[108] Luong, J. H. T., et al. *Biotechnol. Adv.* 2008, *26*, 492-500.

[109] Ferguson, B. S., et al. *Sci. Transl. Med.* 2013, *5*, 213ra165.

[110] Arlett, J. L., et al. *Nat Nano* 2011, *6*, 203-215.

[111] Lofas, S., et al. *Biosens. Bioelectron.* 1995, *10*, 813-822.

[112] Wetter, L.; Deutsch, H. *J. Biol. Chem.* 1951, *192*, 237-242.

[113] Habeeb, A. F. S. A.; Atassi, M. Z. *Biochemistry* 1970, *9*, 4939-4944.

[114] Shetty, J. K.; Kinsella, J. E. *Biochem. J.* 1980, *191*, 269-0.

[115] Hermanson, G. T. In *Bioconjugate techniques*. Academic Press: San Diego, 1996.

[116] Parmar, A. S.; Muschol, M. *Biophys. J.* 2009, *97*, 590-598.

Curriculum Vitae

Norman D. Brault was born in Anchorage, AK. He received his Bachelor of Science in Chemical and Biological Engineering at Montana State University in Bozeman, MT, in 2007, and his Master's in Chemical Engineering at University of Washington in Seattle, WA in 2009.

He is an author on the following publications:

Sundaram HS, Ella-Menye J-R, **Brault N.D.**, Shao Q., Jiang S. Reversibly switchable polymer with cationic/zwitterionic/anionic behavior through synergistic protonation and deprotonation. Chemical Science. 2014;5(1):200-5.

Brault, N.D., A.D. White, A.D. Taylor, Q. Yu, and S. Jiang, *Directly Functionalizable Surface Platform for Protein Arrays in Undiluted Human Blood Plasma.* Analytical Chemistry, 2013. 85(3): p. 1447-1453.

Brault, N.D., H.S. Sundaram, Y.T. Li, C.J. Huang, Q.M. Yu, and S.Y. Jiang, *Dry Film Refractive Index as an Important Parameter for Ultra-Low Fouling Surface Coatings.* Biomacromolecules, 2012. 13(3): p. 589-593.

Brault, N.D., H.S. Sundaram, C.-J. Huang, Y. Li, Q. Yu, and S. Jiang, *Two-Layer Architecture Using Atom Transfer Radical Polymerization for Enhanced Sensing and Detection in Complex Media.* Biomacromolecules, 2012. 12(12): p. 4049-4056.

Huang, C.J.[†], **N.D. Brault**[†], Y.T. Li, Q.M. Yu, and S.Y. Jiang, *Controlled Hierarchical Architecture in Surface-initiated Zwitterionic Polymer Brushes with Structurally Regulated Functionalities.* Advanced Materials, 2012. 24(14): p. 1834-1837.

Keefe, A.J., **N.D. Brault**, and S.Y. Jiang, *Suppressing Surface Reconstruction of Superhydrophobic PDMS Using a Superhydrophilic Zwitterionic Polymer.* Biomacromolecules, 2012. 13(5): p. 1683-1687.

Kirk, J.T., **N.D. Brault**, T. Baehr-Jones, M. Hochberg, S. Jiang, and D.M. Ratner, *Zwitterionic polymer-modified silicon microring resonators for label-free biosensing in undiluted human plasma.* Biosensors and Bioelectronics. Doi: 10.1016/j.bios.2012.10.079.

Huang, C.J., Y.T. Li, J.B. Krause, **N.D. Brault**, and S.Y. Jiang, *Internal Architecture of Zwitterionic Polymer Brushes Regulates Nonfouling Properties.* Macromolecular Rapid Communications, 2012. 33(11): p. 1003-1007.

Li, Y.T., A.J. Keefe, M. Giarmarco, **N.D. Brault**, and S.Y. Jiang, *Simple and Robust Approach for Passivating and Functionalizing Surfaces for Use in Complex Media.* Langmuir, 2012. 28(25): p. 9707-9713.

Cao, Z.Q., **N. Brault**, H. Xue, A. Keefe, and S.Y. Jiang, *Manipulating Sticky and Non-Sticky Properties in a Single Material.* Angewandte Chemie-International Edition, 2011. 50(27): p. 6102-6104.

Krause, J.E., **N.D. Brault**, Y.T. Li, H. Xue, Y.B. Zhou, and S.Y. Jiang, *Photoiniferter-Mediated Polymerization of Zwitterionic Carboxybetaine Monomers for Low-Fouling and Functionalizable Surface Coatings.* Macromolecules, 2011. 44(23): p. 9213-9220.

Brault, N.D., C.L. Gao, H. Xue, M. Piliarik, J. Homola, S.Y. Jiang, and Q.M. Yu, *Ultra-low fouling and functionalizable zwitterionic coatings grafted onto SiO2 via a biomimetic adhesive group for sensing and detection in complex media.* Biosensors & Bioelectronics, 2010. 25(10): p. 2276-2282.

von Muhlen, M.G., **N.D. Brault**, S.M. Knudsen, S.Y. Jiang, and S.R. Manalis, *Label-Free Biomarker Sensing in Undiluted Serum with Suspended Microchannel Resonators.* Analytical Chemistry, 2010. 82(5): p. 1905-1910.

Under Submission/Review:

Zhu, Z., X. Xue, **N.D. Brault**, A.J. Keefe, X. Han, Y. Deng, J. Xu, Q. Yu, and S.Y. Jiang, *Cellulose Paper Sensors Modified with Zwitterionic Poly(carboxybetaine) for Sensing and Detection in Complex Media.* Analytical Chemistry, 2014. Submitted.

Sundaram, H.S., X. Han, A.K. Nowinski, **N.D. Brault**, Y. Li, J-R. Ella-Menye, K.A. Amoaka, K.E. Cook, M. Patrick, K. Senecal, and S.Y. Jiang, *Achieving One-step Surface Coating of Highly Hydrophilic Poly(Carboxybetaine Methacrylate) Polymers on Hydrophobic and Hydrophilic Surfaces*. Applied Materials and Interfaces, 2014. Submitted.

Book Chapters:

Brault, N.D., S. Jiang, and Q. Yu, *Dual-Functional Zwitterionic Carboxybetaine for Highly Sensitive and Specific Cancer Biomarker Detection in Complex Media Using SPR Biosensors*, in *Biosensors for Cancer Diagnostics*, K.E. Herold and A. Rasooly, Editors. 2012, CRC PressINC. p. 69 - 88.

Brault, N.D., S. Jiang, and Q. Yu, *Use of a Surface Plasmon Resonance (SPR) Biosensor to Characterize Zwitterionic Coatings on SiO2 for Cancer Biomarker Detection*, in *Biosensors and Cancer*, V.R. Preedy and V.B. Patel, Editors. 2012, CRC Press. p. 20 – 42.

Patent Applications**:**

U.S. Patent Application PCT/US2012/047745 “Photonic Blood Typing”, **N.D. Brault**, Jill Johnsen, D. Ratner, J. Kirk, J. Lopez, and S. Jiang, filed July 20, 2012.

U.S. Patent Application 61/588,785 “Integrated High- and Low-Density Layers to Achieve Low Fouling and High Immobilization”, **N.D. Brault**, H. Sundaram, Y. Li, C.J. Huang, Q. Yu, J.E. Krause, and S. Jiang, filed Jan. 20, 2012.

U.S. Patent Application 12/891,524 “Zwitterionic Polymers Having Biomimetic Adhesive Linkages”, S. Jiang, C. Gao, G. Li, H. Xue, and **N.D. Brault**, filed Sep. 27, 2010.